

Doctoral thesis

Doctoral theses at NTNU, 2021:233

Yuequn Fu

Atomistic Insights to Interfacial Dynamics

NTNU
Norwegian University of Science and Technology
Thesis for the Degree of
Philosophiae Doctor
Faculty of Engineering
Department of Structural Engineering



Norwegian University of
Science and Technology

Yuequn Fu

Atomistic Insights to Interfacial Dynamics

Thesis for the Degree of Philosophiae Doctor

Trondheim, June 2021

Norwegian University of Science and Technology
Faculty of Engineering
Department of Structural Engineering



Norwegian University of
Science and Technology

NTNU

Norwegian University of Science and Technology

Thesis for the Degree of Philosophiae Doctor

Faculty of Engineering

Department of Structural Engineering

© Yuequn Fu

ISBN 978-82-326-5530-4 (printed ver.)

ISBN 978-82-326-6894-6 (electronic ver.)

ISSN 1503-8181 (printed ver.)

ISSN 2703-8084 (online ver.)

Doctoral theses at NTNU, 2021:233

Printed by NTNU Grafisk senter

Preface

This thesis is submitted to the Norwegian University of Science and Technology (NTNU) for partial fulfillment of the requirements for the degree of Philosophiae doctor (PhD).

The doctoral work has been conducted in the period between August 2017 and June 2021 under the supervision of Professor Jianying He and Professor Zhiliang Zhang. All the simulation work was carried out at NTNU Nanomechanical Lab, Department of Structural Engineering (KT), Faculty of Engineering (IV), Norwegian University of Science and Technology (NTNU), Trondheim, Norway. The thesis comprises of an introductory section, and 3 journal papers (one published and two submitted).

This work is supported by the Research Council of Norway and the China Scholarship Council. All the simulations were carried out on the computational resources provided by Norwegian Metacenter for Computational Science (NOTUR NN9110k and NN9391k).

Yuequn Fu

Trondheim, June 2021

Abstract

For decades, interfacial dynamics is always a hot spot in interface-related fields such as colloidal stabilization, fabrications of new materials, heterogenous catalysis, biosensors, chemical or physical absorption, and many others. Observing the dynamic behavior of the molecules in the interface is significant to explore the mechanisms of the formation of the interface and interfacial mechanics. According to the interfacial geometry, we studied the interfacial dynamics in two parts, curved interface and flat interface. In this thesis, the self-emulsifying microemulsion is targeted as the curved interface, while the ice/graphene is studied as the flat interface.

In part of curved interface, it aims at investigating the mechanical properties of microemulsion droplet and the particle size distribution of the water-oil microemulsion. The mechanical properties of microemulsion droplets and the correlation to their molecular structures are of vital importance to those applications. Here, atomistic modelling was utilized to study the stability, deformation, and rupture of Janus oligomer enabled water-in-oil microemulsion droplets, aiming for revealing their intrinsic relationship to the Janus oligomer-based surfactants and oil structures. The self-emulsifying process from a water, oil and surfactant mixture to a single microemulsion droplet was modulated by the amphiphilicity and the structure of the surfactants. Four microemulsion systems with interfacial thickness in the range of 7.4-17.3Å were self-assembled to explore the effect of the surfactant on the droplet morphology. By applying counter forces on the water core and the surfactant shell, the mechanical stability of microemulsion droplets was probed at different ambient temperatures. A strengthening response and a softening regime before and after a temperature-dependent peak force were identified followed by the final rupture. This work demonstrates a practical strategy to precisely tune the mechanical properties of a single microemulsion droplet, which can be applied in the formation, de-emulsification, and design of microemulsion in oil recovery and production, drug delivery and more other applications. As continuing work, a coarse-grained model with molecular dynamics was built up to simulate a liquid mixture of water, oil, and surfactant molecules, a total of 864000 untied atoms. Hundreds of water-in-oil microemulsion droplets formed in a configuration consisted of a hydrophilic core

and a hydrophobic shell. By observing the size variation of the microemulsion droplets during the self-emulsifying of the microemulsion, the droplets' diameter and particle size distribution was calculated and compared. According to the results of the particle size distribution of the microemulsion, direct aggregating and the water molecules transition between microemulsion droplets and a steep energy barrier were observed clearly. A mechanism found in the results explicated droplets' variation during the preliminary stage of microemulsion emulsifying and explained the reason why microemulsions can be thermodynamically stable. Furthermore, the temperature's effect on the droplet size was also studied by a series of parallel simulations. It indicated that higher thermal energy can lead to a large droplet size. This work compensates for the understanding deeply of the mechanism of water-in-oil microemulsions self-emulsifying and their particle size distribution. Such a theoretical finding suggests some practical strategy to prepare a microemulsion in a desirable size.

In part of the flat interface, mechanical properties of the ice/graphene interface were studied systemically. This work built up the models of oriental-structured materials with diverse arrangement density that were adhered to the ice layer. The mechanical properties of such kind of materials were systematically investigated in terms of different loading rate, pulling direction, arrangement density, and fracture mode. The stress-strain response and the changes in the morphology of an oriental-structured substrate indicated that relatively low loading rate and high arrangement density remained the original morphology of the substrate and exhibited unique reversibility. Increasing the arrangement density reduced the ice adhesion strength and favored ice removal. The shear test with two-mode (concurrent and sequential) and two directions (along and against the structure of substrate) exhibited lower stress along with the oriental structures than against it and finally reached constant shear stress that can be considered as the ice friction force. In general, the findings not only contribute to fundamental knowledge of ice adhesion dynamics but also provide a practical strategy for de-icing or anti-icing surface design.

Acknowledgements

For me, pursuing a Ph.D. is a four-year-long traveling both in vast academics and picturesque Norway, filled with many meaningful memories. Four years ago, being a Ph.D. is cool and honorary in my thought, which also makes me decide to archive it without hesitation. Started as a novice, challengeable tasks and increasing interests lay a foundation of my slowly growing in academic study. Difficulty and challenges in the researches often let me feel disappointed, anxious, painful, even distraught. But I also feel that I am the happiest man in the world who walks home in a jumping style each time some fantastic findings were discovered gradually. Time is flying when we focus on something. Four years later, finishing a Ph.D. is not so amazing and exciting achievement but the bright guidelines for my futural career, even my life. This period helps me find myself and my interest in the research. Keeping learning knowledges and exploring new researches will enhance the clarity of our view on the world, which is a meaningful and everlasting pursuit.

Those work as extensive as this could not have been achieved without significant efforts from many individuals.

My supervisors, Prof. Jianying He and Prof. Zhiliang Zhang, are the person who introduces me to the academic world. They spare no effort to draw up a detailed project plan agreeing with my background and interests in research, at the beginning of my Ph.D. Every time they can give quick and efficient feedback for my questions. They apply a professional solution to support me with their appropriate encouragement and much patience. Their careful guidance helps me recognize the comfortable rhythm of studying. Then they improve my ability and logicity of scientific thinking. In such a way, I have benefited a lot from their wisdom and professional attitude. I would like to appreciate their meticulous efforts and supports. They enrich me very much in the past four years, even in the future.

My mentor, Dr. Senbo Xiao, leads me into the fantastic research field, molecular dynamics simulations. From theory to the computing details, he almost teaches everything to me. His passion and soulful enthusiasm for the research inspire me profoundly. With critical advice and modifications to the content of my research, he

improves greatly the quality and significance of the publications. Here, I would like to express my sincere gratitude for his help, effort, encouragement, and patience.

There are special thanks to Prof. Jianyang Wu and Associate Prof. Xiao Wang for their kind guidance and wonderful corporation in work.

My grateful thanks are also extended to all the colleagues at the Department of Structural Engineering. Here, special thanks are for my dear friends and colleagues: Prof. Kjell Magne Mathisen, Prof. Helge Kristiansen, Mao Wang, Yi Gong, Zhiwei He, Kai Zhao, Haiyang Yu, Yang Li, Øyvind Othar Aunet Persvik, Bjørn Strøm, Verner Håkonsen, Shengwen Tu, Sigrid Rønneberg, Merete Falck, Ingrid Snustad, Li Sun, Yizhi Zhuo, Susanne Sandell, Tong Li, Feng Wang, Sandra Sæther, Xuyan Liu, Sakari Pallaspuuro, Tianle Zhou, Zexin Chang , Junchao Pan, Tengjiao Jiang, Thorstein Wang, Xu Wang, Meichao Lin, Yu Ding, Yuanhao Chang, Rui Ma, Jing He, Paul Rübsamen-von Döhren, Mohammad Javad Sadeghinia, Yang Song, Mingjie Zhang and Pan Wei. We have spent lots of wonderful time together. It is a unique memory in my life. In addition, I want to express heartfelt thanks to my friends, Xiaolan Ma, Meichen Liu, Sienna Li, Jiali Xian, Wei Guan, Jianyu Ma and Qian Long, for your kind helps, company and supports. All of these make Norway a beautiful country where we meet each other.

Last but not least, I want to express my gratitude to my family for their love and support. Especially, I want to thank my beloved girl, Siqi Liu, who knows me, loves me and always be with me. For her, words are powerless to express my gratitude, but all my love and thanks to you.

All of you make me what I am! Please accept my vehement protestations of gratitude!

List of Papers

The thesis is organized based on the following three papers, which have been published or submitted:

- I. **Fu, Y.**; Xiao, S.; Liu, S.; Wu, J.; Wang, X.; Qiao, L.; Zhang, Z.; He, J., Stability, deformation and rupture of Janus oligomer enabled self-emulsifying water-in-oil microemulsion droplets. *Physical Chemistry Chemical Physics* 2020, 22 (43), 24907-24916.
- II. **Fu, Y.**; Xiao, S.; Liu, S.; Zhang, Z.; He, J., Atomistic insights to droplet size distribution in the preliminary stage of self-microemulsifying of a water/surfactant/oil system. *To be submitted*
- III. **Fu, Y.**; Xiao, S.; Zhang, Z.; He, J., Stimuli-responsive surfaces in design for low intrinsic ice adhesion. *Submitted*

The other relevant journal papers that are finished in the PhD study but not include in the thesis are listed in the following:

- I. **Fu, Y.**; Xu, K.; Wu, J.; Zhang, Z.; He, J., The effects of morphology and temperature on the tensile characteristics of carbon nitride nanothreads. *Nanoscale* 2020, 12 (23), 12462-12475.
- II. **Fu, Y.**; Wu, J.; Xiao, S.; Zhang, Z.; He, J., Influences of morphology and temperature on mechanical properties of double-carbon-chains Carbon sulfur nanothreads in orientational order. *To be submitted*

Besides the publication presented above, I have contributed to the following works:

- I. Yang, Y.; Li, L.; Wang, X.; **Fu, Y.**; He, X.; Zhang, S.; Guo, J., A Surfactant for Enhanced Heavy Oil Recovery in Carbonate Reservoirs in High-Salinity and High-Temperature Conditions. *Energies* 2020, 13 (17), 4525.
- II. Chang, Y.; Xiao, S.; **Fu, Y.**; Wang, X.; Zhang, Z.; He, J., Nanomechanical Characteristics of Trapped Oil Droplets with Nanoparticles: A Molecular Dynamics Simulation. *Journal of Petroleum Science and Engineering* 2021, 108649.

- III. Wang, F.; **Fu, Y.**, et al. Morphology memory effect and switching on and off surface wrinkling in ultrathin metal film deposition. *Submitted.*
- IV. Liu, S.; Wan, D.; Shuai, G.; **Fu, Y.**; Ren, X.; Zhang, Z.; He, J., Microstructure and nanomechanical behavior of an additively manufactured high-entropy alloy. *Submitted.*

Conferences

- I. **Fu, Yuequn**; Senbo, Xiao; Jianying, He; Zhiliang, Zhang. (2019) Deformation mechanics of microemulsion droplets by atomistic modeling. International conference on nanofluids; Castello. 2019-06-26 - 2019-06-28.
- II. **Fu, Yuequn**; Senbo, Xiao; Jianying, He; Zhiliang, Zhang. (2019) Mechanical properties of microemulsion droplet from a atomistic simulations. WaterEurope: Multiscale simulations and coarse-grained models for water and aqueous systems; Lausanne. 2019-10-21 - 2019-10-23.

Contents

Preface..... i

Abstract..... iii

Acknowledgements v

List of Papers..... vii

Contents ix

Chapter 1. Introduction 1

 1.1 Background and Motivation 1

 1.2 Research Objectives..... 2

 1.3 Thesis Highlights 2

 1.4 Thesis Outline 3

Chapter 2. Literature Review 5

 2.1 Introduction..... 5

 2.2 The formations of interfaces 6

 2.3 Interfacial dynamics by MD Simulations 17

 2.4 Challenges and Tasks..... 23

Chapter 3. Modelling and Simulation..... 25

 3.1 Modelling of microemulsion and ice/graphene-platelets Systems 25

 3.2 Simulation Details..... 30

Chapter 4. Main Results..... 34

 4.1 Stability of the self-emulsifying microemulsion droplets..... 34

 4.2 Droplets size distribution of the microemulsion system..... 35

 4.3 The dynamics happened on the ice/material interface..... 36

Chapter 5. Recommendations for Further Studies.....	37
Bibliography	39
Appendix A Appended papers.....	53
A.1 Paper I.....	53
A.2 Paper II	87
A.3 Paper III.....	119
Appendix B	146

Chapter 1. Introduction

1.1 Background and Motivation

Interface dynamics attract the decades-long interest of scientists in many fields, such as colloids[1-3], adhesions[4-6], tribology[7, 8], functional-coating materials[9-11], anti-icing[12-14] or de-icing[15, 16], catalysts[17, 18] and so on. Many mechanisms have been explored to understand scientific phenomenon and problems. In recent decades, the spontaneous self-assembly behaviors on the interface are strongly capturing the eyes of researchers in both academia and industry. Especially, by studying the interfaces in colloid systems with normal three phases (water, oil and surfactant phase), it discovered many fundamental knowledges which can provide us practical strategies to fabricate new materials. As an important one of curve-interface colloids, microemulsion systems[19, 20] with core-shell spherical droplets realized the designing and manufacturing of nanoscale materials for a specific function. Although there are many experiments[21-24] and computational calculations[25-27] focusing on the emulsifying mechanism and the stability of microemulsions, atomistic insights to explicate the dynamic processes of these phenomena are far unexplored, due to the limits of the currently available experimental technologies and methods. For a purpose of comprehensive study, standing for flat-morphology interface, as a flat interface, the ice/graphene interface is a typical target for studying the mechanism of the ice adhesion[28-30]. It is easy to measure the values of the ice adhesion with the specific machines. Meanwhile, it is still difficult to capture the detailed dynamic processes of

deformations and atomistic view of interface configurations. So, it is meaningful to study these behaviours and mechanisms happening on the interfaces. The theoretical finds in this thesis are expected to compensate for fundamental understanding on the physical and chemical properties of the interfaces.

1.2 Research Objectives

The present thesis is funded by a NTNU - CSC scholarship program, which aims to explore atomistic insights to fundamental understanding of the interfacial dynamics , including mechanical stability of water-in-oil microemulsion droplets, the droplet size distribution of water-in-oil system during preliminary stage of the micro-emulsification, and the mechanism of de-icing in the ice/graphene-platelets. The primary objective of this thesis is to establish a coarse-grained model of a liquid system containing water, surfactant and oil, trying to observe the detailed information of the self-emulsifying process of a water-in-oil microemulsion. It mainly focused on the information and mechanical properties of the microemulsion, and droplets size distribution during preliminary stage of micro-emulsification of water/surfactant/oil system. Another objective is to build up an ice/graphene-platelets interface model as a tensile test target, aiming at exploring the atomistic insights to the detailly process and mechanism of de-icing in the interface.

1.3 Thesis Highlights

With a series of comprehensive molecular dynamics (MD) simulations, the thesis exhibits results on the self-emulsifying process during the formation of the microemulsion and the mechanisms of the droplet size distribution of a water-in-oil microemulsion system. Except for such a kind of curved interface, the thesis also investigated the mechanical properties of a flat-interface ice/graphene. In summary, the highlights of the thesis are listed in the following:

- The spontaneous emulsification of microemulsion droplets showed that the structure and arrangement of the water and oil interface were dominated by the amphiphilic parts of the linear surfactant molecules. Molecular level insights were explicated to improve the understanding of interfacial behaviors of a water/surfactant/oil system.

- Four microemulsion systems with interfacial thickness in the range of 7.4-17.3Å were self-assembled to explore the effect of the surfactant on the droplet morphology. We found that surfactant molecule can impact on the arrangement density of surfactant monolayer in the water/oil interface and curvature of a microemulsion droplet by their intrinsic molecular length and amphiphilicity.
- The force peak and the rupture work were obtained to identify the softening-to-strengthening transition as lowering the temperature. It is a novel method to measure or quantify the stability of a microemulsion droplet.
- Due to the instability of small microemulsion droplets, the water molecules on the surface of water drop trend to detach from their host droplets, and then redeposit into the large microemulsion droplets. It is detailed atomistic insights to mass transfer of water in water/oil system.
- At the time of 1.8 ns, it is found that there is approximately a Gaussian-like particle size distribution in the water/oil system including 182 droplets, and the size range of the microemulsion droplets is from 4.0 nm to 8.0 nm. A size statistic was introduced to describe the information of droplet-diameter distribution of water/oil system.
- Following the mechanism similar to Ostwald ripening, directly aggregating of two microemulsion droplets and the transition of water molecules from the small microemulsion droplets to the large microemulsion droplets realizes the rapid growth of droplets and brings the system into the next level of stability. This find added atomistic knowledges into the mechanisms of mass transfer in water/oil systems.
- The graphene platelets with dense arrangement reduce the ice fraction force effectively. By using three graphene-platelets substrates with different ordered geometry, we figured out different ice adhesion after the de-icing test.
- suitable knitting or arrangement of the graphene-platelets in materials for anti-icing or de-icing is expected for other researchers to fabricate for de-icing & anti-icing and water collection.

1.4 Thesis Outline

The thesis consists of an introductory section and a collection of three peer-reviewed papers. The introductory section is divided into five chapters. Detailly, in **Chapter 1**,

the background and motivation, research objectives, thesis highlights are stated. **Chapter 2** will review the literatures. **Chapter 3** describes the simulation methods and details involved in the thesis. The main findings are summarized in **Chapter 4**. Finally, recommendations for further work are given in **Chapter 5**.

Chapter 2. Literature Review

2.1 Introduction

Thousands of years ago, people began to recognize that there are various elements consisting of the world or the universe and they can present as simple substances or compounds. Their existence makes it unavoidable to form a number of phases or mixtures. Due to the different properties of these phases, the interfaces naturally appear as boundaries among them, generally including liquid-liquid interfaces (some colloid systems), solid-solid interfaces, gas-liquid interfaces, gas-solid interfaces, liquid-solid interfaces according to their physical states.[31-35] It is no exaggeration to say that the interfacial problems are highly relevant of both our life and academic fields, such as dishes washing by using detergent, fabrication of ice cream, using of daily necessities, grain boundary, interfacial wettability and activity, functional surface coatings and so on. Up to date, the topics about interfaces are keeping the appealing to scientists in many fields. As a branch of interfacial research, interfacial dynamics focuses on interfacial behaviors driven by molecule-level physical and chemical interactions. Studying further on interfacial dynamics is critical for us to enrich our fundamental understanding of nanoscale level phenomenon, which can make basement to develop new techniques and materials, such as drug deliver, nanomaterials' fabrication and coatings of anti-icing & de-icing. In this chapter, formation of some curved and flat interfaces, intermolecular forces at interfaces and previous studies will be emphatically introduced.

2.2 The formations of interfaces

2.2.1 Intermolecular forces at interfaces

As known well, the intermolecular interactions presented at interfaces are namely called intermolecular forces (IMF, or secondary forces)[36], such as hydrogen bonding[37], ionic bonding[38-40], ion-induced dipole forces[41], ion-dipole forces[42] and van der Waals forces[43, 44] (Keesom force, Debye force, and London dispersion force[45, 46]), weaker than intramolecular forces[47, 48], as shown in Figure 2.1. They can also be divided into strong and weak interactions, according to their bonding energy and intrinsic strength. The following text will introduce them separately.

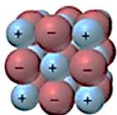

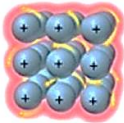

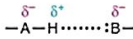




Force	Model	Basis of Attraction	Energy (kJ/mol)	Example
Bonding				
Ionic		Cation-anion	400-4000	NaCl
Covalent		Nuclei-shared e ⁻ pair	150-1100	H-H
Metallic		Cations-delocalized electrons	75-1000	Fe
Nonbonding (Intermolecular)				
Ion-dipole		Ion charge-dipole charge	40-600	Na ⁺ ·····O ⁻ H
H bond		Polar bond to H-dipole charge (high EN of N, O, F)	10-40	:O ⁻ -H·····H-O ⁺ -H H H
Dipole-dipole		Dipole charges	5-25	I-Cl·····I-Cl
Ion-induced dipole		Ion charge-polarizable e ⁻ cloud	3-15	Fe ²⁺ ·····O ₂
Dipole-induced dipole		Dipole charge-polarizable e ⁻ cloud	2-10	H-Cl·····Cl-Cl
Dispersion (London)		Polarizable e ⁻ clouds	0.05-40	F-F·····F-F

Figure 2.1 Different intermolecular interaction types and their energy. Taken from <http://slideplayer.com/slide/2740266/>

Hydrogen bonding (H-bond)[49] is normally seen as a covalent bond to describe the electrostatic attractions between a hydrogen atom (hydrogen acceptor) and an electronegative atom or functional group (hydrogen donor), primarily the second-row elements oxygen, nitrogen, or fluorine. Interestingly, hydrogen bonds can be intermolecular or intramolecular interactions occurring among separate molecules or the parts of the same molecule, which is a kind of strong attraction but weaker than covalent or ionic bonds.[50-52] For example, the intermolecular hydrogen bonds make the high boiling point of water (100 °C).[53] There are also some weaker hydrogen bonding whose donor is sulfur (S) or chlorine (Cl).[54] In protein-ligand interfaces, there have been proven to be many hydrogen bonding between hydrogen atom with halogen element (nitrogen, oxygen, sulfur, fluorine, chlorine, bromine and iodine), as Figure 2.2 shows. A computer program figured out that such hydrogen bonding interactions occurred in the active sites, as a sphere of 10 Å radius around the ligand.[55] An experimental study exhibits that self-assembled adsorption at the liquid-solid interface formed and stabilized through hydrogen bonds, shown in Figure 2.3. And the intermolecular N···H–O H-bonds dominated the interactions and afford the main driving force for the self-assembly behaviors. For water in crude oil emulsion systems, hydrogen bonding (such as pyrrole, carboxylic, thiophene, sulfhydryl, and related functional groups)[56] also contributes significantly to their formation and stability.

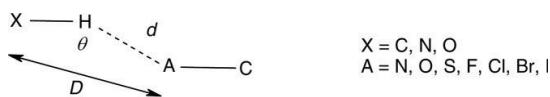


Figure 2.2 Representative hydrogen bond. A–C is a single or double bond.

Reprinted from Ref [54].

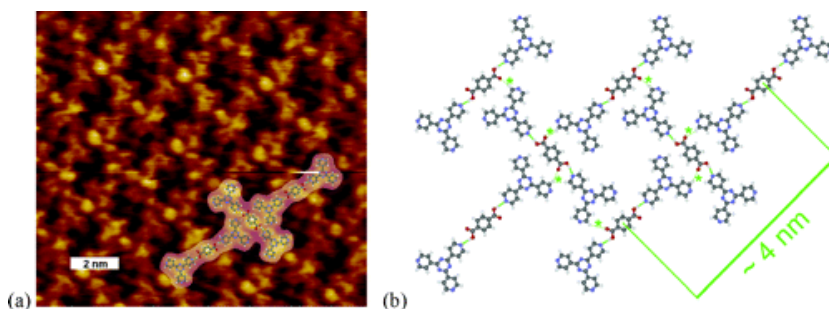


Figure 2.3 (a) Scanning tunneling microscopy (STM) topograph of the 80° TPT (trimesic acid)–TPA (terephthalic acid) cocrystal on highly oriented pyrolytic graphite (HOPG) (0001). TPT molecules appear as several bright, triangularly arranged features, whereas TPA appears as a single round feature. (b) Molecular model of the 90° TPT–TPA structure (the bold dashed green lines indicate the $N \cdots H-O$ H-bonds of the TPT–TPA–TPT basic units, and the fine green lines (additionally marked with asterisks) indicate weaker $C-H \cdots O$ H-bonds between these building blocks), reprinted from Ref [55].

Ionic bonding[57], as one kind of chemical bonding, is produced by the electrostatic attraction from the ions charged by opposite charge or atoms with entirely distinct electronegativities. In a Pickering emulsion[58], amphiphilic Fe_3O_4 nanoparticles were utilized as surfactant with their interfacial activity of ionic head part, to stabilize the emulsions system, as Figure 2.4 shows. It is an efficient extraction system to separate chlorobenzene, phenol, and methyl orange from many kinds of aqueous solutions by utilizing the intermolecular ionic bonding.

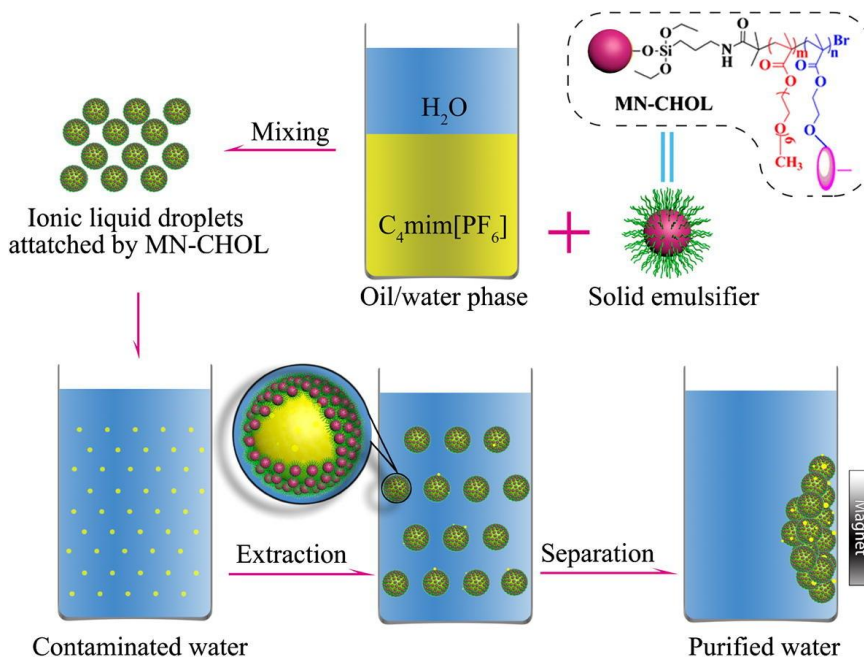


Figure 2.4 Smart magnetic ionic liquid-based Pickering emulsions stabilized by amphiphilic Fe_3O_4 nanoparticles: Highly efficient extraction systems for water purification, reprinted from Ref[58].

Van der Waals force[59, 60] is a distance-dependent interaction between the chemical electronic bonds, differing from ionic and covalent bonds. It can describe the attraction and repulsions among atoms, molecules and surfaces, similar to other intermolecular interactions. Normally, the Lennard-Jones potential is used as an approximate calculation method for performing van der Waals force.[61] From the view of molecular physics, van der Waals is weaker than the covalent and ionic bonds, not directional, short-range, and mostly temperature-independent except for the dipole-dipole interactions. [62]The van der Waals emulsion is a result of using van der Waals forces to trap the particles in the water-oil interface, which enables a practical strategy for the design and fabrications of new materials, as Figure 2.5 shows.

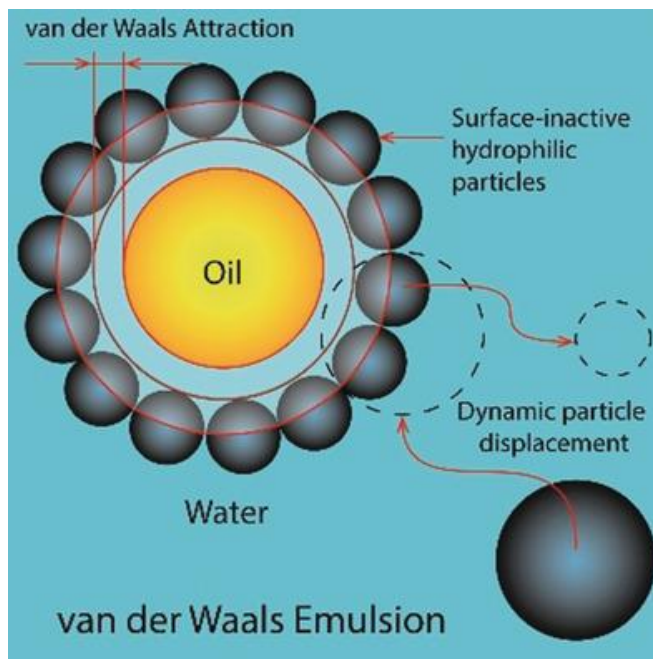


Figure 2.5 Van der Waals Emulsions: Emulsions Stabilized by Surface-Inactive, Hydrophilic Particles via van der Waals Attraction, reprinted from Ref[62].

In most cases, the interactions presented in the interfaces normally are quite complex, not only depending on the kinds of atoms or molecules but also being determined by the morphology of the interface, such as their roughness[63] and

curvature. It is also possible to include one or several ones of intermolecular forces in one case.

2.2.2 Curved water/oil interfaces and microemulsion system

A mixture of water, surfactant and oil, can form an emulsion system that can be prepared by dry gum, wet gum, *In-situ* soap and mechanical method.[31, 64] It can be divided into emulsions[65, 66], microemulsions[31, 67] and nanoemulsions[68] that are multi-phases colloid systems containing water, oil and surfactant & cosurfactant. They possess various particle sizes and morphologies, as Figure 2.6 shows. For example, emulsion systems can be divided into three types: water-in-oil, oil-in-water, and multiple emulsions, according to their dispersed and continuous phases, as Figure 2.7 shows. Most of them are in spherical or lamellar shape with various sizes. In such polydisperse solutions, the dispersed phase is isolated from the continuous phase by a surfactant & cosurfactant monolayer, which leads to the different surface tension of two sides of the monolayer. A curved interface is a quite reasonable configuration to balance this difference between their surface tensions. Meanwhile, the surfactant and cosurfactant also have been trapped tightly in the interfaces. So, the strength of the monolayer dominates the stability of these emulsified systems.

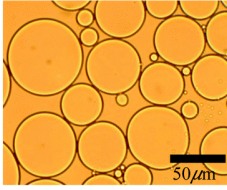
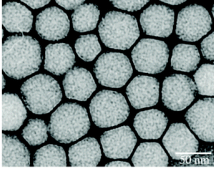
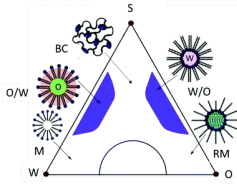
	macroemulsions	nanoemulsions	microemulsions
			
size	1-100 μm	20-500 nm	10-100 nm
shape	spherical	spherical	spherical, lamellar
stability	thermodynamically unstable, weakly kinetically stable	thermodynamically unstable, kinetically stable	thermodynamically stable
method of preparation	high & low energy methods	high & low energy methods	low energy method
polydispersity	often high (>40%)	typically low (<10-20%)	typically low (<10%)

Figure 2.6 Comparison of macroemulsions, nanoemulsions (also referred to as miniemulsions) and microemulsions with respect to size, shape, stability, method of preparation, and polydispersity. Nanoemulsions and microemulsions have a larger surface area per unit volume than do macroemulsions because of their size. In addition, due to strong kinetic stability, nanoemulsions are less sensitive to physical and chemical changes. The nanoemulsion TEM image has been reprinted with permission. Copyright (2006) by IOP Publishing. Reprinted from Ref [68].

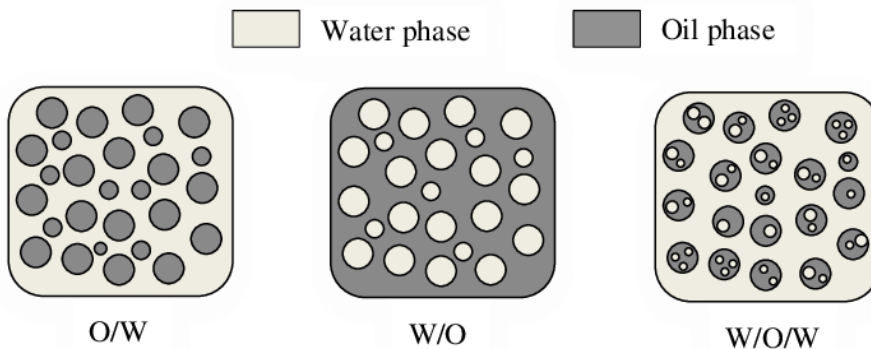


Figure 2.7 Classification of oil emulsions, reprinted from Ref [69].

Microemulsions are transparent, thermodynamically stable multiphase liquid systems, differing from emulsions or nanoemulsions[70, 71]. Self-emulsifying is a unique character of some microemulsions, such as self-emulsifying drug delivery systems (SEDDS)[21, 23, 72]. For example, developing a self-microemulsifying drug delivery system was applied to enhance antiplatelet activity and bioavailability of ticagrelor, as Figure 2.8 shows[73]. In a self-emulsifying system, surfactant and cosurfactant play an important role that can function as emulsifiers or stabilizers in emulsion or microemulsion. These amphiphilic materials that work as an emulsifier, can adsorb on the immiscible water/oil interface and reduce the interfacial tension[74], finally trapped in the interface. This process can be seen as a minimization of the system's total energy. During this process, surfactant automatically arranges in the interface by a self-assembly way, forming a surfactant monolayer or double layer with mechanical strength.[75] Under different conditions, the microscopic configuration of the solution will be various, as Figure 2.9 shows.

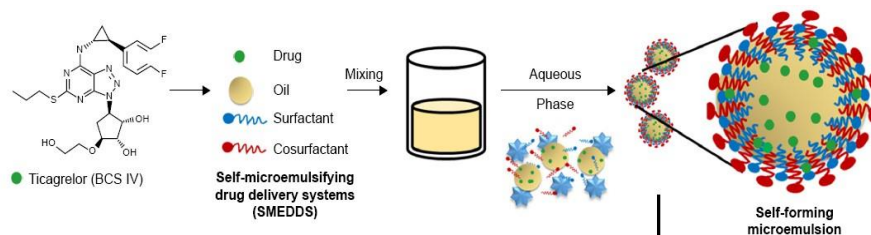


Figure 2.8 Schematic design of a drug delivery systems by preparing a microemulsion, reprinted from Ref [73].

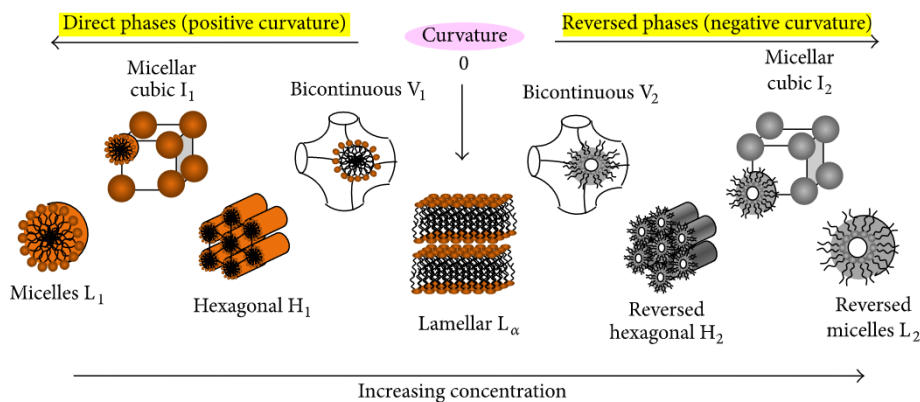


Figure 2.9 Schematic representation of a typical progression of phases as a function of concentration for an amphiphile dissolved in a selective solvent, reprinted from Ref [75].

2.2.4 Flat ice/graphene-platelets interface and the adhesion mechanism

Differing from the curved interfaces, flat interfaces are commonly related to liquid-solid interfaces or solid-solid interfaces. Herein, our topic focuses on the ice/graphene-platelets interfaces, starting from interfacial configurations to their mechanical properties (ice adhesion, shear force, pulling force, and so on).[76] In a low-temperature condition, the water or its vapor tends to accrete into a solid ice. During the freezing, the stabilizing hydrogen bonds will push water molecules away a bit from each other, resulting in an expansion of the water volume, as Figure 2.10 shows.[77, 78] The formation of hydrogen bonds makes water crystallize and organize in order. Specifically, Figure 2.11 shows the details about phase diagrams of water, which exhibits process of phase transition during frosting and deicing. Under low temperature and atmospheric pressure, vapor is easy to frost, from gaseous state into solid state. If the temperature and atmospheric pressure increase, the frost attend to evaporate into vapor, which can be called deicing process. Meanwhile, the nucleation way can be controlled by the designed surface, as **Figure 2.12** shows. The interfaces formed between the ice layer and material, and such a combination is quite tightened. Furthermore, unwanted ice is a serious problem in many fields, such as power line[79, 80], turbine[16, 81, 82], aircraft[83-85] and so on. Different anti-icing and de-icing materials and techniques have been developed well.[12, 83, 86-88]

As water freezes the hydrogen bonds push the H_2O molecules farther apart from each other increasing the intermolecular space resulting in expansion.

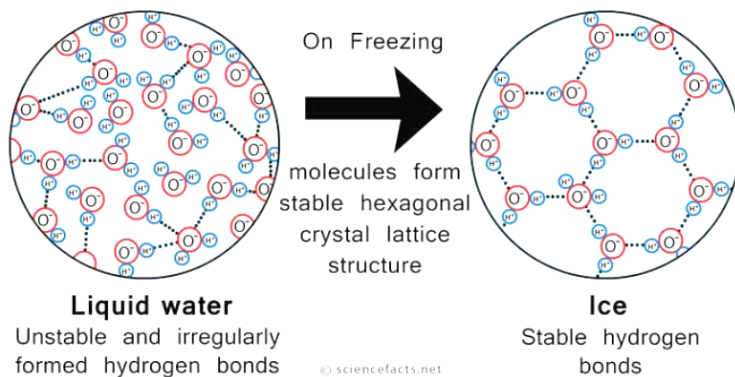


Figure 2.10 Schematic diagram shows how water expand when it freezes, copyright © sciencefacts.net.

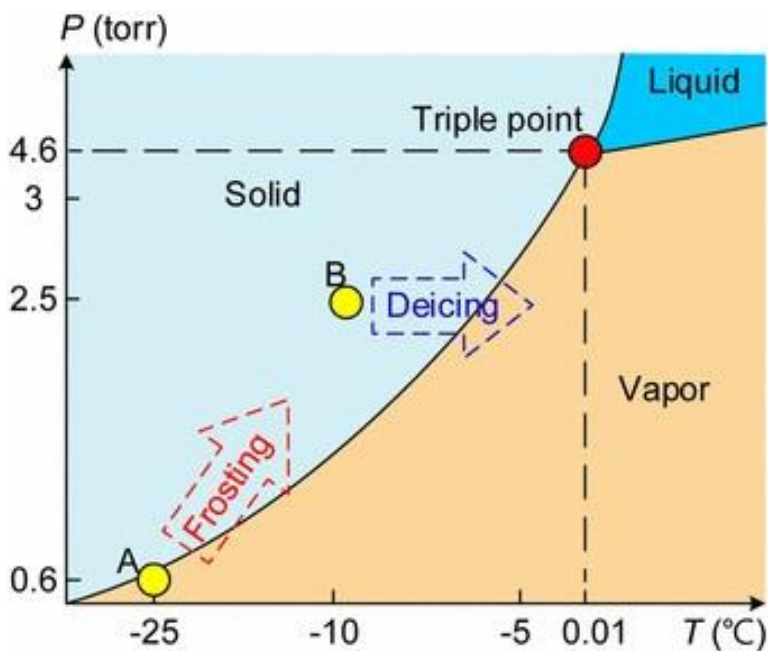


Figure 2.11 Phases diagram of water, Reprinted from Ref [78].

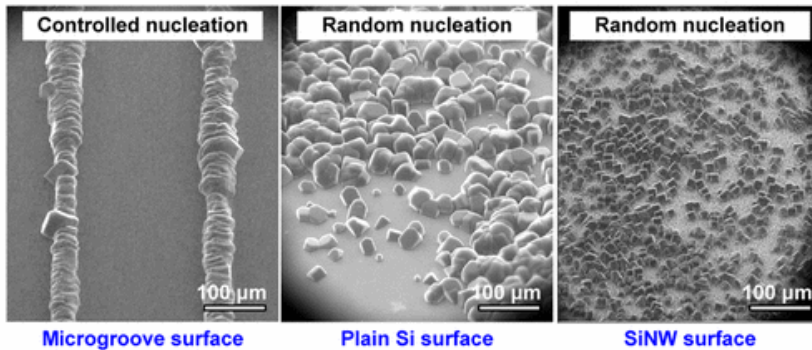


Figure 2.12 Control of ice formation leading by the types of surfaces, where SiNW is Si nanowire, reprinted from Ref [78].

Adhesion[4] is the tendency of different materials or surfaces to adhering to one another, which is a process of exothermal reaction. Taking the intermolecular forces and some mechanical effects into the consideration, the mechanisms of adhesion can be divided into the following five mechanisms: mechanical adhesion, chemical adhesion, dispersive adhesion, electrostatic adhesion and diffusive adhesion. This also works for ice adhesion.

- Mechanical adhesion. Due to the roughness of materials or surfaces including the voids and pores, interlocking is highly possible to be observed on multi scales. As Figure 2.13 shows, the “peak-valley” interface affords a wonderful configuration to produce mechanical interlocking[89].
- Chemical adhesion. Two kinds of materials or surfaces may make a new compound at the joint parts, as Figure 2.14 shows. By forming covalent bonds, ionic bonds or hydrogen bonds, two surfaces form the adhesion, even a complex network of these bonds at the interface. Such adhesion has been applied widely to many materials fabrications[90, 91].
- Dispersive adhesion. It is also known as physisorption or adsorptive adhesion, resulting from van der Waals forces or hydrogen bonding[92]. This adhesion is the most important part of adhesion due to its presence[93, 94] in all kinds of adhesive examples and its great strength.
- Electrostatic adhesion. It also is called electroadhesion, created by an electrostatic force between the conducting materials. [95]Figure 2.15 shows

us the principle of electroadhesion on conductive and semi-conductive substrates.

- Diffusive adhesion. It stems from the diffusive forces, acting a role like mechanical tethering at the molecular scale.

Actually, every adhesion case is controlled by the combination of several ones of these five mechanisms. In addition to these mechanisms, adhesion is influenced strongly by other crucial effects, such as stringing[96, 97], microstructures[98, 99], polymer-polymer hysteresis[100], wettability & absorption[96], and lateral adhesion[101, 102]. So, case-dependent adhesion is a result caused by the accumulation of the above factors.

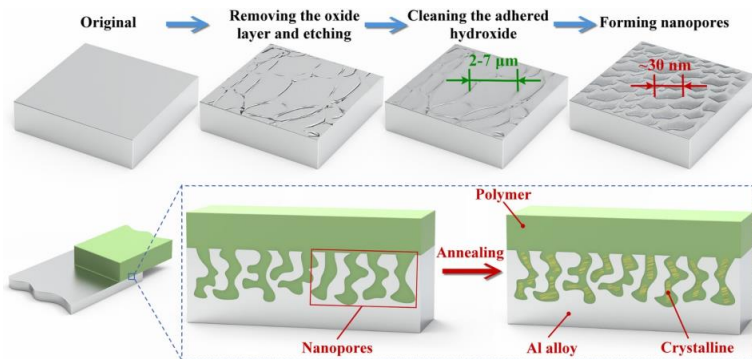


Figure 2.13 Large-area mechanical interlocking via nanopores: Ultra-high-strength direct bonding of polymer and metal materials, reprinted from Ref [89].

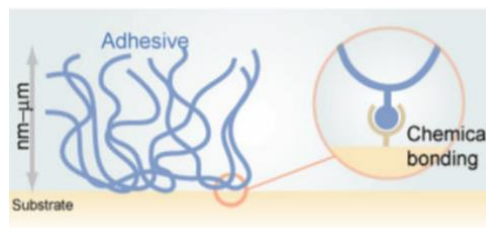


Figure 2.14 Chemical bonding for adhesion, reprinted from Ref [103].

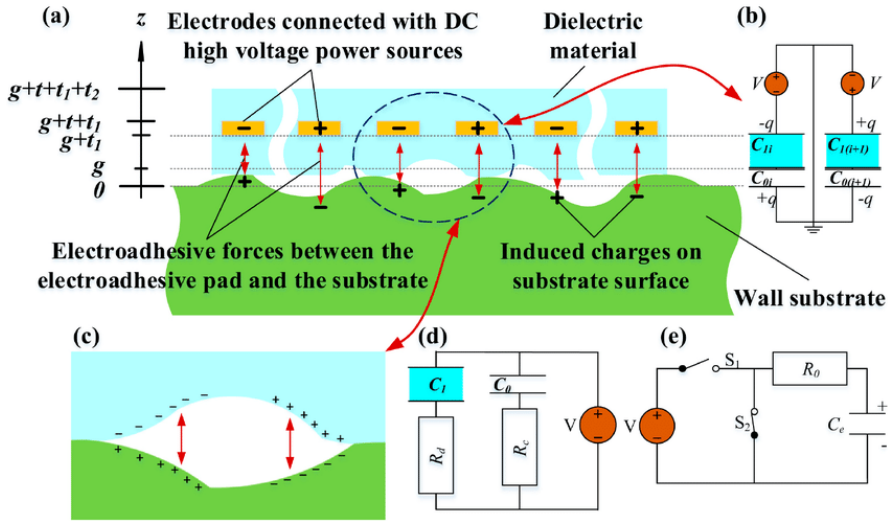


Figure 2.15 Principle of electroadhesion on conductive and semi-conductive substrates: (a) is the cross sectional view of the electroadhesive system, (b) is the equivalent circuit of two adjacent electrodes in series, (c) is charges accumulated between the non-contact areas[104], (d) is the equivalent circuit of the J–R type electroadhesive[104], and (e) is the equivalent circuit of the Coulomb type electroadhesive[105], reprinted from Ref [95].

2.3 Interfacial dynamics by MD Simulations

Limited by present techniques and methods, to observe a nanoscale interface is a very challenging task, not to mention capturing the detailed dynamic process that happens on the nanoscale view. As expected, computer simulation, such as first-principle[106, 107], Monte Carlo simulation[108, 109], density functional theory[110, 111], and molecular dynamics simulations[112, 113], was explored and developed into a mature method of quantum and physicochemical calculations based on the fundamental quantum, physics, and chemistry theory. As an important part of computational simulations, molecular dynamics simulations related with this thesis will be mentioned specially here.

2.3.1 The studies about particles' self-assembly on the water/oil interface

For recent decades, the self-assembly properties of surfactants on the interface attracts a lot of interest from academia and industry. Molecular dynamics simulations (MD simulations) were chosen to observe molecule-level phenomena and predict some properties. According to time and length scales in liquid surfactant solutions, the

approaches to modelling them can be concluded into quantum mechanics, atomistic, coarse grain, mesoscale, and fluid mechanics, as Figure 2.16 shows.[114] Molecular dynamics simulations are adapted for atomistic simulations (full atom), coarse-grained modeling, and mesoscale modeling (dissipative particle dynamics, DPD) of surfactant solutions. The followings are previous studies by common MD simulations methods including atomistic simulations, coarse-grained modelling and mesoscale modelling.

- Atomistic simulations. In such simulations, all information of all the atoms is explicitly represented. When running the simulations,[114] five kinds of intermolecular or intramolecular interactions are mainly taken into consideration, including bond potentials[115], angle interactions, dihedral potentials, electrostatic interactions and non-bonded & non-electrostatic potentials. For example, using fully atomistic molecular dynamics simulations represent how ionic surfactants adsorb and aggregate at liquid/solid interface, as Figure 2.17 shows.[116] Such kind of simulations have some disadvantage, such as the large amount of calculations, the limitation of simulation scale and low running speed.
- Coarse-grained modeling.[114] By this method, it needs to make a specific number of atoms group together as on one united atom, meanwhile the information of angle, dihedral or electrostatic potentials will be absent. [117]For instance, a coarse-grained molecular dynamics simulation was employed into observing the interfacial self-assembly behaviour of the micelle of a cationic surfactant (CTAB), shown in Figure 2.18. This simulations method can save a large number of cup hours, but it also ignores detailed information of simulated system. It can have high speed of calculations although the scale of system is quite large.
- Mesoscale modeling. Here, dissipative particle dynamics (DPD) is introduced, which is adapted well for a liquid solution system at the mesoscopic level.[118, 119] Compared to coarse-grained simulations, DPD can describe more atoms in one site, suitable for mesoscale simulated system. By this method, large-scale systems, such as vesicle and nanoemulsion systems, can be simulated and run a long simulated time, from separated phases to microstructure in order.[120, 121] These studies performed a complete dynamic process of particles' self-assembling.

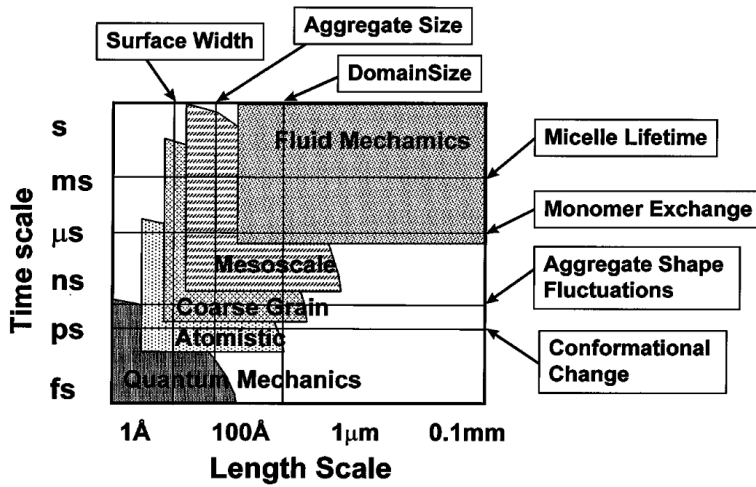


Figure 2.16 Time and length scales in surfactant solutions. A log-log schematic diagram of the length- and time-scale ranges present in surfactant solutions and rough estimates for the range of applicability of various approaches to modeling surfactant solutions. The labeled horizontal and vertical lines are estimates for the lower bounds of the length- and time-scales relevant for a common surfactant, sodium dodecylsulfate, in water near equilibrium, reprinted from Ref [114].

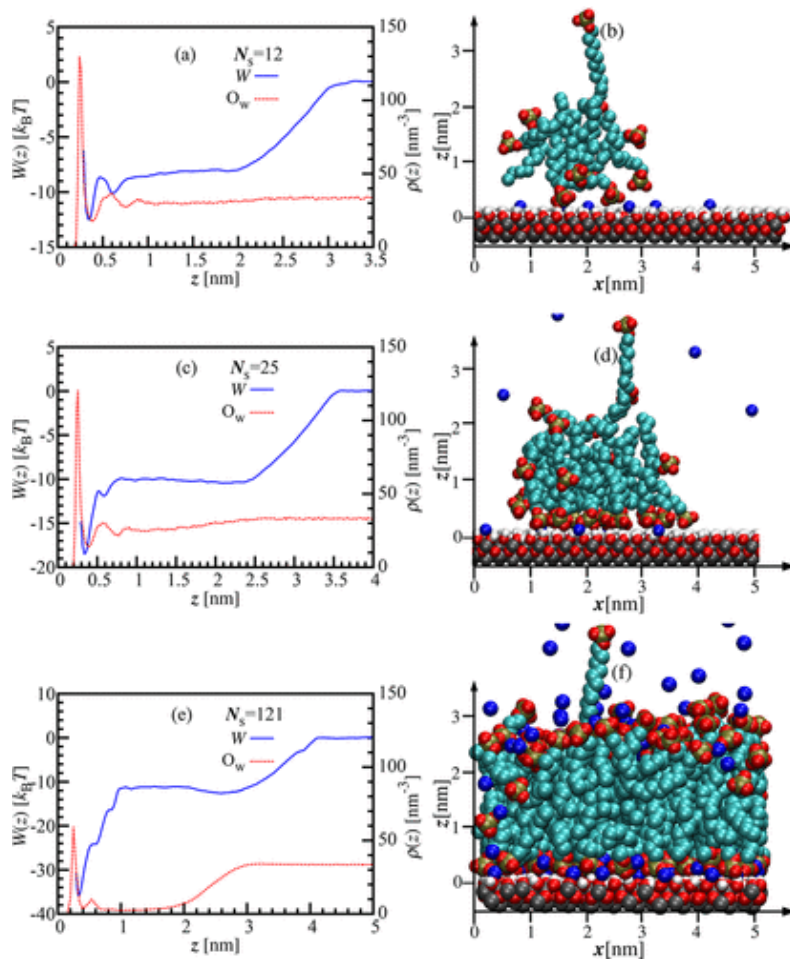


Figure 2.17 Free energy of transferring one SDS surfactant molecule from the bulk solution to the alumina surface with adsorbed SDS aggregates, reprinted from Ref[116].

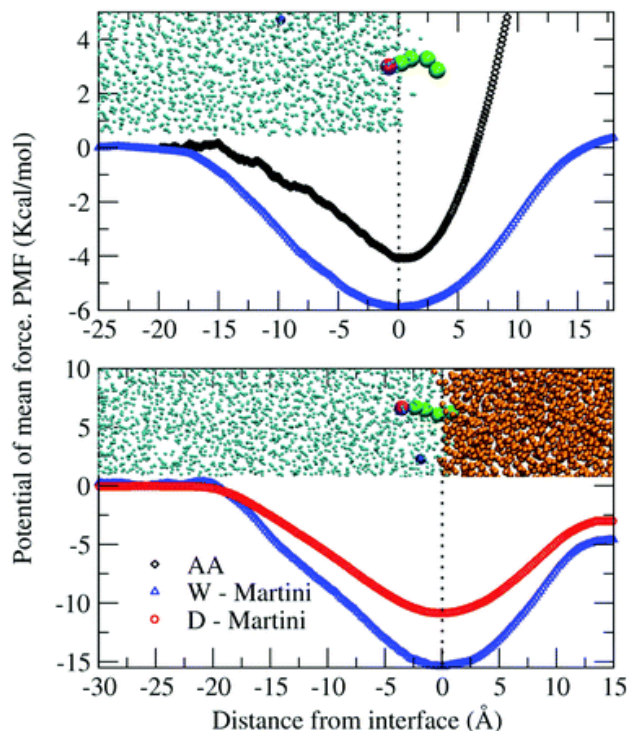


Figure 2.18 Potential of mean force (PMF) of a CTA⁺ (Hexadecyltrimethylammonium bromide)surfactant as a function of the distance from the interface in two situations: a water slab in contact with a vacuum (top panel) and a water slab in contact with an organic solvent slab (bottom panel), reprinted from Ref [117].

2.3.2 The studies of ice/materials interface

With the increasing interest in the formation[122] & mechanics of ice/materials interface, molecular dynamics simulation was more frequently employed into simulating such an interfacial structure at the atomistic level. Focusing on the ice formation on the crystalline substrate,[123] the results of seeded molecular dynamics simulations demonstrate that ice nucleation on the orientation of hydroxylated (001) kaolinite grows exclusively in the shape of hexagonal ice polytype, as shown in Figure 2.19. It approved that the critical nucleus size of hexagonal ice is about half of the critical nucleus size of homogeneous water freezing under the condition of supercooling. Some nuclei automatically form at the surface, but the ones in the initial stages of heterogeneous ice nucleation form only on the particular kaolinite surface.

There are also other studies of MD simulations to explore the mechanism of ice nucleation on various surfaces[122, 124, 125]. On the other hand, many solutions[12, 126-128] and materials[129-131] have been designed for anti-icing or de-icing of unwanted ice or frost, as shown in Figure 2.20. This work exhibits Heterogeneous SEEDing (HSEED) method to tackle the MD simulations of heterogeneous ice nucleation on crystalline surfaces. Comparing with coarse-grained mW water freezing model, fully atomistic TIP4P/Ice water turning into ice on crystals, it has been proved that the HSEED method is able to pinpoint the combination of ice polytype and crystalline face. For exploring atomistic ice adhesion mechanics, a full atom modeling was developed to investigate the effect with or without water layer on the detaching and shearing force of the ice cube.[132]

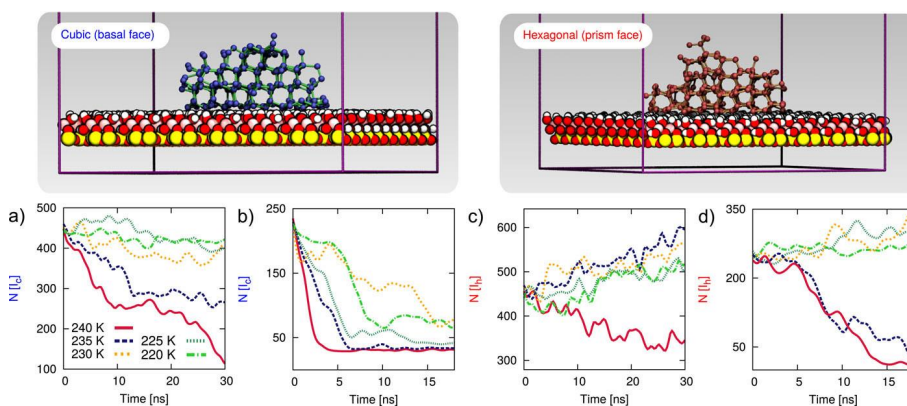


Figure 2.19 Seeded MD simulations of heterogeneous ice nucleation on the KAO_{OH} surface. Ice nuclei of I_c (top, blue) and I_h (bottom, red), as obtained from metadynamics simulations provided high-quality starting points in terms of the hydrogen bond network between ice and the kaolinite surface. The number λ of ice-like molecules within the largest connected cluster is reported as a function of time for seeds with initial sizes of about 250 and 450 ice molecules of I_c [(a) and (b)] and I_h [(c) and (d)]. For each seed five different temperatures (220, 225, 230, 235 and 240 K) have been considered, reprinted from Ref [123].

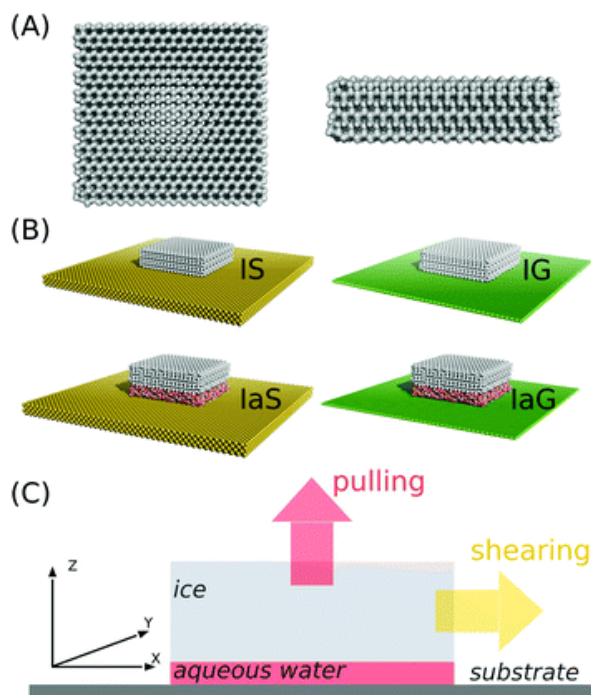


Figure 2.20 Atomistic models and simulation setup. (A) Atomistic ice cube model both from the top view on the basal face (left) and the side view (right). (B) Four simulation systems studied in this study, including IS, IaS, IG and IaG. (C) Molecular dynamics simulation setup with force acting on the center of mass of the ice cube. The force application directions for detachment pulling and shearing are indicated in the figure. Simulation box axes are indicated in the figure, reprinted from Ref [132].

2.4 Challenges and Tasks

Based on the above literature's reviews, the topics about interfacial dynamics attract the interests of scientists from many fields. It also shows that detailed molecule-level information of interfacial dynamics was unexplored although a series of interfacial mechanisms were proven by many experiments. It will be meaningful to deepen atomistic insights to interfacial dynamics. But challenge and tasks are still reminded for future research. Here, they will be mentioned by two kinds of interfaces including curved interface and flat interface depending on their geometry.

For curved interface, microemulsion was targeted to study behaviors and mechanical stability of water/oil interface. It is needed to build up large-scale coarse-grained modeling of microemulsion systems. During the self-emulsifying process, we will

investigate the dynamic variation of the microemulsion's morphology, then apply a suitable pulling force solution to measure and quantify the mechanical strength of the single microemulsion droplet, and finally get the separation of water and oil phase. In addition, a larger microemulsion system will be studied further, in order to get the droplet size distribution.

For flat interface, ice/graphene interface was chosen as a subject. The main challenge is to build up a suitable simulated model and find a solution to make pulling and shearing force. Another task is to organize the configuration of the graphene substrate. This is aiming at figuring out the effect of different-arranged graphene substrates on the adhesion and mechanical properties of this ice/graphene interface.

Chapter 3. Modelling and Simulation

This chapter summarizes the methods and simulations details used in this thesis. It includes

3.1 Modelling of microemulsion and ice/graphene-platelets Systems

Generally, we need to choose a suitable molecule structure for these systems, then apply force field parameters for the interactions considered in the simulations. Herein, the molecular dynamics simulations in this thesis are obtained by Large-scale Atomic/Molecular Massively Parallel Simulator (LAMMPS) package[133] and GROMACS software package[134].

3.1.1 Modeling for self-emulsifying microemulsion system

In order to realize meaningful microemulsion droplet size for mechanical tests in MD simulations, the transferable potentials for phase equilibria (TraPPE) united-atom parameters[135] were adopted for modeling oil and surfactant molecules, combined with the coarse-grained water, the mW model with many-body force field[136], to build simulation systems[137]. Briefly, the TraPPE united-atom parameters treated non-polar groups, such as the CH₂ group, as one combined atom in the system. The mW water model also considered one water molecule as one combined atom and used a 3-body Stillinger-Weber potential for capturing the appropriate non-bonded interactions among different water molecules[136]. The mW Water model was found to well reproduce the thermodynamic properties of water in many studies[137-139]. Here, dodecane and hexane were modeled as the oil phase. To represent the amphiphile, the linear diblock

oligomer surfactants with a varied length of hydrophilic (labeled as L) and hydrophobic (labeled as B) parts were used by modifying the value of force-field parameters between different parts, with details given in Figure 3.1, following the similar way with a minimalist model[140]. The bonded potentials, including carbon-carbon single bond, angles, and dihedrals, for the linear oil and surfactant molecules, were borrowed from TraPPE parameters for alkanes[139]. The Lennard-Jones potential (eq (3.1)) was applied between oil, surfactant and mW water atoms, as details listed in Table 3.1, similar to the previous studies[135, 141-144]. All the nonbonded interactions were truncated at 9 Å. One can see the energy depth, ϵ of U_{ij} for water atoms (directly borrowed from the mW water model) was two orders of magnitude higher than that for hydrophobic oil atoms (CH₂, directly borrowed from TraPPE parameters[135]), which enabled phase separation between the two. It should be noted that the purpose of the atomic parameters used was for predicting the qualitative microemulsion droplet rupture mechanics rather than the quantitative value of any specific property.

$$E = 4\epsilon\left[\left(\frac{\sigma}{r}\right)^{12} - \left(\frac{\sigma}{r}\right)^6\right] \quad (3.1)$$

Four systems were built containing surfactants with different length of hydrophobic and hydrophilic patches (termed L2B4, L2B10, and L4B8) and oil type, as shown in Figure 3.1 and Table 3.2. These systems contained the same amount of water (6144), oil (3072) and surfactant (1024) molecules, aiming to form water-in-oil microemulsions. The oil, water, and surfactants were initially distributed orderly in the periodic simulation boxes (209.097 Å × 209.097 Å × 209.097 Å). In addition, a large multiphase system consisting of water molecules (32928), L2B10 surfactant molecules (5488) and dodecane oil molecules (16464) was constructed. For comparison, we also built up an oil-in-water microemulsion system consisting of water molecules (47928), L2B10 surfactant molecules (5488) and dodecane oil molecules (16464). All systems formed stable water-in-oil or oil-in-water microemulsions, which demonstrated the validity of the molecular model and the applied potential.

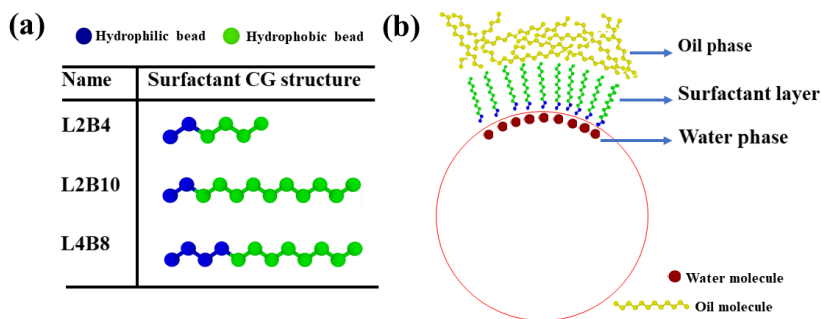


Figure 3.1 Atomistic models. (a) Janus oligomeric surfactants and their hydrophilic and hydrophobic patches. (b) Schematic of a microemulsion droplet, with a red circle representing the droplet shape. Representative water, surfactant and oil molecules and their locations at the interface of a stable droplet are depicted.

Table 3.1 The parameters in LJ potential between different atoms.

	ϵ (kcal/mol)	σ (Å)
H₂O: H₂O	SW[136]	SW[136]
H₂O: L	0.602	3.558
H₂O: B	0.119	3.558
H₂O: Oil-CH₂	0.119	3.558
L: L	0.602	3.558
L: B	0.091	3.95
L: Oil-CH₂	0.091	3.95
B: B	0.091	3.95
B: Oil-CH₂	0.091	3.95
Oil-CH₂: Oil-CH₂	0.091	3.95

Table 3.2 Four systems with different surfactants and oil molecules. The surfactants were named by the number of hydrophilic and hydrophobic patches, as depicted in Figure 3.1.

System	Surfactant	Oil
A	L2B4	Hexane
B	L2B4	Dodecane
C	L2B10	Dodecane
D	L4B8	Dodecane

3.1.2 Modeling for ice/materials system

The global model is the oriented graphene platelets coated by an ice layer, as Figure 3.2 (e) shows. Each graphene platelet has a uniform morphology and size (a single graphene layer, and its area is $\sim 2.3 \times 2.3 \text{ nm}^2$, as shown in Figure 3.2 (a), which is placed on XZ plane, in the arrangement of squama-like shape, as shown in Figure 3.2 (b-d). There is some overlapping between the adjacent graphene platelets. The graphene platelets follow a tilting orientation along with the X - and Z -axis direction. Such kind of structure can perform perfectly how the fish-scale-like surface is torn from the ice layer against the atomistic interactions. Totally, two ways to fix the carbon atoms were selected to produce the behavior of graphene platelets, namely sequential mode, and concurrent mode. In sequential mode, only there anchor carbon atoms are fixed, and on the same XZ plane area ($10.4 \times 10.4 \text{ nm}^2$), a various number of the graphene platelets (4×4 , 5×5 , 8×8) were spread homogenously, which specifically combined with ice atoms into three systems, labeled as “4”, “5” and “8”, as Figure 3.2 (b-d) shows. In concurrent mode, all of the carbon atoms are fixed, and others are completely same with the ones in sequential mode, labeled as “C4”, “C5” and “C8”. So, three models with different graphene platelet density are built up to perform the difference between them. Herein, hexagonal ice is chosen for this work. To obey the practical condition, the ice with a thickness of about $\sim 2 \text{ nm}$ is set as a periodic structure in X - and Z -boundaries, and its area is the same size with the simulation box area in XZ plane area. And its basal face is set as (0 0 0 1). At the beginning of the simulation, the ice has no overlapping with graphene platelets, which enables a fast adhesion process of ice and prepare an equilibrium system for the following pulling and shearing measurements. Every model has both concurrent and sequential mode to fix the graphene platelets. for

the sequential way, three carbon atoms at the bottom corner of each graphene platelet are fixed on the XZ plane. For the concurrent way, every carbon atom of the graphene platelets is fixed.

The detailed simulation parameters used in this work are directed borrowed from the previous studies of de-icing[145, 146]. The tip4p/ice[147] was chosen to model the ice, and OPLS force-field[148] was used for the graphene platelets parameters. Table 3.3 gives the parameters of the graphene platelets. And both the carbon and hydrogen atoms in the graphene platelets are electrically neutral. The interaction between the graphene platelets and ice is performed by van der Waals forces. A cutoff distance of 1.0 nm is employed for the non-bond interaction.

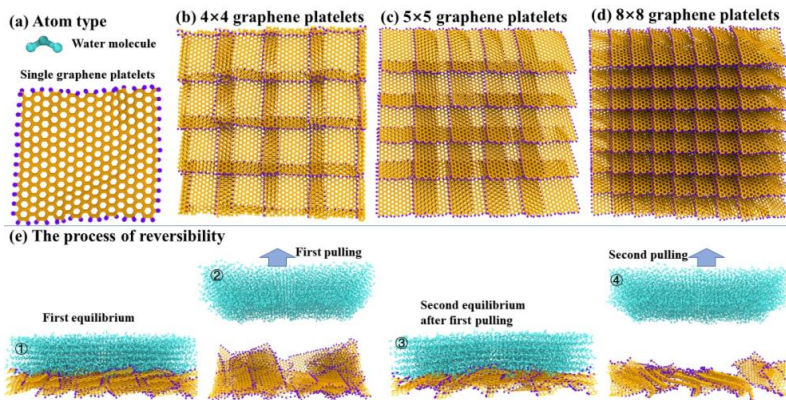


Figure 3.2 (a) the molecule structure used in the model; (b-d) the graphene platelets substrate of three systems; (e) the scheme of the process of pulling and re-pulling to prove the reversibility of the function of the graphene platelets.

Table 3.3 The simulation parameters value of van der Waals radius (σ) and energy well depth (ϵ) for the carbon (C) and hydrogen (H) atoms in the graphene platelets.

Parameter	C	H
σ (nm)	0.355	0.242
ϵ (KJ/mol/nm ²)	0.293	0.126

3.2 Simulation Details

3.2.1 Simulation details of microemulsion system

For this system, all the MD simulations were performed by using the LAMMPS package[133]. Energy minimization was first carried out with each initial system, employing the steepest descent algorithm. Each system was then equilibrated under the NVT ensemble for 50 ns with a temperature of 400 K by the Nose-Hoover method with a coupling constant of 1 ps with 10 fs time step[149]. The purpose of this high-temperature equilibration was to fully mix the oil, water and surfactant molecules in the systems. Subsequently, the systems run for another 50 ns under the NpT ensemble with a temperature of 300 K. The Parrinello-Rahman barostat was used to keep the system pressure to be 1 bar, with a coupling constant of 1 ps[150]. One stable microemulsion droplet then formed in each system, which was then subjected to mechanical testing and rupturing. The simulations before reaching the equilibrium state were run with a constant timestep 10 fs, and during the mechanical deformation and rupture with a constant timestep of 1fs.

To probe the nanoscale de-emulsification mechanics of microemulsion droplets, counter pulling forces were applied onto the water core and the surfactant shell of each microemulsion droplets, in the same manner as former studies[146, 151]. Briefly, harmonic springs were linked to the center-of-mass of the water core and the surfactant shell, and then displaced at a constant speed. The counter pulling forces were generated and applied onto the droplet owing to the extension of the harmonic springs. In all the droplet rupturing tests, the springs had the same force constant $400 \text{ kcal/mol/\AA}^2$ and moving speed 5 nm/ns. Each microemulsion droplet was ruptured at different temperatures in the range of 280~360 K. All simulations end when the core of each microemulsion droplet was separated from the surfactant shell. The rupture work was calculated by integral of pull force on displacement between the water core and the surfactant shell. In another continuing work, we build up a larger system and try to analyse the diameter of all microemulsion droplets in the simulation box. Firstly, we have hidden the oil and surfactant molecules, to make every water drop visible. Then with neighbouring distance of 3.2 \AA , every water drop was captured by labelled with

different colours, detailly as Figure 3.3 shows. For a simple calculation, each water cluster was approximately seen as a sphere. By counting the number of water molecules in each water clusters, the diameter and total surface area of each microemulsion droplets were carried out, according to the equation (3.2) and (3.3).

$$D = \sqrt[3]{\frac{29.9 \cdot N_W \cdot 6}{\pi}} \quad (3.2)$$

$$A = \pi D^2 \quad (3.3)$$

Finally, we can get the diameter distribution of the microemulsion system in every trajectory. Due to the temperature's effect on the microemulsion droplets' size, the temperature range of 280 K- 400 K was chosen to study the thermal influence on the microemulsion droplets' behaviour. In addition, a small microemulsion system containing only two droplets was established to explore more details about the mechanism of droplets' variations in the microemulsion.

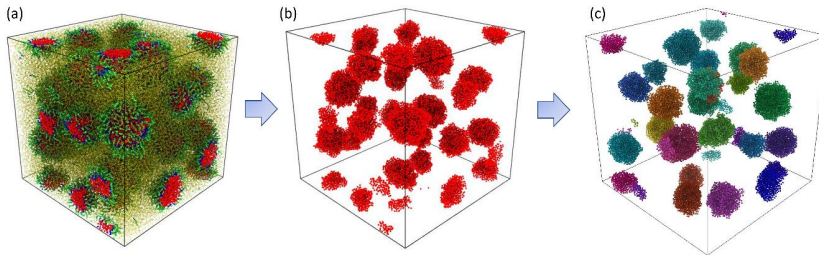


Figure 3.3 the method to calculate the number of every water cluster was shown here. (a) the general view of the whole simulation box. (b) the oil molecules and surfactant molecules were hidden. (c) different water clusters were captured and labeled with different colors. And the number of water molecules in every water cluster were recorded for the following calculation.

3.2.2 Simulation details of ice/graphene-platelets system

For this work, all MD simulations work were performed by the package GROMACS 5.0.7.[134] all simulation boxes are periodic boundaries conditions. But, on the Y -axis, the length of simulation boxes is more than 2 times longer than the length of simulated matters in the Y -axis direction, due to show non-periodic boundary condition influence

in the Y -axis. Before any running of all simulation systems, the first step is energy minimization to prepare a reasonable spatial structure for the next work. The NVT (constant number of particles, a constant volume of the simulation box, and constant temperature of 180 K) ensemble is chosen for all systems. The Nosé–Hoover coupling method with the coupling time of 0.4 ps, is used to control the temperature of the simulation systems. A 100 ns time is taken to run for an equilibrated state of all systems when the ice will contact slowly with the graphene platelets. Finally, the systems with the ice adhesion to the surface of the graphene platelets are prepared well for the next pulling and shearing force-probe of MD simulation.

To enable pulling force and shearing force to work, a virtual spring with an elastic constant of 2000 kJ/mol/nm^2 is tethered with the center of the mass (COM) of the ice. For pulling mode, the spring moves in the speed of 0.5 nm/ns along with the Y -axis direction, also vertically with the interface between the ice and graphene platelets. For shearing mode, the moving direction of the spring is along or against with Z -axis direction. During the running simulation, the particle trajectories and the pulling force with displacement between the ice and the spring will be recorded per 5 ps. By applying such forces, the ice adhering stress (σ , is calculated by pulling force divided by interface area (A) between the ice and graphene platelets, as shown in equation (3.4)), the rupture stress (σ , is the peak value of the pulling stress), and shearing stress (τ , is obtained by the shearing force divided by interface area (A) between the ice and graphene platelets, as shown in equation (3.5) will be calculated out. Likewise, the effects of various loading rates of spring on the stress are also taken into consideration for the evaluation of the mechanical properties of the systems. For the statistical significance, five independent simulations were carried out for every pulling test. The rupture work was calculated by the integral of pulling force on displacement between the ice and the graphene platelets. In order to prove the reversibility of the graphene platelets, there are designed to take a double-round pulling test, as shown in Figure 3.2 (e). This process can be divided into four parts. Firstly, an equilibrium system is prepared well from the initially designed morphology. Then, first pulling is applying into the ice layer until there is an obvious separation between the ice layer and the graphene platelets, which describes the deformation of the graphene substrate and the ice fracture on the organic surface. Following the re-equilibrium of the system, second pulling is taken to make

the ice fracture true. By analysis of the results of the two pulling tests, it can prove the reversibility of the function of the graphene substrate.

$$\sigma = \frac{F_{Pulling}}{A} \quad (3.4)$$

$$\tau = \frac{F_{shearing}}{A} \quad (3.5)$$

Chapter 4. Main Results

4.1 Stability of the self-emulsifying microemulsion droplets

As first part of studying curved interface, we have utilized atomistic modeling and molecular dynamics simulation to scrutinize the nanoscale mechanical properties of the microemulsion and resolve the determinants of the droplet stability. The spontaneous emulsification of microemulsion droplets showed that the structure and arrangement of water and oil interface were dominated by the amphiphilic parts of the linear surfactant molecules. The effects of the chemical composition of the surfactant, the surfactant packing structure and temperature on the droplet rupturing were explored by performing a series of tensile tests. The force peak and the rupture work were obtained to evaluate the robustness of the microemulsions and identify the softening-to-strengthening transition as lowering the temperature. Compared to the previous studies [19, 152, 153], this work from the view of MD simulation investigated the morphologies of W/O microemulsion droplets and evaluated their dynamic deformation process. It is the first attempt to scrutinize the mechanical properties of a single microemulsion droplet. Although the loading manner could be different from possible shearing force a microemulsion droplet experienced in experiments, the amplitude of the rupturing force should be proportional to the mechanical stability of the microemulsion droplets. Furthermore, the findings contribute to establishing an atomistic view on microemulsion fluids and provide a general guide to design a stable

microemulsion system, such as oil recovery and production, drug delivery, materials fabrication, chemical sensors, and other related fields. [133, 154]

4.2 Droplets size distribution of the microemulsion system

Continuing with above study, this work explored deeply the particle size distribution of a W/O microemulsion system and illuminated detailly the mechanism about how the microemulsion droplets' configuration and size varied during the spontaneous process of microemulsion emulsifying, by a series of molecular dynamics simulations. A coarse-grained model modified by a hybrid force field potential was built up to perform the polydisperse liquid system (water, dodecane oil, and Janus oligomer surfactant). Beginning from a homodisperse mixture of water, oil, and surfactant, there formed fast many single core-shell droplets consisted of a water core coated by some hydrophilic head groups of surfactants, and hydrophobic shell comprised of tail groups of surfactants. Due to the instability of small microemulsion droplets, the water molecules on the surface of water drop trend to detach from their host droplets, and then redeposit into the large microemulsion droplets. At the time of 1.8 ns, it is found that there is approximately a Gaussian-like particle size distribution in the microemulsion system including 182 droplets, and the size range of the microemulsion droplets is from 4.0 nm to 8.0 nm. Following the mechanism similar to Ostwald ripening, directly aggregating of two microemulsion droplets and the transition of water molecules from the small microemulsion droplets to the large microemulsion droplets realizes the rapid growth of droplets and brings the system into the next level of stability. Afterward, the number and speed of water transitions between droplets decrease, only leading to a slight variation of the droplets. Finally, the droplets' size trend to be uniform in a close value, caused by the steep energy barrier occurring in an equilibrium state. Besides, we also studied the thermal effect on the average diameter of microemulsion droplets, by setting different ambient temperature. This funding is expected to approve some fundamental knowledge on understanding the mechanism of droplets' variation during microemulsion emulsifying, which can support guidelines to the designs and fabrications of nanomaterials by the assistance of microemulsion.

4.3 The dynamics happened on the ice/material interface

As a finding of flat interface, the dynamics of the interface between ice and the oriental-arranged substrate were systematically studied. The pulling with slow loading rate maintained the most of initial configuration of the substrate, which suggested that slow de-icing speed can make the substrate remain the retrievability. A series of double-round pulling tests on systems 4, 5, and 8, the rupture stress of them was observed to be distributed like an upside-down “U” shape, intending to indicate that a suitable increasing the arrangement density of the substrate can decrease the ice adhesion. Both with different pulling mode and direction, the reversibility of the structural morphologies of the oriental-arranged graphene platelets was approved. In the shearing part, an interesting difference appeared between the results of shearing along the substrate and the shearing against the substrate. Finally, the value of the shearing stress will vibrate around the ice fracture force. The graphene platelets with dense arrangement reduce the ice fracture force effectively. By this finding, suitable knitting or arrangement of the graphene platelets for anti-icing or de-icing is encouraged for other researchers to synthesize a surface or coatings for deicing and water collection. Additionally, the study of the mechanics of ice was performed to supply fundamental knowledge for reducing ice fraction.

Chapter 5. Recommendations for Further Studies

We have done some work on the interfacial dynamics, focusing on atomistic-level morphology and detailed process of interfacial behavior with molecular dynamics simulations. Furthermore, there is still much room to improve the fundamental understanding of the mechanisms.

- Except for chemical or physical activity of a molecule, the molecular length and structure is a key factor to affect molecular behavior. The molecular length and structure of oil and surfactant also play an important role in the microemulsion system. So, a series of different-length oil and surfactant molecules should be used in the microemulsion system, to investigate the effect of the morphology of oil and surfactant molecules on the properties of the microemulsion system.
- It has been studied that droplet size distribution in the preliminary stage of water-in-oil microemulsion's self-emulsifying. The final state of the microemulsion in this finding is a relatively equilibrium, not really stable. So, longer-time simulations should be archived to make sure the final state of droplets size distribution and try to make a further theoretical acknowledgment on the mechanism of stability of microemulsion system.
- It is well known that the morphology of oil & surfactant and temperature have an influence on the droplet size distribution of the microemulsion system. For a comprehensive mechanism of microemulsion droplets' control, more factors (including pressure, the kind of oil & surfactant) should be figured out how to impact the microemulsion droplets' size.

- Based on the above findings, a lot of result data can be input information for the next work by a machine learning method. It is expected to provide a systematic guideline to design and control accurately the microemulsion droplets' size for material fabrication and drug delivery.
- Starting from anti-icing or de-icing, other material or method can be seen as a new measuring substrate in the ice/material interface system by MD simulations. This further work aims to find out material for anti-icing or de-icing and predict the direction of the development of new materials.

Bibliography

1. Hunter, R. J., *Introduction to modern colloid science*. Oxford University Press Oxford: 1993; Vol. 7.
2. Everett, D. H., *Basic principles of colloid science*. Royal society of chemistry: 2007.
3. Hiemenz, P. C.; Hiemenz, P. C., *Principles of colloid and surface chemistry*. M. Dekker New York: 1986; Vol. 188.
4. Lee, L.-H., *Fundamentals of adhesion*. Springer Science & Business Media: 2013.
5. Kinloch, A., The science of adhesion. *Journal of materials science* **1980**, 15, (9), 2141-2166.
6. Johnson, K., Mechanics of adhesion. *Tribology International* **1998**, 31, (8), 413-418.
7. Bhushan, B., *Introduction to tribology*. John Wiley & Sons: 2013.
8. Stachowiak, G.; Batchelor, A. W., *Engineering tribology*. Butterworth-Heinemann: 2013.
9. Wicks Jr, Z. W., Coatings. *Encyclopedia of Polymer Science and Technology* **2002**.
10. Tracton, A. A., *Coatings technology handbook*. CRC press: 2005.
11. Kinloch, A. J., *Adhesion and adhesives: science and technology*. Springer Science & Business Media: 2012.
12. Farhadi, S.; Farzaneh, M.; Kulinich, S., Anti-icing performance of superhydrophobic surfaces. *Applied Surface Science* **2011**, 257, (14), 6264-6269.
13. Wang, N.; Xiong, D.; Deng, Y.; Shi, Y.; Wang, K., Mechanically robust superhydrophobic steel surface with anti-icing, UV-durability, and corrosion resistance properties. *ACS applied materials & interfaces* **2015**, 7, (11), 6260-6272.
14. Zhuo, Y.; Xiao, S.; Håkonsen, V.; He, J.; Zhang, Z., Anti-icing Ionogel Surfaces: Inhibiting Ice Nucleation, Growth, and Adhesion. *ACS Materials Letters* **2020**, 2, (6), 616-623.
15. Laforte, J.; Allaire, M.; Laflamme, J., State-of-the-art on power line de-icing. *Atmospheric Research* **1998**, 46, (1-2), 143-158.

16. Parent, O.; Ilinca, A., Anti-icing and de-icing techniques for wind turbines: Critical review. *Cold regions science and technology* **2011**, 65, (1), 88-96.
17. Sips, R., On the structure of a catalyst surface. *The Journal of Chemical Physics* **1948**, 16, (5), 490-495.
18. Lippens, B.; Linsen, B.; De Boer, J., Studies on pore systems in catalysts I. The adsorption of nitrogen; apparatus and calculation. *Journal of Catalysis* **1964**, 3, (1), 32-37.
19. Patole, A. S.; Patole, S. P.; Kang, H.; Yoo, J.-B.; Kim, T.-H.; Ahn, J.-H., A facile approach to the fabrication of graphene/polystyrene nanocomposite by in situ microemulsion polymerization. *Journal of Colloid and Interface Science* **2010**, 350, (2), 530-537.
20. Jang, J.; Yoon, H., Novel Fabrication of Size - Tunable Silica Nanotubes Using a Reverse - Microemulsion - Mediated Sol - Gel Method. *Advanced Materials* **2004**, 16, (9 - 10), 799-802.
21. Pouton, C. W., Formulation of self-emulsifying drug delivery systems. *Advanced drug delivery reviews* **1997**, 25, (1), 47-58.
22. Itoh, K.; Tozuka, Y.; Oguchi, T.; Yamamoto, K., Improvement of physicochemical properties of N-4472 part I formulation design by using self-microemulsifying system. *International journal of pharmaceutics* **2002**, 238, (1-2), 153-160.
23. Gursoy, R. N.; Benita, S., Self-emulsifying drug delivery systems (SEDDS) for improved oral delivery of lipophilic drugs. *Biomedicine & pharmacotherapy* **2004**, 58, (3), 173-182.
24. Goddeeris, C.; Cuppo, F.; Reynaers, H.; Bouwman, W.; Van den Mooter, G., Light scattering measurements on microemulsions: estimation of droplet sizes. *International journal of pharmaceutics* **2006**, 312, (1-2), 187-195.
25. Ma, J.; Song, X.; Luo, J.; Zhao, T.; Yu, H.; Peng, B.; Zhao, S., Molecular Dynamics Simulation Insight into Interfacial Stability and Fluidity Properties of Microemulsions. *Langmuir* **2019**, 35, (42), 13636-13645.
26. Benson, S. P.; Pleiss, J. r., Molecular dynamics simulations of self-emulsifying drug-delivery systems (SEDDS): influence of excipients on droplet nanostructure and drug localization. *Langmuir* **2014**, 30, (28), 8471-8480.

27. Ma, J.; Song, X.; Peng, B.; Zhao, T.; Luo, J.; Shi, R.; Zhao, S.; Liu, H., Multiscale molecular dynamics simulation study of polyoxyethylated alcohols self-assembly in emulsion systems. *Chemical Engineering Science* **2020**, 116252.
28. Kulinich, S.; Farzaneh, M., Ice adhesion on super-hydrophobic surfaces. *Applied Surface Science* **2009**, 255, (18), 8153-8157.
29. Makkonen, L., Ice adhesion—theory, measurements and countermeasures. *Journal of Adhesion Science and Technology* **2012**, 26, (4-5), 413-445.
30. Varanasi, K. K.; Deng, T.; Smith, J. D.; Hsu, M.; Bhate, N., Frost formation and ice adhesion on superhydrophobic surfaces. *Applied Physics Letters* **2010**, 97, (23), 234102.
31. Kale, S. N.; Deore, S. L., Emulsion micro emulsion and nano emulsion: a review. *Systematic Reviews in Pharmacy* **2017**, 8, (1), 39.
32. McClements, D. J.; Jafari, S. M., Improving emulsion formation, stability and performance using mixed emulsifiers: A review. *Advances in colloid and interface science* **2018**, 251, 55-79.
33. Leal-Calderon, F.; Schmitt, V.; Bibette, J., *Emulsion science: basic principles*. Springer Science & Business Media: 2007.
34. Anton, N.; Benoit, J. P.; Saulnier, P., Design and production of nanoparticles formulated from nano-emulsion templates - A review. *Journal of Controlled Release* **2008**, 128, (3), 185-199.
35. McClements, D. J.; Rao, J., Food-Grade Nanoemulsions: Formulation, Fabrication, Properties, Performance, Biological Fate, and Potential Toxicity. *Critical Reviews in Food Science and Nutrition* **2011**, 51, (4), 285-330.
36. Stone, A., *The theory of intermolecular forces*. oUP oxford: 2013.
37. McNaught, A. D.; Wilkinson, A., *Compendium of chemical terminology*. Blackwell Science Oxford: 1997; Vol. 1669.
38. Schneider, H. J., Ionic Interactions in Supramolecular Complexes. In Wiley Online Library: 2012; pp 35-47.
39. Biedermann, F.; Schneider, H.-J., Experimental Binding Energies in Supramolecular Complexes. *Chemical Reviews* **2016**, 116, (9), 5216-5300.
40. Grabowski, S. J., *Hydrogen bonding: new insights*. Springer: 2006; Vol. 3.

41. Li, P.; Merz Jr, K. M., Taking into account the ion-induced dipole interaction in the nonbonded model of ions. *Journal of chemical theory and computation* **2014**, 10, (1), 289-297.
42. Yoder, C. H., Teaching ion-ion, ion-dipole, and dipole-dipole interactions. *Journal of Chemical Education* **1977**, 54, (7), 402.
43. Tschumper, G. S., 2 Reliable Electronic Structure Computations for Weak Noncovalent Interactions in Clusters. *Reviews in Computational Chemistry* **2009**, 26, 39.
44. Mahan, G. D., *Quantum mechanics in a nutshell*. Princeton University Press: 2008.
45. French, R. H., Origins and applications of London dispersion forces and Hamaker constants in ceramics. *Journal of the American Ceramic Society* **2000**, 83, (9), 2117-2146.
46. Kristyán, S.; Pulay, P., Can (semi) local density functional theory account for the London dispersion forces? *Chemical physics letters* **1994**, 229, (3), 175-180.
47. Green, J.-B. D. V.; Novoradovsky, A.; Lee, G. U., Method for measuring intramolecular forces by atomic force. In Google Patents: 1999.
48. Wüster, S., Quantum zeno suppression of intramolecular forces. *Physical review letters* **2017**, 119, (1), 013001.
49. Scheiner, S., *Hydrogen bonding: a theoretical perspective*. Oxford University Press on Demand: 1997.
50. Jeffrey, G. A.; Jeffrey, G. A., *An introduction to hydrogen bonding*. Oxford university press New York: 1997; Vol. 12.
51. Pihko, P. M., *Hydrogen bonding in organic synthesis*. John Wiley & Sons: 2009.
52. Jeffrey, G. A.; Saenger, W., *Hydrogen bonding in biological structures*. Springer Science & Business Media: 2012.
53. Sabin, J. R., Hydrogen bonds involving sulfur. I. Hydrogen sulfide dimer. *Journal of the American Chemical Society* **1971**, 93, (15), 3613-3620.
54. Panigrahi, S. K.; Desiraju, G. R., Strong and weak hydrogen bonds in the protein–ligand interface. *Proteins: Structure, Function, and Bioinformatics* **2007**, 67, (1), 128-141.

55. Kampschulte, L.; Griessl, S.; Heckl, W. M.; Lackinger, M., Mediated Coadsorption at the Liquid– Solid Interface: Stabilization through Hydrogen Bonds. *The Journal of Physical Chemistry B* **2005**, 109, (29), 14074-14078.
56. Kilpatrick, P. K., Water-in-crude oil emulsion stabilization: review and unanswered questions. *Energy & Fuels* **2012**, 26, (7), 4017-4026.
57. Nič, M.; Jiráť, J.; Košata, B.; Jenkins, A.; McNaught, A., IUPAC compendium of chemical terminology. *IUPAC, Research Triangle Park, NC* **2009**.
58. Yang, H.; Zhang, H.; Peng, J.; Zhang, Y.; Du, G.; Fang, Y., Smart magnetic ionic liquid-based Pickering emulsions stabilized by amphiphilic Fe₃O₄ nanoparticles: Highly efficient extraction systems for water purification. *Journal of colloid and interface science* **2017**, 485, 213-222.
59. Landragin, A.; Courtois, J.-Y.; Labeyrie, G.; Vansteenkiste, N.; Westbrook, C.; Aspect, A., Measurement of the van der Waals force in an atomic mirror. *Physical review letters* **1996**, 77, (8), 1464.
60. Andersson, Y.; Hult, E.; Rydberg, H.; Apell, P.; Lundqvist, B. I.; Langreth, D. C., Van der Waals interactions in density functional theory. In *Electronic Density Functional Theory*, Springer: 1998; pp 243-260.
61. Schneider, H.-J. r., Dispersive interactions in solution complexes. *Accounts of chemical research* **2015**, 48, (7), 1815-1822.
62. Marina, P. F.; Cheng, C.; Sedev, R.; Stocco, A.; Binks, B. P.; Wang, D., Van der Waals Emulsions: Emulsions Stabilized by Surface - Inactive, Hydrophilic Particles via van der Waals Attraction. *Angewandte Chemie* **2018**, 130, (30), 9654-9658.
63. He, Y.; Zhang, X.; Hooton, R.; Zhang, X., Effects of interface roughness and interface adhesion on new-to-old concrete bonding. *Construction and Building Materials* **2017**, 151, 582-590.
64. Canselier, J.; Delmas, H.; Wilhelm, A.; Abismail, B., Ultrasound emulsification—an overview. *Journal of dispersion science and technology* **2002**, 23, (1-3), 333-349.
65. Kokal, S. L., Crude oil emulsions: A state-of-the-art review. *SPE Production & facilities* **2005**, 20, (01), 5-13.
66. Barnes, H. A., Rheology of emulsions—a review. *Colloids and Surfaces A: Physicochemical and Engineering Aspects* **1994**, 91, 89-95.

67. Kumar, P.; Mittal, K. L., *Handbook of microemulsion science and technology*. CRC press: 1999.
68. Mason, T. G.; Wilking, J. N.; Meleson, K.; Chang, C. B.; Graves, S. M., Nanoemulsions: formation, structure, and physical properties. *Journal of Physics: condensed matter* **2006**, 18, (41), R635.
69. Akbari, S.; Nour, A. H., Emulsion types, stability mechanisms and rheology: A review. *International Journal of Innovative Research and Scientific Studies* **2018**, 1, (1), 14-21.
70. McClements, D. J., Nanoemulsions versus microemulsions: terminology, differences, and similarities. *Soft matter* **2012**, 8, (6), 1719-1729.
71. Shakeel, F.; Ramadan, W.; Faisal, M. S.; Rizwan, M.; Faiyazuddin, M.; Mustafa, G.; Shafiq, S., Transdermal and topical delivery of anti-inflammatory agents using nanoemulsion/microemulsion: an updated review. *Current nanoscience* **2010**, 6, (2), 184-198.
72. Pouton, C. W., Lipid formulations for oral administration of drugs: non-emulsifying, self-emulsifying and 'self-microemulsifying' drug delivery systems. *European journal of pharmaceutical sciences* **2000**, 11, S93-S98.
73. Na, Y.-G.; Byeon, J.-J.; Wang, M.; Huh, H. W.; Son, G.-H.; Jeon, S.-H.; Bang, K.-H.; Kim, S.-J.; Lee, H.-J.; Lee, H.-K., Strategic approach to developing a self-microemulsifying drug delivery system to enhance antiplatelet activity and bioavailability of ticagrelor. *International journal of nanomedicine* **2019**, 14, 1193.
74. Lam, R. S.; Nickerson, M. T., Food proteins: a review on their emulsifying properties using a structure–function approach. *Food chemistry* **2013**, 141, (2), 975-984.
75. Lombardo, D.; Kiselev, M. A.; Magazù, S.; Calandra, P., Amphiphiles self-assembly: basic concepts and future perspectives of supramolecular approaches. *Advances in Condensed Matter Physics* **2015**, 2015.
76. Li, Q.; Guo, Z., Fundamentals of icing and common strategies for designing biomimetic anti-icing surfaces. *Journal of Materials Chemistry A* **2018**, 6, (28), 13549-13581.
77. Zaritzky, N., Physical–chemical principles in freezing. *Handbook of frozen food processing and packaging* **2011**, 2.

78. Lo, C.-W.; Sahoo, V.; Lu, M.-C., Control of ice formation. *ACS nano* **2017**, 11, (3), 2665-2674.
79. Volat, C.; Farzaneh, M.; Leblond, A. In *De-icing/anti-icing techniques for power lines: current methods and future direction*, Proceedings of the 11th International Workshop on Atmospheric Icing of Structures, Montreal, Canada, 2005; 2005.
80. Farzaneh, M., *Atmospheric icing of power networks*. Springer Science & Business Media: 2008.
81. Villalpando, F.; Reggio, M.; Ilinca, A., Prediction of ice accretion and anti-icing heating power on wind turbine blades using standard commercial software. *Energy* **2016**, 114, 1041-1052.
82. Kreutz, M.; Ait-Alla, A.; Varasteh, K.; Oelker, S.; Greulich, A.; Freitag, M.; Thoben, K.-D., Machine learning-based icing prediction on wind turbines. *Procedia CIRP* **2019**, 81, 423-428.
83. Thomas, S. K.; Cassoni, R. P.; MacArthur, C. D., Aircraft anti-icing and de-icing techniques and modeling. *Journal of aircraft* **1996**, 33, (5), 841-854.
84. Pellissier, M.; Habashi, W.; Pueyo, A., Optimization via FENSAP-ICE of aircraft hot-air anti-icing systems. *Journal of Aircraft* **2011**, 48, (1), 265-276.
85. Su, Q.; Chang, S.; Zhao, Y.; Zheng, H.; Dang, C., A review of loop heat pipes for aircraft anti-icing applications. *Applied Thermal Engineering* **2018**, 130, 528-540.
86. Lv, J.; Song, Y.; Jiang, L.; Wang, J., Bio-inspired strategies for anti-icing. *ACS nano* **2014**, 8, (4), 3152-3169.
87. Farzaneh, M.; Volat, C.; Leblond, A., Anti-icing and de-icing techniques for overhead lines. In *Atmospheric icing of power networks*, Springer: 2008; pp 229-268.
88. Wang, Y.; Xu, Y.; Huang, Q., Progress on ultrasonic guided waves de-icing techniques in improving aviation energy efficiency. *Renewable and Sustainable Energy Reviews* **2017**, 79, 638-645.
89. Xie, Y.; Zhang, J.; Zhou, T., Large-area mechanical interlocking via nanopores: Ultra-high-strength direct bonding of polymer and metal materials. *Applied Surface Science* **2019**, 492, 558-570.

90. Picard, L.; Phalip, P.; Fleury, E.; Ganachaud, F., Chemical adhesion of silicone elastomers on primed metal surfaces: A comprehensive survey of open and patent literatures. *Progress in Organic Coatings* **2015**, 80, 120-141.
91. Speranza, G.; Gottardi, G.; Pederzolli, C.; Lunelli, L.; Canteri, R.; Pasquardini, L.; Carli, E.; Lui, A.; Maniglio, D.; Brugnara, M., Role of chemical interactions in bacterial adhesion to polymer surfaces. *Biomaterials* **2004**, 25, (11), 2029-2037.
92. Lee, L.-H., *Adhesive bonding*. Springer Science & Business Media: 2013.
93. Choi, T.; Kim, S. J.; Park, S.; Hwang, T. Y.; Jeon, Y.; Hong, B. H., Roll-to-roll continuous patterning and transfer of graphene via dispersive adhesion. *Nanoscale* **2015**, 7, (16), 7138-7142.
94. Wiesing, M.; De Los Arcos, T.; Gebhard, M.; Devi, A.; Grundmeier, G., Analysis of dispersive interactions at polymer/TiAlN interfaces by means of dynamic force spectroscopy. *Physical Chemistry Chemical Physics* **2018**, 20, (1), 180-190.
95. Guo, J.; Bamber, T.; Chamberlain, M.; Justham, L.; Jackson, M., Optimization and experimental verification of coplanar interdigital electroadhesives. *Journal of Physics D: Applied Physics* **2016**, 49, (41), 415304.
96. Kendall, K., Adhesion: molecules and mechanics. *Science* **1994**, 263, (5154), 1720-1725.
97. Newby, B.-m. Z.; Chaudhury, M. K.; Brown, H. R., Macroscopic evidence of the effect of interfacial slippage on adhesion. *Science* **1995**, 269, (5229), 1407-1409.
98. Hanaor, D. A.; Gan, Y.; Einav, I., Static friction at fractal interfaces. *Tribology International* **2016**, 93, 229-238.
99. Majumder, A.; Ghatak, A.; Sharma, A., Microfluidic adhesion induced by subsurface microstructures. *Science* **2007**, 318, (5848), 258-261.
100. Maeda, N.; Chen, N.; Tirrell, M.; Israelachvili, J. N., Adhesion and friction mechanisms of polymer-on-polymer surfaces. *Science* **2002**, 297, (5580), 379-382.
101. Tadmor, R.; Bahadur, P.; Leh, A.; N'guessan, H. E.; Jaini, R.; Dang, L., Measurement of lateral adhesion forces at the interface between a liquid drop and a substrate. *Physical review letters* **2009**, 103, (26), 266101.

102. Tadmor, R.; Das, R.; Gulec, S.; Liu, J.; E. N'guessan, H.; Shah, M.; S. Wasnik, P.; Yadav, S. B., Solid–liquid work of adhesion. *Langmuir* **2017**, 33, (15), 3594-3600.
103. Donohue, M. D. *Supercritical Fluid Spray Application Process for Adhesives and Primers*; JOHNS HOPKINS UNIV LAUREL MD: 2003.
104. Qin, S.; McTeer, A., Wafer dependence of Johnsen–Rahbek type electrostatic chuck for semiconductor processes. *Journal of Applied Physics* **2007**, 102, (6), 064901.
105. Shim, G. I.; Sugai, H., Dechuck operation of Coulomb type and Johnsen-Rahbek type of electrostatic chuck used in plasma processing. *Plasma and Fusion Research* **2008**, 3, 051-051.
106. Zhu, B.; Zhang, L.; Cheng, B.; Yu, J., First-principle calculation study of tri-s-triazine-based g-C₃N₄: a review. *Applied Catalysis B: Environmental* **2018**, 224, 983-999.
107. Jin, Y.; Liu, M.; Zhang, C.; Leygraf, C.; Wen, L.; Pan, J., First-principle calculation of Volta potential of intermetallic particles in aluminum alloys and practical implications. *Journal of The Electrochemical Society* **2017**, 164, (9), C465.
108. Mooney, C. Z., *Monte carlo simulation*. Sage publications: 1997; Vol. 116.
109. Moglestue, C., *Monte Carlo simulation of semiconductor devices*. Springer Science & Business Media: 2013.
110. Engel, E.; Dreizler, R. M., *Density functional theory*. Springer: 2013.
111. Sholl, D.; Steckel, J. A., *Density functional theory: a practical introduction*. John Wiley & Sons: 2011.
112. Hansson, T.; Oostenbrink, C.; van Gunsteren, W., Molecular dynamics simulations. *Current opinion in structural biology* **2002**, 12, (2), 190-196.
113. Hospital, A.; Goñi, J. R.; Orozco, M.; Gelpí, J. L., Molecular dynamics simulations: advances and applications. *Advances and applications in bioinformatics and chemistry: AABC* **2015**, 8, 37.
114. Shelley, J. C.; Shelley, M. Y., Computer simulation of surfactant solutions. *Current opinion in colloid & interface science* **2000**, 5, (1-2), 101-110.

115. Liu, Y.-P.; Kim, K.; Berne, B.; Friesner, R. A.; Rick, S. W., Constructing ab initio force fields for molecular dynamics simulations. *The Journal of chemical physics* **1998**, 108, (12), 4739-4755.
116. Jiménez-Ángeles, F.; Khoshnood, A.; Firoozabadi, A., Molecular Dynamics Simulation of the Adsorption and Aggregation of Ionic Surfactants at Liquid–Solid Interfaces. *The Journal of Physical Chemistry C* **2017**, 121, (46), 25908-25920.
117. Illa-Tuset, S.; Malaspina, D. C.; Faraudo, J., Coarse-grained molecular dynamics simulation of the interface behaviour and self-assembly of CTAB cationic surfactants. *Physical Chemistry Chemical Physics* **2018**, 20, (41), 26422-26430.
118. Wu, H.; Xu, J.; He, X.; Zhao, Y.; Wen, H., Mesoscopic simulation of self-assembly in surfactant oligomers by dissipative particle dynamics. *Colloids and Surfaces A: Physicochemical and Engineering Aspects* **2006**, 290, (1-3), 239-246.
119. Deng, X.; Yang, Y.; Ma, Y.; Sun, X.; Zhou, G.; Wu, H.; Lu, G., Self-assembled structure of sulfonic gemini surfactant solution. *AIP Advances* **2018**, 8, (7), 075003.
120. Arai, N.; Yasuoka, K.; Zeng, X. C., Self-assembly of Janus oligomers into onion-like vesicles with layer-by-layer water discharging capability: A minimalist model. *ACS nano* **2016**, 10, (8), 8026-8037.
121. Li, J.; Wang, J.; Yao, Q.; Yan, Y.; Li, Z.; Zhang, J., Manipulating Hybrid Nanostructures by the Cooperative Assembly of Amphiphilic Oligomers and Triblock Janus Nanoparticles. *The journal of physical chemistry letters* **2020**, 11, (9), 3369-3375.
122. Liu, J.; Zhu, C.; Liu, K.; Jiang, Y.; Song, Y.; Francisco, J. S.; Zeng, X. C.; Wang, J., Distinct ice patterns on solid surfaces with various wettabilities. *Proceedings of the National Academy of Sciences* **2017**, 114, (43), 11285-11290.
123. Sosso, G. C.; Tribello, G. A.; Zen, A.; Pedevilla, P.; Michaelides, A., Ice formation on kaolinite: Insights from molecular dynamics simulations. *The Journal of Chemical Physics* **2016**, 145, (21), 211927.
124. Pedevilla, P.; Fitzner, M.; Sosso, G. C.; Michaelides, A., Heterogeneous seeded molecular dynamics as a tool to probe the ice nucleating ability of crystalline surfaces. *The Journal of chemical physics* **2018**, 149, (7), 072327.

125. Geng, H.; Liu, X.; Shi, G.; Bai, G.; Ma, J.; Chen, J.; Wu, Z.; Song, Y.; Fang, H.; Wang, J., Graphene oxide restricts growth and recrystallization of ice crystals. *Angewandte Chemie* **2017**, 129, (4), 1017-1021.
126. Guo, P.; Zheng, Y.; Wen, M.; Song, C.; Lin, Y.; Jiang, L., Icephobic/anti - icing properties of micro/nanostructured surfaces. *Advanced Materials* **2012**, 24, (19), 2642-2648.
127. Bäckström, M.; Karlsson, S.; Bäckman, L.; Folkesson, L.; Lind, B., Mobilisation of heavy metals by deicing salts in a roadside environment. *Water research* **2004**, 38, (3), 720-732.
128. Hartley, R. A.; Wood, D. H., Deicing solution. In Google Patents: 2001.
129. Wang, K.; Nelsen, D. E.; Nixon, W. A., Damaging effects of deicing chemicals on concrete materials. *Cement and concrete composites* **2006**, 28, (2), 173-188.
130. Golovin, K.; Dhyani, A.; Thouless, M.; Tuteja, A., Low-interfacial toughness materials for effective large-scale deicing. *Science* **2019**, 364, (6438), 371-375.
131. Zhao, H.; Wu, Z.; Wang, S.; Zheng, J.; Che, G., Concrete pavement deicing with carbon fiber heating wires. *Cold Regions Science and Technology* **2011**, 65, (3), 413-420.
132. Xiao, S.; He, J.; Zhang, Z., Nanoscale deicing by molecular dynamics simulation. *Nanoscale* **2016**, 8, (30), 14625-14632.
133. Plimpton, S.; Hendrickson, B., Parallel molecular dynamics algorithms for simulation of molecular systems. In ACS Publications: 1995.
134. Abraham, M. J.; Murtola, T.; Schulz, R.; Páll, S.; Smith, J. C.; Hess, B.; Lindahl, E., GROMACS: High performance molecular simulations through multi-level parallelism from laptops to supercomputers. *SoftwareX* **2015**, 1-2, 19-25.
135. Martin, M. G.; Siepmann, J. I., Transferable potentials for phase equilibria. 1. United-atom description of n-alkanes. *Journal of Physical Chemistry B* **1998**, 102, (14), 2569-2577.
136. Stillinger, F. H.; Weber, T. A., Computer simulation of local order in condensed phases of silicon. *Physical review B* **1985**, 31, (8), 5262-5271.
137. Molinero, V.; Moore, E. B., Water modeled as an intermediate element between carbon and silicon. *The Journal of Physical Chemistry B* **2008**, 113, (13), 4008-4016.

138. Vega, C.; Abascal, J. L., Simulating water with rigid non-polarizable models: a general perspective. *Physical Chemistry Chemical Physics* **2011**, 13, (44), 19663-88.
139. Noid, W. G., Perspective: Coarse-grained models for biomolecular systems. *The Journal of chemical physics* **2013**, 139, (9), 090901.
140. Arai, N.; Yasuoka, K.; Zeng, X. C., Self-Assembly of Janus Oligomers into Onion-like Vesicles with Layer-by-Layer Water Discharging Capability: A Minimalist Model. *ACS Nano* **2016**, 10, (8), 8026-37.
141. Jacobson, L. C.; Hujo, W.; Molinero, V., Amorphous precursors in the nucleation of clathrate hydrates. *Journal of the American Chemical Society* **2010**, 132, (33), 11806-11.
142. Raubenolt, B.; Gyawali, G.; Tang, W.; Wong, K. S.; Rick, S. W., Coarse-Grained Simulations of Aqueous Thermoresponsive Polyethers. *Polymers (Basel)* **2018**, 10, (5), 475.
143. Song, B.; Molinero, V., Thermodynamic and structural signatures of water-driven methane-methane attraction in coarse-grained mW water. *The Journal of chemical physics* **2013**, 139, (5), 054511.
144. Gyawali, G.; Sternfield, S.; Kumar, R.; Rick, S. W., Coarse-Grained Models of Aqueous and Pure Liquid Alkanes. *Journal of Chemical Theory and Computation* **2017**, 13, (8), 3846-3853.
145. Xiao, S.; He, J.; Zhang, Z., Nanoscale deicing by molecular dynamics simulation. *Nanoscale* **2016**, 8, (30), 14625-32.
146. Xiao, S.; Skallerud, B. H.; Wang, F.; Zhang, Z.; He, J., Enabling sequential rupture for lowering atomistic ice adhesion. *Nanoscale* **2019**, 11, (35), 16262-16269.
147. Abascal, J. L.; Sanz, E.; Garcia Fernandez, R.; Vega, C., A potential model for the study of ices and amorphous water: TIP4P/Ice. *J Chem Phys* **2005**, 122, (23), 234511.
148. Jorgensen, W. L.; Maxwell, D. S.; Tirado-Rives, J., Development and testing of the OPLS all-atom force field on conformational energetics and properties of organic liquids. *Journal of the American Chemical Society* **1996**, 118, (45), 11225-11236.

-
149. Evans, D. J.; Holian, B. L., The Nose-Hoover Thermostat. *Journal of Chemical Physics* **1985**, 83, (8), 4069-4074.
 150. Parrinello, M.; Rahman, A., Polymorphic Transitions in Single-Crystals - a New Molecular-Dynamics Method. *Journal of Applied Physics* **1981**, 52, (12), 7182-7190.
 151. Xiao, S.; Zhang, Z.; He, J., Atomistic dewetting mechanics of Wenzel and monostable Cassie-Baxter states. *Physical Chemistry Chemical Physics* **2018**, 20, (38), 24759-24767.
 152. Muzaffar, F.; Singh, U.; Chauhan, L., Review on microemulsion as futuristic drug delivery. *International Journal of Pharmacy and Pharmaceutical Sciences* **2013**, 5, (3), 39-53.
 153. Zolfaghari, R.; Fakhru'l-Razi, A.; Abdullah, L. C.; Elnashaie, S. S. E. H.; Pendashteh, A., Demulsification techniques of water-in-oil and oil-in-water emulsions in petroleum industry. *Separation and Purification Technology* **2016**, 170, 377-407.
 154. Simon, M.; Schneck, E.; Noirez, L.; Rahn, S.; Davidovich, I.; Talmon, Y.; Gradzielski, M., Effect of Polymer Architecture on the Phase Behavior and Structure of Polyelectrolyte/Microemulsion Complexes (PEMECs). *Macromolecules* **2020**, 53, (10), 4055-4067.

Appendix A Appended papers

Paper I

A.1 Paper I

Stability, Deformation and Rupture of Janus Oligomer Enabled Self-Emulsifying Water-in-Oil Microemulsion Droplet

Authors: Yuequn Fu, Senbo Xiao, Siqu Liu, Jianyang Wu, Xiao Wang, Lijie Qiao, Zhiliang Zhang and Jianying He

Physical Chemistry Chemical Physics 2020, 22 (43), 24907-24916.

Stability, deformation and rupture of Janus oligomer enabled self-emulsifying water-in-oil microemulsion droplet

Yuequn Fu,^a Senbo Xiao,^{*a} Siqi Liu,^a Jianyang Wu,^b Xiao Wang,^c Lijie Qiao,^d

Zhiliang Zhang^a and Jianying He^{*†a,d}

^aNTNU Nanomechanical Lab, Norwegian University of Science and Technology
(NTNU), Trondheim 7491, Norway

^bDepartment of Physics, Research Institute for Biomimetics and Soft Matter, Jiujiang
Research Institute and Fujian Provincial Key Laboratory for Soft Functional Materials
Research, Xiamen University, Xiamen 361005, China

^cReservoir Engineering Research Institute, Palo Alto, California 94301, United States

^dBeijing Advanced Innovation Center for Materials Genome Engineering, University
of Science and Technology Beijing, Beijing 100083, China

*Corresponding author.

E-mail addresses: senbo.xiao@ntnu.no (S. Xiao), jianying.he@ntnu.no (J. He).

†Currently on sabbatical as a visiting professor at ^dBeijing Advanced Innovation
Center for Materials Genome Engineering, University of Science and Technology
Beijing.

Abstract

Microemulsion exists widely in nature, daily life and industrial manufacturing, including petroleum production, food processing, drug delivery, new materials fabrication, sewage treatment, etc. The mechanical properties of microemulsion droplets and the correlation to their molecular structures are of vital importance to those applications. Despite researches on their physicochemical determinants, there are lots of challenges to explore the mechanical properties of microemulsion by experimental studies. Herein, atomistic modelling was utilized to study the stability, deformation, and rupture of Janus oligomer enabled water-in-oil microemulsion droplets, aiming for revealing their intrinsic relationship to the Janus oligomer based surfactants and oil structures. The self-emulsifying process from a water, oil and surfactant mixture to a single microemulsion droplet was modulated by the amphiphilicity and the structure of the surfactants. Four microemulsion systems with interfacial thickness in the range of 7.4-17.3Å were self-assembled to explore the effect of the surfactant on the droplet morphology. By applying counter forces on the water core and the surfactant shell, the mechanical stability of microemulsion droplets was probed at different ambient temperatures. A strengthening response and a softening regime before and after a temperature-dependent peak force were identified followed by the final rupture. This work demonstrates a practical strategy to precisely tune the mechanical properties of a single microemulsion droplet, which can be applied in the formation, de-emulsification, and design of microemulsion in oil recovery and production, drug delivery and many other applications.

Key Words: Self-emulsifying; microemulsion droplet; stability; deformation; rupture; molecular dynamics simulation.

1 INTRODUCTION

The microemulsion is thermodynamic-stable mixtures of multiphase system, and in many cases presents as droplets of one liquid dispersed inside the other surrounding liquid¹⁻³. Because microemulsion plays an important role in daily life and applications including wastewater treatment^{4, 5}, drug-delivery⁶, electro-kinetic chromatography^{7, 8}, enhanced oil recovery⁹, fabrication of new materials¹⁰, nanoparticle synthesis¹¹, and many others, it has been the focus of many research fields for decades.

Research on microemulsions started in 1943 when microemulsion as a scientific concept was first promoted by Hoar and Schulman¹². With limited experimental characterization methods, spontaneous formation of globular micelles with size ~ 120 Å in diameter was identified, which clearly explained how the orientated non-ionized amphipathic molecules prevented the ion-pairs of soap from the repulsion. In 1959 microemulsion was characterized by electron microscopy and demonstrated a uniformly dispersed spherical oil or water core in water or oil droplet¹³. The detailed structural and dynamic properties of the chemical ingredients of microemulsion were then investigated by Fourier transform nuclear magnetic resonance (FT-NMR), which provided a clear picture of the polydisperse nature of the complex multiphase system¹⁴⁻¹⁶. Other experimental methodologies, such as infrared and Raman spectroscopy, were also applied in studying microemulsion to gain a better understanding of nanoscale morphologies^{17, 18}. It is generally accepted nowadays in the nanotechnology era that microemulsion is a colloid system consisting of small droplets of water (or oil), which could be on the

nanometer scale, dispersed in a continuum medium of oil (or water) phase by adding surfactant and/or cosurfactant as stabilizer. The highly complicated nature of the surfactant layer on microemulsion droplets is currently attracting attention from different research fields, and continually provides new multi-disciplinary insights^{19,20}.

The most important property of the microemulsion is its thermodynamic stability^{21,22}. The surfactant and cosurfactant coating on the surface of the emulsion droplets greatly reduces the interfacial tension between the continuum phase and the interior of the droplet, minimizing the overall free energy of the microemulsion system²³. There are many factors affecting the stability of a microemulsion system, including temperature, salinity, surfactant structure, oil composition, cosolvent, and immiscible solids, and their effects are inherently intertwined^{24,25}. It is highly challenging in experiments to clarify the intricate relationship between each factor and the stability of the microemulsion system. In contrast, atomistic modeling and molecular dynamic (MD) simulations can provide resolution extending the experimental limits in investigating microemulsion. For instance, a series of MD simulations were performed to probe the properties of water/trichloroethylene (TCE) interface absorbed with sodium alkyl sulfate (SDS-type) surfactant monolayers, and further to elucidate the underlying connections between the parameters of a microemulsion system. The results revealed that the tail order of the surfactants was dependent on their interfacial coverage, while the interface thickness (in the range of 10-25 Å) was interestingly dependent on tail length rather than the surface coverage²⁶.

Comparing to the fast accumulation of synthesis and physicochemical knowledge on microemulsion, the mechanical stability of microemulsion still awaits a thorough

investigation. The mechanical stability of microemulsion is crucially important in many production and application processes²⁷⁻²⁹. For instance, microemulsion was utilized in drug delivery, where the mechanical robustness of the microemulsion droplets are critical to the transport and the release of the loaded drug³⁰. The nanomechanics of microemulsion droplets is the determinant of the de-emulsification process on oil/water separation in oil production, which prominently influences the production cost in the petroleum industry³¹. However, there are still lots of challenges for experimental methods to explore the mechanical properties of the microemulsion from the view of atomic size. Unlike other solid materials, a single microemulsion droplet is very difficult to be separated from a microemulsion solution as only investigated target, not even measuring its mechanical properties. Besides, their structure is too tiny to be captured for current experimental methods. Until now, there is no efficient means to evaluate the mechanical properties of a microemulsion droplet.

This work aims to probe the nanomechanics in rupturing microemulsion droplets and to establish the connections between nanoscale mechanical properties of surfactant coated droplets and the molecular structures of microemulsion. Following similar approaches utilizing atomistic modeling and MD simulations³²⁻³⁴, stable microemulsion droplets were constructed and subjected to rupturing forces. The effects of surfactant structure and the environmental temperature on the droplet rupturing mechanics were scrutinized, which for the first time provided theoretical fundamentals for experimental studies on microemulsion as well as design and processing in practice.

2 MODELS AND METHOD

2.1 Atomistic modeling

In order to realize meaningful microemulsion droplet size for mechanical tests in MD simulations, the transferable potentials for phase equilibria (TraPPE) united-atom parameters³⁵ were adopted for modeling oil and surfactant molecules, combined with the coarse-grained water, the mW model with many-body force field³⁶, to build simulation systems³⁷. Briefly, the TraPPE united-atom parameters treated non-polar groups, such as the CH₂ group, as one combined atom in the system. The mW water model also considered one water molecule as one combined atom and used a 3-body Stillinger-Weber potential for capturing the appropriate non-bonded interactions among different water molecules³⁶. The mW Water model was found to well reproduce the thermodynamic properties of water in many studies³⁷⁻³⁹. Here, dodecane and hexane were modeled as the oil phase. To represent the amphiphile, the linear diblock oligomer surfactants with a varied length of hydrophilic (labeled as L) and hydrophobic (labeled as B) parts were used by modifying the value of force-field parameters between different parts, with details given in Fig. 1, following the similar way with a minimalist model⁴⁰. The bonded potentials, including carbon-carbon single bond, angles, and dihedrals, for the linear oil and surfactant molecules, were borrowed from TraPPE parameters for alkanes³⁹. The Lennard-Jones potential (eq (1)) was applied between oil, surfactant and mW water atoms, as details listed in Table 1, similar to the previous studies^{35, 41-44}. All the nonbonded interactions were truncated at 9 Å. One can see the energy depth, ϵ of U_{ij} for water atoms (directly borrowed from the mW water model) was two orders of magnitude higher than that for hydrophobic oil atoms (CH₂, directly borrowed from TraPPE parameters³⁵), which enabled phase separation between the two. It should be noted that the purpose of the atomic parameters used was for predicting the qualitative microemulsion droplet rupture mechanics rather than the quantitative value of any specific property.

$$E = 4\epsilon\left[\left(\frac{\sigma}{r}\right)^{12} - \left(\frac{\sigma}{r}\right)^6\right] \quad (1)$$

Four systems were built containing surfactants with different length of hydrophobic and hydrophilic patches (termed L2B4, L2B10, and L4B8) and oil type, as shown in Fig. 1 and Table 2. Other systems consisting of different surfactants can be found in supporting information (Fig. S1). These systems contained the same amount of water (6144), oil (3072) and surfactant (1024) molecules, aiming to form water-in-oil microemulsions. The oil, water, and surfactants were initially distributed orderly in the periodic simulation boxes ($209.097 \text{ \AA} \times 209.097 \text{ \AA} \times 209.097 \text{ \AA}$), as shown in Fig. 2 (a). In addition, a large multiphase system consisting of water molecules (32928), L2B10 surfactant molecules (5488) and dodecane oil molecules (16464) was constructed, as shown in Fig. 2 (f)-(j) and Fig. S2. For comparison, we also built up an oil-in-water microemulsion system consisting of water molecules (47928), L2B10 surfactant molecules (5488) and dodecane oil molecules (16464), as shown in Fig. S2. All systems formed stable water-in-oil or oil-in-water microemulsions, which demonstrated the validity of the molecular model and the applied potential.

2.2 Molecular dynamics (MD) simulations

All the MD simulations were performed by using the LAMMPS package⁴⁵. Energy minimization was first carried out with each initial system, employing the steepest descent algorithm. Each system was then equilibrated under the NVT ensemble for 50 ns with a temperature of 400 K by the Nose-Hoover method with a coupling constant of 1 ps with 10 fs time step⁴⁶. The purpose of this high-temperature equilibration was to fully mix the oil, water and surfactant molecules in the systems. Subsequently, the systems run for another 50 ns under the NpT ensemble with a temperature of 300 K. The Parrinello-

Rahman barostat was used to keep the system pressure to be 1 bar, with a coupling constant of 1 ps⁴⁷. One stable microemulsion droplet then formed in each system, as shown in Fig. 2 (d), which was then subjected to mechanical testing and rupturing. The simulations before reaching the equilibrium state were run with a constant timestep 10 fs, and during the mechanical deformation and rupture with a constant timestep of 1fs.

To probe the nanoscale de-emulsification mechanics of microemulsion droplets, counter pulling forces were applied onto the water core and the surfactant shell of each microemulsion droplets, in the same manner as former studies^{48, 49}. Briefly, harmonic springs were linked to the center-of-mass of the water core and the surfactant shell, and then displaced at a constant speed. The counter pulling forces were generated and applied onto the droplet owing to the extension of the harmonic springs. In all the droplet rupturing tests, the springs had the same force constant 400 kcal/mol/Å² and moving speed 5 nm/ns. Each microemulsion droplet was ruptured at different temperatures in the range of 280~360 K. All simulations end when the core of each microemulsion droplet was separated from the surfactant shell. The rupture work was calculated by integral of pull force on displacement between the water core and the surfactant shell.

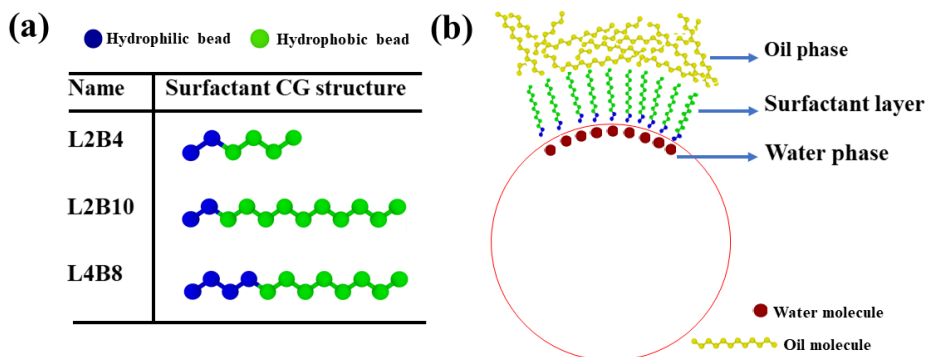


Figure 1. Atomistic models. (a) Janus oligomeric surfactants and their hydrophilic and hydrophobic patches. (b) Schematic of a microemulsion droplet, with a red circle representing the droplet shape. Representative water, surfactant and oil molecules and their locations at the interface of a stable droplet are depicted.

Table 1 The parameters in LJ potential between different atoms.

	ϵ	σ
	(kcal/mol)	(Å)
H ₂ O: H ₂ O	SW ³⁶	SW ³⁶
H ₂ O: L	0.602	3.558
H ₂ O: B	0.119	3.558
H ₂ O: Oil-CH ₂	0.119	3.558
L: L	0.602	3.558
L: B	0.091	3.95
L: Oil-CH ₂	0.091	3.95
B: B	0.091	3.95

B: Oil-CH ₂	0.091	3.95
Oil-CH ₂ : Oil- CH ₂	0.091	3.95

Table 2 Four systems with different surfactants and oil molecules. The surfactants were named by the number of hydrophilic and hydrophobic patches, as depicted in Fig. 1.

System	Surfactant	Oil
A	L2B4	Hexane
B	L2B4	Dodecane
C	L2B10	Dodecane
D	L4B8	Dodecane

3 RESULTS AND DISCUSSION

3.1 Spontaneous formation of stable microemulsion droplets

For evaluating the mechanical properties of microemulsion droplets, four stable microemulsion systems coated with surfactants were prepared with three surfactants and two oil types. Following the defined simulation process of mixing in the NVT ensemble at 400 K and equilibration in the NpT ensemble at 300 K, the final state of all the microemulsion droplets featured a spherical core of water fully coated by surfactants and surrounded by oil molecules, as the representative sequential snapshots are shown in Fig.

2(a-d) and a short video in the supplement (spontaneous-process.MP4). The representative system potential energy profile monitored in preparing the microemulsion droplet was given in Fig. 2(e). Both in the high-temperature mixing simulation and in equilibration, the system potential reached a plateau in a very short time and maintained at that state. The surfactants were packed around the water core, forming an ordered curvature with the hydrophilic patches facing the water. In order to demonstrate the formation process, a larger water-in-oil microemulsion multiphase system was also simulated, as shown in Fig. 2(f-j). The potential energy profile and the packing of surfactants at the oil/water interface agreed with the results predicted in former studies⁵⁰.

As shown in Fig. 2, the prepared microemulsion droplets featured the most frequently observed structures, namely water core structure coated by a well-defined surfactant monolayer in the continuous oil phase. The mass ratio between water and oil in the systems was 0.21. The surfactant shell had long been identified to be critically important to the properties of the microemulsion and was previously found to have an interfacial tension at a threshold of 10^{-3} mN/m⁵¹. It is known that the interfacial tension of the surfactant layer can compensate for the dispersion entropy of the microemulsion droplets, which contributes to the stability of the microemulsion system^{52, 53}. The prepared microemulsion droplets should thus be able to withstand certain pulling force and provide rupturing events for probing the nanoscale de-emulsification.

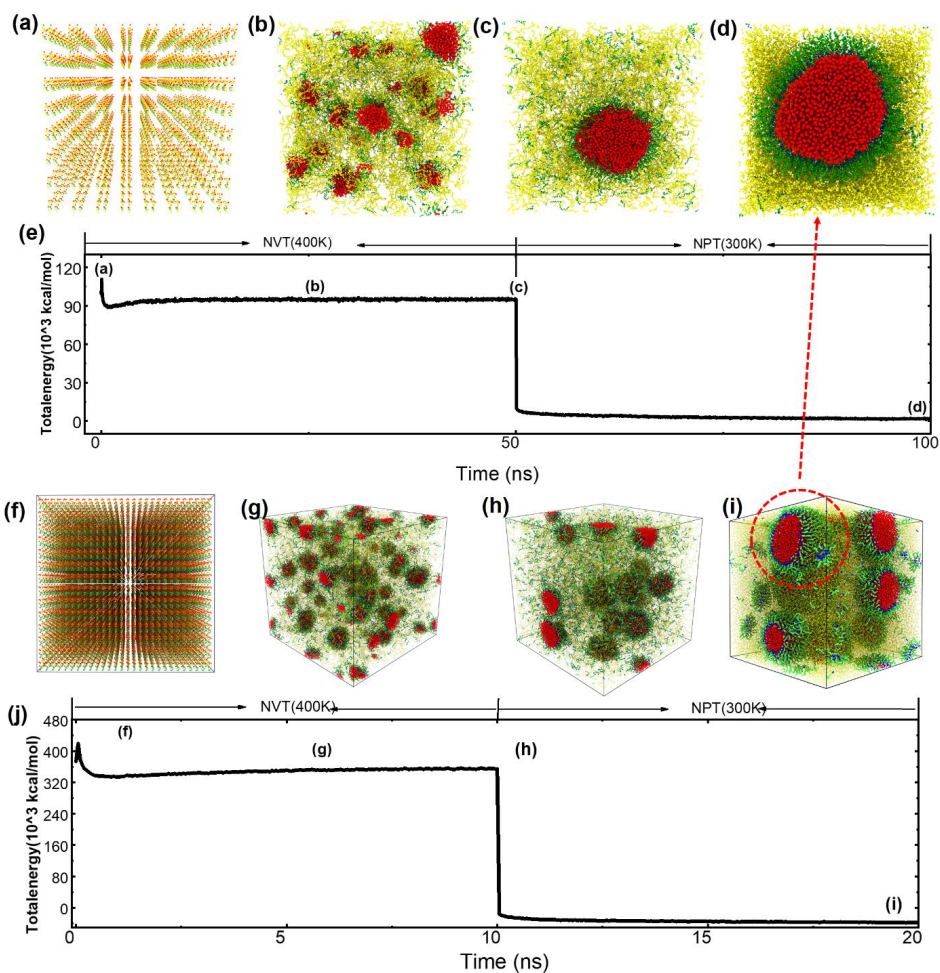


Figure 2. Spontaneous formation of microemulsion droplets, represented by system C. (a) Initial atomistic structure of the systems, with all the components in an orderly arrangement. (b) Disordered and mixing of oil, water and surfactant molecules at 400 K. (c) A complete microemulsion droplet formed at the end of high temperature mixing in the NVT ensemble; (d) The microemulsion droplet at the end of 50 ns equilibration at 300 K in the NpT ensemble. (e) Total system potential energy. (f-j) the self-emulsifying processes of a multiphase system consisting of water molecules (32928), L2B10

surfactant molecules (5488) and dodecane oil molecules (16464) and the total potential energy.

3.2 The internal structure of the microemulsion droplets

The difference in the surfactants and the oil molecules led to noticeable deviations in the internal structures of the final microemulsion droplets, as shown in Fig. 3. System A and B consisted of the same surfactant but different oil species, namely hexane and dodecane, respectively. The final structure of the two microemulsion droplets showed similar morphologies at the stable state, which suggested that the molecular sizes of hexane and dodecane did not lead to obvious differences in the microemulsion droplet. As shown in Fig. 3 (a-b) and (e-f), the shape of two microemulsion droplets fluctuated in equilibrium, with surfactant molecules randomly adsorbing to and escaping from the oil/water interface. A small fraction of the surfactant molecules could even diffuse into the oil phase as well as into the water core. The result could be attributed to the relatively weak phase preference of the L2B4 molecules (2 hydrophilic and 4 hydrophobic sites in the linear molecule). The stronger hydrophobic or hydrophilic property was needed for the surfactant molecules to firmly coat the internal core of a microemulsion droplet, which was clearly illustrated by comparing the final microemulsion droplets in system B and C, as shown in Fig. 3 (b-c) and (f-g). If the surfactant molecules contained a long hydrophobic patch, 10 hydrophobic atoms in L2B10 instead of 4 in L2B4, the surfactant molecules could not diffuse into the water core, as shown in Fig. 3(c). Thanks to the longer hydrophobic patch in the molecule, the L2B10 surfactant showed more ordered packing at the oil/water interface, and resulted in a more spherical droplet in system C. Because the L2B10 surfactant molecules had the same length of the hydrophilic patch as

L2B4 in system A and B, a small fraction of L2B10 were able to escape from the oil/water interface in system C, as shown in Fig. 3(g) and Fig. 4(c). In comparison, system D with L4B8 surfactants was the only system that had a clean oil phase as shown in Fig. 3(h) and Fig. 4(d). Despite the same molecule length of L4B8 surfactants as L2B10, longer hydrophilic patch of L4B8 resulted in the fully locking of all the surfactants at the oil/water interface and an almost perfectly spherical droplet in equilibrium. The packing of the surfactants in system D was the most ordered among the four systems (Fig. 3(d) and Fig. 4(d)). All the results indicated that the surfactant chemistry was the most determining factor of the final state of microemulsion droplets at the nanoscale, consistent with the experimental work^{54, 55}.

The molecular length and packing orderliness of the surfactants defined the thickness of the microemulsion droplet shell. As shown in Fig. 4(e-h), the shell thicknesses in system A, B, C, and D were 10 ± 2.9 , 8 ± 0.6 , 15.5 ± 2.1 and 12.4 ± 3.5 Å, respectively (comparison in Fig. S3). The thickness and the packing order of surfactants further influenced the rigidity of the microemulsion droplets, which would induce different de-emulsification behaviour. Besides, the radius of microemulsion droplets in the larger system were in the range of 4-8 nm after equilibration of 2 ns, as shown in Fig. S4. Although the microemulsion system was thermodynamically stable, the size of the microemulsion droplet changed with time due to droplet coalescence. The average radius became larger and larger while the speed of radius increase was getting slower. The speed and the average radius varied from case to case. It was also the reason why different microemulsion systems could keep stable for various time lengths.

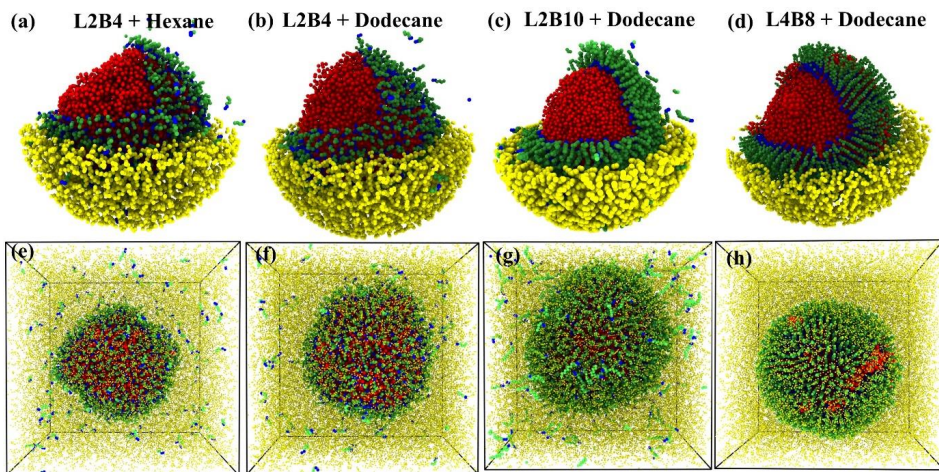


Figure 3. Structures of microemulsion droplets in equilibrium. (a-d) Dissection of the four equilibrated microemulsion droplets with the surfactant and the oil types given on each figure. (e-h) The final system snapshots of the four equilibrated systems in respective order as (a) to (d).

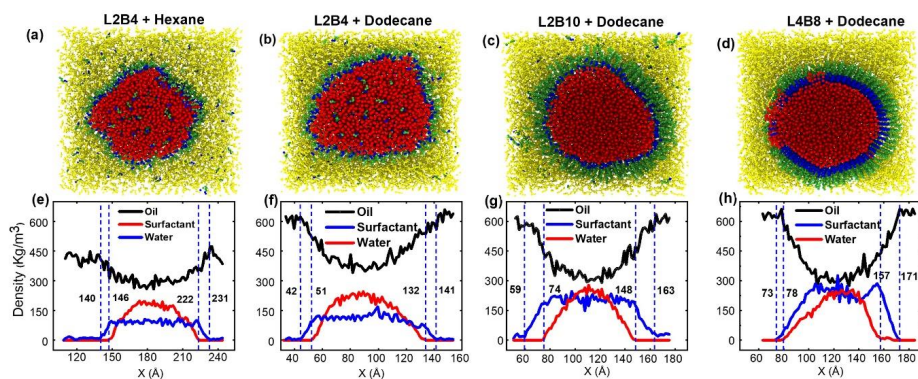


Figure 4. Surfactant shell thickness of the four microemulsion droplets in equilibrium. (a-d) Cross-section view of the four equilibrated droplets, with surfactant and oil type given on top of each figure. (e-h) Representative density distributions of oil, water, and surfactants in representative equilibrated snapshots of the four systems in respective order as (a) to (d).

order to (a) to (d). The surfactant shell thickness was quantified as the projected distance on the X-coordinate of the simulation box between the initial point of increasing density of water and surfactant. The blue dash-lines in (e-h) highlight the initial point of increasing density of water and surfactants with coordinates given. The distance between the near-by blue dash-line pair is the surfactant shell thickness.

3.3 Rupture mechanics of microemulsion droplets

3.3.1 Rupturing in nanoscale de-emulsification

The water core and the surfactant shell of each microemulsion droplet were attached to harmonic springs moving on opposite directions, which generated the counterforce on the droplet. Because of the thermodynamic stability of the droplets, a significant force was needed to rupture apart the water core from the surfactant shell, as example system C shown in Fig. 5 and a short video in the supplement (rupture-process.MP4). Force profiles monitored in rupturing all the microemulsion droplets at a temperature below 340 K showed the same pattern of a steady increase to peak values and then a gradual decrease to a low plateau, as shown in Fig. 5. The highest force peak corresponded to the opening of the surfactant shell, while the low force plateau resulted from the friction of the deformed water core with the surfactant shell and the oil phase. For comparison, extra simulations were performed to examine rupture events and rupture forces of the same microemulsion droplets by using different timesteps of 1 and 2 fs. As shown in Fig. S5, the effect of simulation timestep on the rupture behaviour was negligible.

The pulling force monitored before the opening of the surfactant shell showed an almost linear increase, indicating a strengthening behavior of the microemulsion droplet

following with a softening process, as shown by the initial part of the force profile and system snapshot 1 in Fig. 5. Releasing the external pulling force before the surfactant shell opening (the peak force value) led to a restoration of the original droplet shape. Such strengthening property was essential to the mechanical stability of microemulsion droplets in experiments, relevant cases of which were drug-carrying droplets transporting through narrow channels.

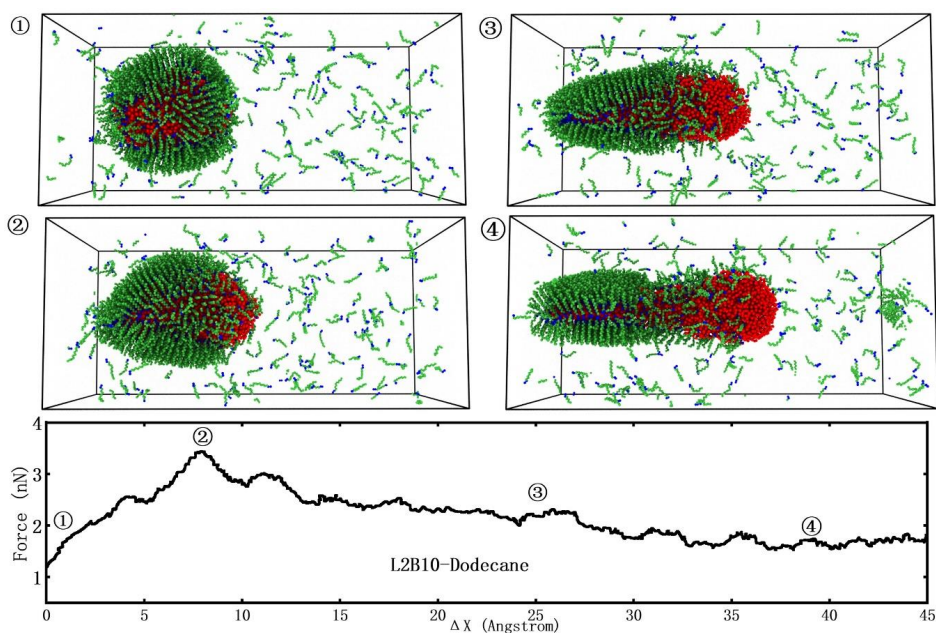


Figure 5. Nanoscale rupturing behaviour of microemulsion droplets represented by system C. Sequential system snapshots, ① - ④, were taken from the one continuous simulation trajectory. The oil molecules were not shown in the figure for a clear view of the microemulsion droplets in the rupturing process. The average force profile monitored in the simulations is given at the bottom, with labels ① - ④ indicating the above corresponding system snapshots. The initial average force is not 0 nN in the figure, which

was resulted from the diffusing and shape fluctuation of the droplet. ΔX is the separation distance of the two pulling harmonic spring along with opposite pulling directions.

3.3.2 Temperature effect

The mechanical properties of the microemulsion droplets were greatly affected by temperature owing to the viscosity of the liquid, namely lower temperature resulting in more robust droplets. The four microemulsion droplets were subjected to rupturing force with the same simulation parameters at the varied temperature of 280, 300, 320, 340, and 360 K. The results indicated that temperature played a major effect on the surfactant shell to influence the mechanical properties of the whole microemulsion droplets. By comparing the force profiles, as shown in Fig. 6, lower temperature resulted in higher peak force and rupture work. High temperature could even diminish the general pattern of the monitored pulling force shown in Fig. 5, especially in system A where the surfactants could easily escape from the oil/water interface (Fig. 3 (a) and (e)). The missing of the force peak at the high temperature indicated that the microemulsion droplet was marginally stable, which coincided with previous experimental observations⁵⁶ of high temperature enhancing the thermal motion of the molecules, enlarging the intermolecular distances, and thus weakening the surfactant shell coating on each droplet. The requirement for microemulsion stability differs in the application fields. For instance, robust microemulsion droplets are preferred during transport through channels like in oil production and drug delivery, while weak microemulsions are favorable for subsequent oil separation and drug release^{57, 58}. For environments where the temperature range is a non-negligible factor, special attention should be paid to the surfactant composition in the microemulsion system for its stability.

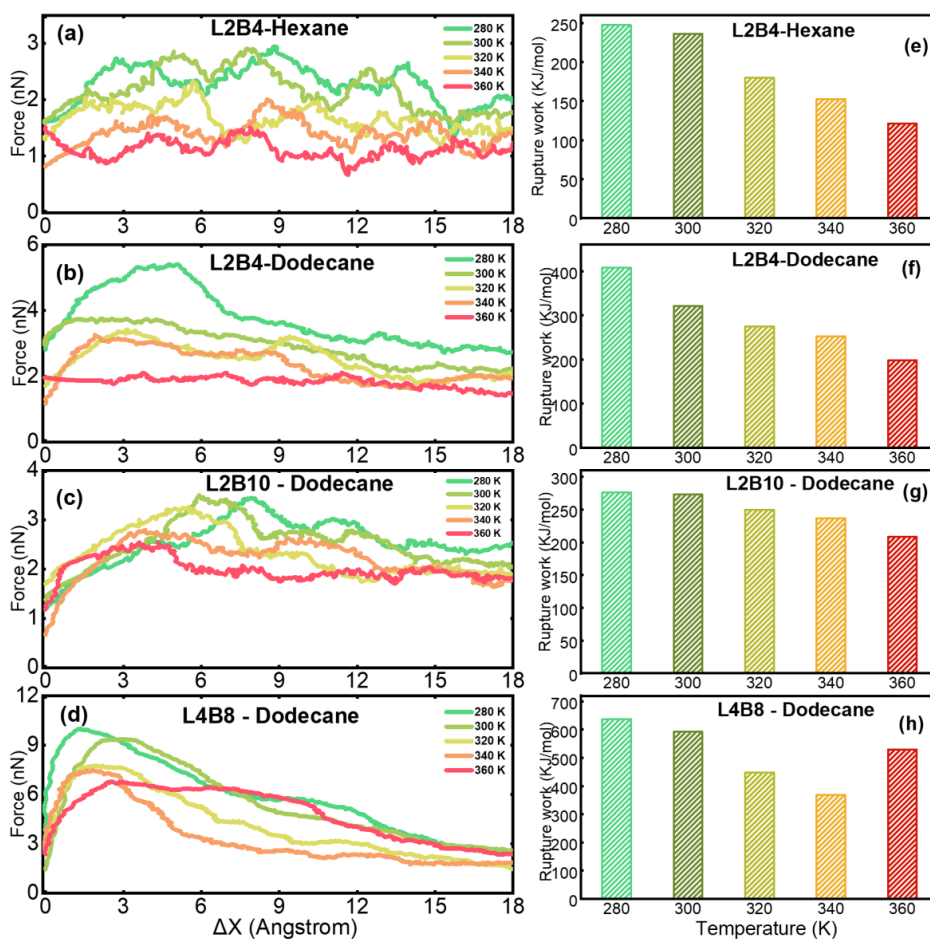


Figure 6. Temperature effect on rupturing the four microemulsion droplets. Force profiles of the four droplet rupturing events are given in (a-d) in the four systems. The surfactant and oil types of each system are given in each figure. The force profiles obtained at different temperatures of 280 K, 300 K, 320 K, 320 K, 340 and 360 K, are labeled by different colors with corresponding legends; the work of fracture of each system at the different temperatures are shown in (e-f).

3.3.3 Surfactant composition effect

The microemulsion droplets in the four systems demonstrated varied mechanical response to the increasing temperature, as shown in Fig. 6. The most robust droplet in system D with a surfactant shell of L4B8 could strongly endure pulling force at the simulation temperature range of 280 ~ 360 K, leading to obvious force peaks compared to its counterparts. As shown in Fig. 3 (d) and (h), the L4B8 surfactant molecules were highly packed and firmly adsorbed at the oil/water interface. The high orderliness of the surfactants was a result of the optimized amphiphilicity of the molecules and synergically contributed to the mechanical stability of the droplet. Comparing the force profiles of rupturing the four microemulsion droplets at 280 K in Fig. 7, the force peak for opening the L4B8 surfactant shell in system D outperformed its three counterparts. Yet, the highest force peak in system D was observed at the smallest separation distance of two pulling harmonic spring (ΔX) among the four force profiles. As discussed above, the deformed microemulsion droplet could restore its spherical structure and maintain integrity before the opening of the surfactant shell. Highly rigid microemulsion droplets could be difficult to transport through narrow channels if deformation in the droplet shape is required. The other three microemulsion droplets showed much lower surfactant shell opening peak force with larger droplet shape deformation. There is a tendency of higher surfactant packing order leading to higher peak force, more rupture work and smaller droplet deformation in the rupturing simulations.

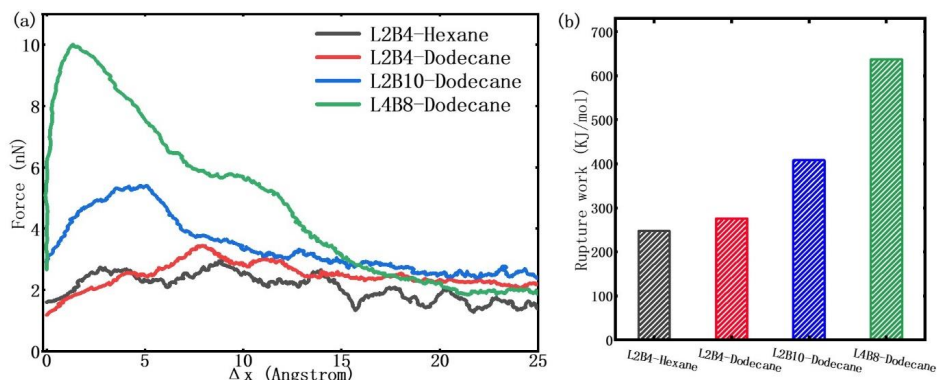


Figure 7. Pulling force profiles with peak values observed in rupturing the four microemulsion droplets in systems A, B, C and D at the temperature of 280 K, shown in (a). the work of fracture of four systems at 280 K are collected into (b). The surfactant and oil types in each system are given as legends.

4 CONCLUSIONS

We have utilized atomistic modeling and molecular dynamics simulation to scrutinize the nanoscale mechanical properties of the microemulsion and resolve the determinants of the droplet stability. The spontaneous emulsification of microemulsion droplets showed that the structure and arrangement of water and oil interface were dominated by the amphiphilic parts of the linear surfactant molecules. The effects of the chemical composition of the surfactant, the surfactant packing structure and temperature on the droplet rupturing were explored by performing a series of tensile tests. The force peak and the rupture work were obtained to evaluate the robustness of the microemulsions and identify the softening-to-strengthening transition as lowering the temperature. Compared to the previous studies⁵⁹⁻⁶¹, this work from the view of MD simulation investigated the

morphologies of W/O microemulsion droplets and evaluated their dynamic deformation process. It is the first attempt to scrutinize the mechanical properties of a single microemulsion droplet. Although the loading manner could be different from possible shearing force a microemulsion droplet experienced in experiments, the amplitude of the rupturing force should be proportional to the mechanical stability of the microemulsion droplets. Furthermore, the findings contribute to establishing an atomistic view on microemulsion fluids and provide a general guide to design a stable microemulsion system, such as oil recovery and production, drug delivery, materials fabrication, chemical sensors, and other related fields.^{45, 62}

CONFLICTS OF INTEREST

There are no conflicts to declare.

ACKNOWLEDGMENTS

This work is financially supported by the Research Council of Norway (Grant No. 234626) and the Chinese Scholarship Council. The supercomputer CPU hours were provided by the Norwegian Metacenter for Computational science (Project ID: NN9110K and NN9391K).

REFERENCES

1. M. K. Ali, R. M. Moshikur, R. Wakabayashi, M. Moniruzzaman, N. Kamiya and M. Goto, *ACS Sustainable Chemistry & Engineering*, 2020, **8**, 6263-6272.
2. E. Ruckenstein and J. C. Chi, *Journal of the Chemical Society-Faraday Transactions II*, 1975, **71**, 1690-1707.
3. A. J. Zarur and J. Y. Ying, *Nature*, 2000, **403**, 65-67.
4. S. Bhattacharya and S. K. Samanta, *Journal of Physical Chemistry Letters*, 2011, **2**, 914-920.

5. Y. Guo, H. Y. Li, Y. H. Yuan, J. Huang, J. Diao and B. Xie, *Journal of Hazardous Materials*, 2020, **386**, 121948.
6. G. Kaur and S. K. Mehta, *International Journal of Pharmaceutics*, 2017, **529**, 134-160.
7. R. Ryan, K. Altria, E. McEvoy, S. Donegan and J. Power, *Electrophoresis*, 2013, **34**, 159-177.
8. A. Fernandez-Pumarega, S. Amezcua, E. Fuguet and M. Roses, *Analytica Chimica Acta*, 2019, **1078**, 221-230.
9. M. Tagavifar, S. Herath, U. P. Weerasooriya, K. Sepehrnoori and G. Pope, *SPE Journal*, 2018, **23**, 66-83.
10. M. R. Kaiser, Z. Ma, X. Wang, F. Han, T. Gao, X. Fan, J. Z. Wang, H. K. Liu, S. Dou and C. Wang, *ACS Nano*, 2017, **11**, 9048-9056.
11. H. Xie, E. Chen, Y. Ye, S. Xu and T. Guo, *The Journal of Physical Chemistry Letters*, 2020, **11**, 1428-1434.
12. T. P. Hoar and J. H. Schulman, *Nature*, 1943, **152**, 102-103.
13. J. H. Schulman, W. Stoeckenius and L. M. Prince, *The Journal of Physical Chemistry*, 1959, **63**, 1677-1680.
14. H. Mateos, A. Valentini, G. Colafemmina, S. Murgia, E. Robles, A. Brooker and G. Palazzo, *Colloids and Surfaces A: Physicochemical and Engineering Aspects*, 2020, 124801.
15. Y. Cohen, L. Avram and L. Frish, *Angewandte Chemie-International Edition*, 2005, **44**, 520-554.
16. D. P. Acharya and P. G. Hartley, *Current Opinion in Colloid & Interface Science*, 2012, **17**, 274-280.
17. C. D'Andrea, J. Bochterle, A. Toma, C. Huck, F. Neubrech, E. Messina, B. Fazio, O. M. Marago, E. Di Fabrizio, M. Lamy de La Chapelle, P. G. Gucciardi and A. Pucci, *ACS Nano*, 2013, **7**, 3522-3531.
18. A. Paul, K. Meyer, J. P. Ruiken, M. Illner, D. N. Muller, E. Esche, G. Wozny, F. Westad and M. Maiwald, *Measurement Science and Technology*, 2017, **28**, 035502.
19. Y. H. Jin, S. Lohstreter, D. T. Pierce, J. Parisien, M. Wu, C. Hall and J. X. J. Zhao, *Chemistry of Materials*, 2008, **20**, 4411-4419.
20. E. Goldmünz, A. Aserin and N. Garti, *Colloids and Surfaces A: Physicochemical and Engineering Aspects*, 2020, **586**, 124213.
21. M. Rodríguez-Hakim, S. Anand, J. Tajuelo, Z. Yao, A. Kannan and G. G. Fuller, *Journal of Rheology*, 2020, **64**, 799-816.

22. P. Rastogi, N. S. Kaisare and M. G. Basavaraj, *Energy & Fuels*, 2019, **33**, 12227-12235.
23. S. H. Chen and R. Rajagopalan, *Micellar solutions and microemulsions: structure, dynamics, and statistical thermodynamics*, Springer Science & Business Media, 2012.
24. M. Bourrel and R. S. Schechter, *Microemulsions and related systems: formulation, solvency, and physical properties*, Editions Technip, 2010.
25. M. Simon, E. Schneck, L. Noirez, S. Rahn, I. Davidovich, Y. Talmon and M. Gradzielski, *Macromolecules*, 2020.
26. M. L. Klein and W. Shinoda, *Science*, 2008, **321**, 798-800.
27. F. A. Maulvi, A. R. Desai, H. H. Choksi, R. J. Patil, K. M. Ranch, B. A. Vyas and D. O. Shah, *International Journal of Pharmaceutics*, 2017, **524**, 193-204.
28. S. N. Kale and S. L. Deore, *Systematic Reviews in Pharmacy*, 2017, **8**, 39-47.
29. N. Pal, N. Kumar and A. Mandal, *Langmuir*, 2019, **35**, 2655-2667.
30. S. P. Callender, J. A. Mathews, K. Kobernyk and S. D. Wettig, *International Journal of Pharmaceutics*, 2017, **526**, 425-442.
31. R. Nguele, K. Sasaki, Y. Sugai, B. Omondi, H. S. Al-Salim and R. Ueda, *Energy & Fuels*, 2017, **31**, 255-270.
32. N. Arai, K. Yasuoka and X. C. Zeng, *ACS Nano*, 2016, **10**, 8026-8037.
33. S. E. Sherman, Q. Xiao and V. Percec, *Chemical Reviews*, 2017, **117**, 6538-6631.
34. J. Li, J. Wang, Q. Yao, Y. Yan, Z. Li and J. Zhang, *The Journal of Physical Chemistry Letters*, 2020, **11**, 3369-3375.
35. M. G. Martin and J. I. Siepmann, *Journal of Physical Chemistry B*, 1998, **102**, 2569-2577.
36. F. H. Stillinger and T. A. Weber, *Physical review B*, 1985, **31**, 5262-5271.
37. V. Molinero and E. B. Moore, *The Journal of Physical Chemistry B*, 2008, **113**, 4008-4016.
38. C. Vega and J. L. Abascal, *Physical Chemistry Chemical Physics*, 2011, **13**, 19663-19688.
39. W. G. Noid, *The Journal of chemical physics*, 2013, **139**, 090901.
40. N. Arai, K. Yasuoka and X. C. Zeng, *ACS Nano*, 2016, **10**, 8026-8037.
41. L. C. Jacobson, W. Hujo and V. Molinero, *Journal of the American Chemical Society*, 2010, **132**, 11806-11811.
42. B. Raubenolt, G. Gyawali, W. Tang, K. S. Wong and S. W. Rick, *Polymers (Basel)*, 2018, **10**, 475.
43. B. Song and V. Molinero, *The Journal of chemical physics*, 2013, **139**, 054511.

44. G. Gyawali, S. Sternfield, R. Kumar and S. W. Rick, *Journal of Chemical Theory and Computation*, 2017, **13**, 3846-3853.
45. S. Plimpton and B. Hendrickson, ACS Publications, 1995.
46. D. J. Evans and B. L. Holian, *Journal of Chemical Physics*, 1985, **83**, 4069-4074.
47. M. Parrinello and A. Rahman, *Journal of Applied Physics*, 1981, **52**, 7182-7190.
48. S. Xiao, B. H. Skallerud, F. Wang, Z. Zhang and J. He, *Nanoscale*, 2019, **11**, 16262-16269.
49. S. Xiao, Z. Zhang and J. He, *Physical Chemistry Chemical Physics*, 2018, **20**, 24759-24767.
50. J. B. Rosenholm, *Advances in Colloid and Interface Science*, 2020, **276**, 102047.
51. G. Lemahieu, J. Aguilhon, H. Strub, V. Molinier, J. F. Ontiveros and J.-M. Aubry, *RSC Advances*, 2020, **10**, 16377-16389.
52. J. L. Salager, A. M. Forgiarini, L. Marquez, L. Manchego and J. Bullon, *Journal of Surfactants and Detergents*, 2013, **16**, 631-663.
53. X. C. Liu, Y. X. Zhao, Q. X. Li and J. P. Niu, *Colloids and Surfaces a-Physicochemical and Engineering Aspects*, 2016, **494**, 201-208.
54. M. Filippousi, M. Angelakeris, M. Katsikini, E. Paloura, I. Efthimiopoulos, Y. J. Wang, D. Zambouis and G. Van Tendeloo, *Journal of Physical Chemistry C*, 2014, **118**, 16209-16217.
55. P. Golwala, S. Rathod, R. Patil, A. Joshi, D. Ray, V. K. Aswal, P. Bahadur and S. Tiwari, *Colloids and Surfaces B: Biointerfaces*, 2020, **186**, 110736.
56. M. Domschke, M. Kraska, R. Feile and B. Stuhn, *Soft Matter*, 2013, **9**, 11503-11512.
57. C. Torres-Luna, N. Hu, A. Koolivand, X. Fan, Y. Zhu, R. Domszy, J. Yang, A. Yang and N. S. Wang, *Pharmaceutics*, 2019, **11**, 262.
58. B. Hajjar, K.-I. Zier, N. Khalid, S. Azarmi and R. Löbenberg, *Journal of Pharmaceutical Investigation*, 2018, **48**, 351-362.
59. W. X. Shi and H. X. Guo, *The Journal of Physical Chemistry B*, 2010, **114**, 6365-6376.
60. F. Muzaffar, U. Singh and L. Chauhan, *International Journal of Pharmacy and Pharmaceutical Sciences*, 2013, **5**, 39-53.
61. R. Zolfaghari, A. Fakhru'l-Razi, L. C. Abdullah, S. S. E. H. Elnashaie and A. Pendashteh, *Separation and Purification Technology*, 2016, **170**, 377-407.
62. M. Simon, E. Schneck, L. Noirez, S. Rahn, I. Davidovich, Y. Talmon and M. Gradzielski, *Macromolecules*, 2020, **53**, 4055-4067.

Supporting Information

Stability, deformation and rupture of Janus oligomer enabled self-emulsifying water-in-oil microemulsion droplet

Yuequn Fu,^a Senbo Xiao,^{*a} Siqi Liu,^a Jianyang Wu,^b Xiao Wang,^c Lijie Qiao,^d Zhiliang Zhang^a and Jianying He^{*†a,d}

^aNTNU Nanomechanical Lab, Norwegian University of Science and Technology (NTNU),
Trondheim 7491, Norway

^bDepartment of Physics, Research Institute for Biomimetics and Soft Matter, Jiujiang
Research Institute and Fujian Provincial Key Laboratory for Soft Functional Materials
Research, Xiamen University, Xiamen 361005, China

^cReservoir Engineering Research Institute, Palo Alto, California 94301, United States

^dBeijing Advanced Innovation Center for Materials Genome Engineering, University of
Science and Technology Beijing, Beijing 100083, China

*Corresponding author.

E-mail addresses: Senbo.xiao@ntnu.no (S. Xiao), Jianying.he@ntnu.no (J. He).

†Currently on sabbatical as a visiting professor at ^dBeijing Advanced Innovation Center for
Materials Genome Engineering, University of Science and Technology Beijing.

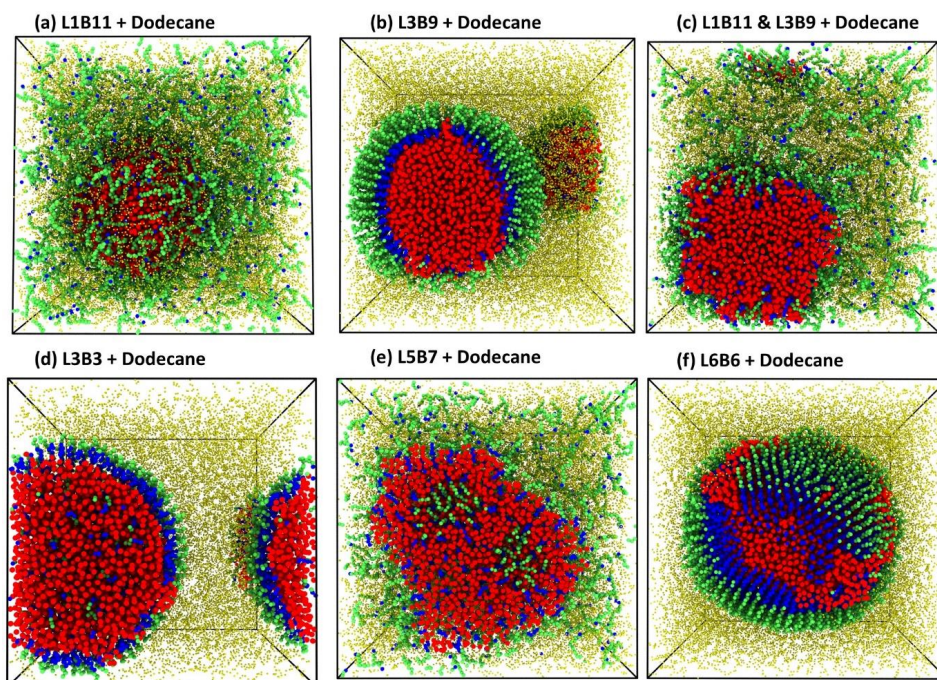
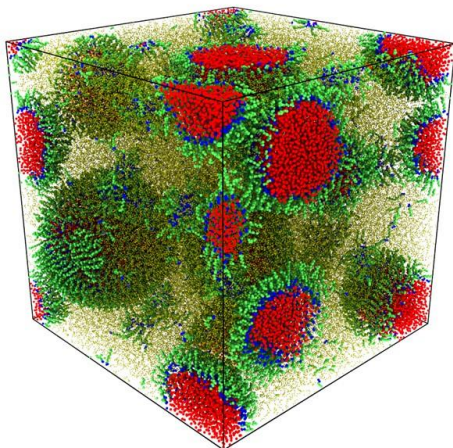


Figure S1 Atoms with red color are water molecules; atoms with blue and green color are janus oligomer molecules; the yellow atoms are oil molecules. With same mole ratio of water:surfactant:oil (6144:1024:3072), three microemulsion droplet were built up. (a) water, surfactant L1B11 (512)+ L3B9 (512), and dodecane oil; (b) water, surfactant L3B9 and dodecane oil; (c) water, surfactant L1B11 (512)+ L3B9 (512), and dodecane oil; (d) water, surfactant L3B3 and dodecane oil; (e) water, surfactant L5B7 and dodecane oil; (f) water, surfactant L6B6 and dodecane oil.

(a) Water in oil microemulsion system



(b) Oil in water microemulsion system

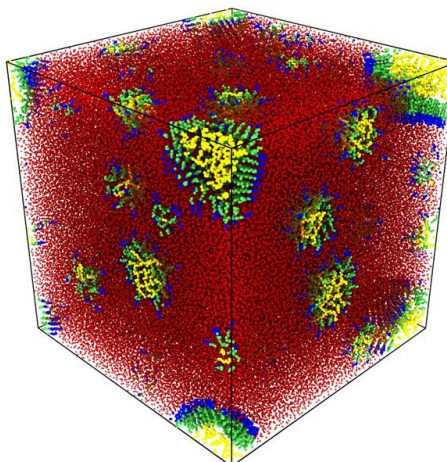


Figure S2 With same forcefield parameter, two microemulsion systems were simulated. (a) water in oil microemulsion system consisting of water molecules (32928), L2B10 surfactant molecules (5488) and dodecane oil molecules (16464); (b) oil in water microemulsion system consisting of water molecules (47928), L2B10 surfactant molecules (5488) and dodecane oil molecules (16464).

In order to get a statistical significance, we calculated the thickness of interface of each system from X-, Y-, and Z- axis direction.

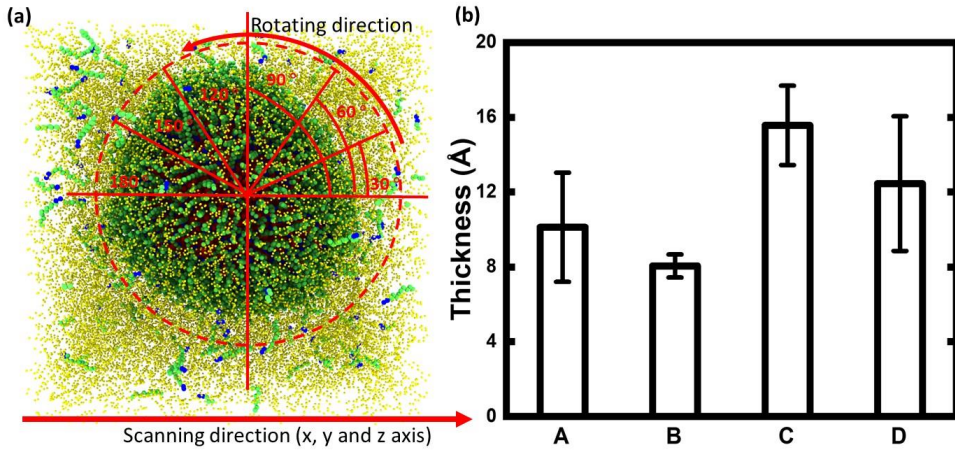


Figure S3 The method to scan the density of the system. (a) When the scanning direction is fixed, the rotating angle is set to 30° , 60° , 90° , 120° , 150° and 180° , that is to say, in every axis direction six density values are calculated. All density values of four systems are collected into (b).

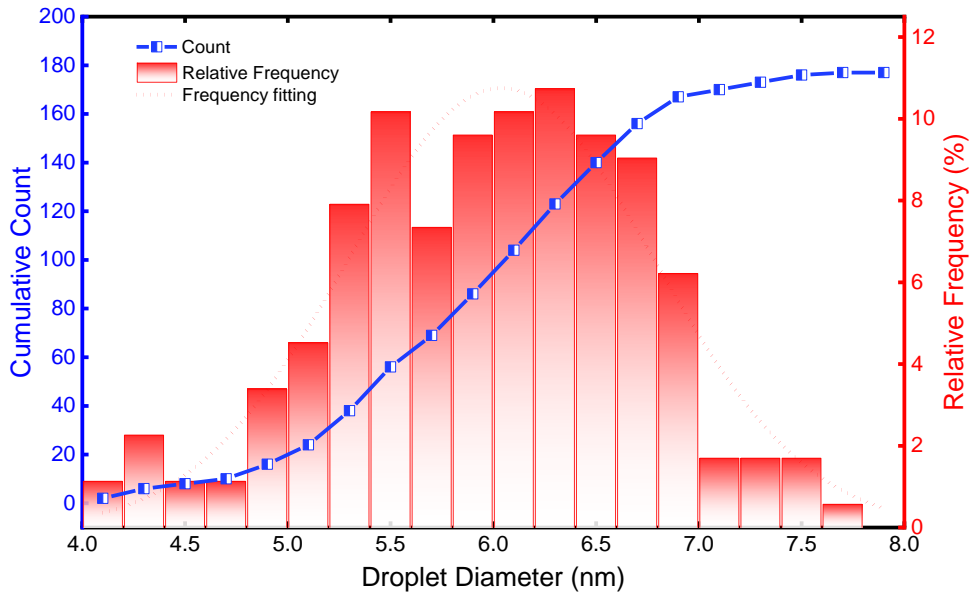


Figure S4 The microemulsion droplets diameter distribution in a large system.

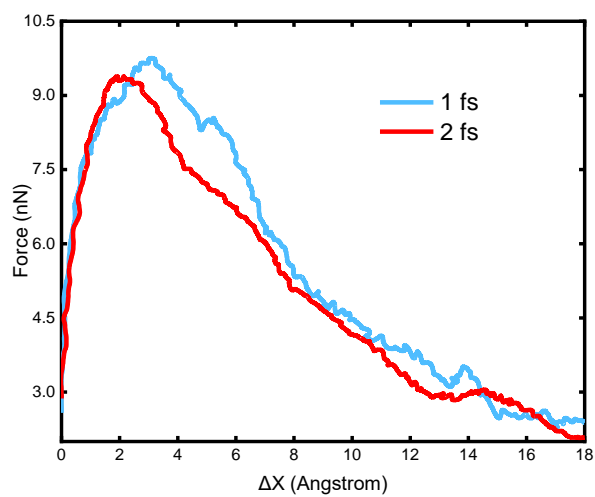


Figure S5 Rupturing force profiles of the same microemulsion droplet using timesteps of 1 and 2 fs.

A.2 Paper II

Atomistic Insights to Droplet Size Distribution in the Preliminary Stage of Self-microemulsifying of a Water/surfactant/oil System

Authors: Yuequn Fu, Senbo Xiao, Siqu Liu, Zhiliang Zhang and Jianying He

To be submitted 2021

This paper is awaiting publication and is not included in NTNU Open

A.3 Paper III

Paper III

Stimuli-responsive Surfaces in Design for Low Intrinsic Ice Adhesion

Authors: Yuequn Fu, Senbo Xiao, Bjørn Helge Skallerud, Zhiliang Zhang and Jianying He

Submitted 2021

This paper is awaiting publication and is not included in NTNU Open

Appendix B

List of previous PhD theses at Department of Structural Engineering

DEPARTMENT OF STRUCTURAL ENGINEERING
NORWEGIAN UNIVERSITY OF SCIENCE AND TECHNOLOGY

N-7491 TRONDHEIM, NORWAY

Telephone: +47 73 59 47 00

"Reliability Analysis of Structural Systems using Nonlinear Finite Element Methods",
C. A. Holm, 1990:23, ISBN 82-7119-178-0.

"Uniform Stratified Flow Interaction with a Submerged Horizontal Cylinder",
Ø. Arntsen, 1990:32, ISBN 82-7119-188-8.

"Large Displacement Analysis of Flexible and Rigid Systems Considering
Displacement-Dependent Loads and Nonlinear Constraints",
K. M. Mathisen, 1990:33, ISBN 82-7119-189-6.

"Solid Mechanics and Material Models including Large Deformations",
E. Levold, 1990:56, ISBN 82-7119-214-0, ISSN 0802-3271.

"Inelastic Deformation Capacity of Flexurally-Loaded Aluminium Alloy Structures",
T. Welo, 1990:62, ISBN 82-7119-220-5, ISSN 0802-3271.

"Visualization of Results from Mechanical Engineering Analysis",
K. Aamnes, 1990:63, ISBN 82-7119-221-3, ISSN 0802-3271.

"Object-Oriented Product Modeling for Structural Design",
S. I. Dale, 1991:6, ISBN 82-7119-258-2, ISSN 0802-3271.

"Parallel Techniques for Solving Finite Element Problems on Transputer Networks",
T. H. Hansen, 1991:19, ISBN 82-7119-273-6, ISSN 0802-3271.

"Statistical Description and Estimation of Ocean Drift Ice Environments",
R. Korsnes, 1991:24, ISBN 82-7119-278-7, ISSN 0802-3271.

"Properties of concrete related to fatigue damage: with emphasis on high strength
concrete",
G. Petkovic, 1991:35, ISBN 82-7119-290-6, ISSN 0802-3271.

"Turbidity Current Modelling",
B. Brørs, 1991:38, ISBN 82-7119-293-0, ISSN 0802-3271.

"Zero-Slump Concrete: Rheology, Degree of Compaction and Strength. Effects of Fillers as Part Cement-Replacement",

C. Sørensen, 1992:8, ISBN 82-7119-357-0, ISSN 0802-3271.

"Nonlinear Analysis of Reinforced Concrete Structures Exposed to Transient Loading",
K. V. Høiseth, 1992:15, ISBN 82-7119-364-3, ISSN 0802-3271.

"Finite Element Formulations and Solution Algorithms for Buckling and Collapse Analysis of Thin Shells",

R. O. Bjærum, 1992:30, ISBN 82-7119-380-5, ISSN 0802-3271.

"Response Statistics of Nonlinear Dynamic Systems",

J. M. Johnsen, 1992:42, ISBN 82-7119-393-7, ISSN 0802-3271.

"Digital Models in Engineering. A Study on why and how engineers build and operate digital models for decision support",

J. Høyte, 1992:75, ISBN 82-7119-429-1, ISSN 0802-3271.

"Sparse Solution of Finite Element Equations",

A. C. Damhaug, 1992:76, ISBN 82-7119-430-5, ISSN 0802-3271.

"Some Aspects of Floating Ice Related to Sea Surface Operations in the Barents Sea",
S. Løset, 1992:95, ISBN 82-7119-452-6, ISSN 0802-3271.

"Modelling of Cyclic Plasticity with Application to Steel and Aluminium Structures",
O. S. Hopperstad, 1993:7, ISBN 82-7119-461-5, ISSN 0802-3271.

"The Free Formulation: Linear Theory and Extensions with Applications to Tetrahedral Elements

with Rotational Freedoms",

G. Skeie, 1993:17, ISBN 82-7119-472-0, ISSN 0802-3271.

"Høyfast betongs motstand mot piggedekkslitasje. Analyse av resultater fra prøving i Veisliter'n",

T. Tveter, 1993:62, ISBN 82-7119-522-0, ISSN 0802-3271.

"A Nonlinear Finite Element Based on Free Formulation Theory for Analysis of Sandwich Structures",

O. Aamlid, 1993:72, ISBN 82-7119-534-4, ISSN 0802-3271.

"The Effect of Curing Temperature and Silica Fume on Chloride Migration and Pore Structure of High Strength Concrete",

C. J. Hauck, 1993:90, ISBN 82-7119-553-0, ISSN 0802-3271.

"Failure of Concrete under Compressive Strain Gradients",

G. Markeset, 1993:110, ISBN 82-7119-575-1, ISSN 0802-3271.

"An experimental study of internal tidal amphidromes in Vestfjorden",
J. H. Nilsen, 1994:39, ISBN 82-7119-640-5, ISSN 0802-3271.

"Structural analysis of oil wells with emphasis on conductor design",
H. Larsen, 1994:46, ISBN 82-7119-648-0, ISSN 0802-3271.

"Adaptive methods for non-linear finite element analysis of shell structures",
K. M. Okstad, 1994:66, ISBN 82-7119-670-7, ISSN 0802-3271.

"On constitutive modelling in nonlinear analysis of concrete structures",
O. Fyrileiv, 1994:115, ISBN 82-7119-725-8, ISSN 0802-3271.

"Fluctuating wind load and response of a line-like engineering structure with emphasis
on motion-induced wind forces",
J. Bogunovic Jakobsen, 1995:62, ISBN 82-7119-809-2, ISSN 0802-3271.

"An experimental study of beam-columns subjected to combined torsion, bending and
axial actions",
A. Aalberg, 1995:66, ISBN 82-7119-813-0, ISSN 0802-3271.

"Scaling and cracking in unsealed freeze/thaw testing of Portland cement and silica
fume concretes",
S. Jacobsen, 1995:101, ISBN 82-7119-851-3, ISSN 0802-3271.

"Damping of water waves by submerged vegetation. A case study of laminaria
hyperborea",
A. M. Dubi, 1995:108, ISBN 82-7119-859-9, ISSN 0802-3271.

"The dynamics of a slope current in the Barents Sea",
Sheng Li, 1995:109, ISBN 82-7119-860-2, ISSN 0802-3271.

"Modellering av delmaterialenes betydning for betongens konsistens",
Ernst Mørtzell, 1996:12, ISBN 82-7119-894-7, ISSN 0802-3271.

"Bending of thin-walled aluminium extrusions",
Birgit Sjøvik Opheim, 1996:60, ISBN 82-7119-947-1, ISSN 0802-3271.

"Material modelling of aluminium for crashworthiness analysis",
Torodd Berstad, 1996:89, ISBN 82-7119-980-3, ISSN 0802-3271.

"Estimation of structural parameters from response measurements on submerged
floating tunnels",
Rolf Magne Larssen, 1996:119, ISBN 82-471-0014-2, ISSN 0802-3271.

-
- “Numerical modelling of plain and reinforced concrete by damage mechanics”,
Mario A. Polanco-Loria, 1997:20, ISBN 82-471-0049-5, ISSN 0802-3271.
- “Nonlinear random vibrations - numerical analysis by path integration methods”,
Vibeke Moe, 1997:26, ISBN 82-471-0056-8, ISSN 0802-3271.
- “Numerical prediction of vortex-induced vibration by the finite element method”,
Joar Martin Dalheim, 1997:63, ISBN 82-471-0096-7, ISSN 0802-3271.
- “Time domain calculations of buffeting response for wind sensitive structures”,
Ketil Aas-Jakobsen, 1997:148, ISBN 82-471-0189-0, ISSN 0802-3271.
- "A numerical study of flow about fixed and flexibly mounted circular cylinders",
Trond Stokka Meling, 1998:48, ISBN 82-471-0244-7, ISSN 0802-3271.
- “Estimation of chloride penetration into concrete bridges in coastal areas”,
Per Egil Steen, 1998:89, ISBN 82-471-0290-0, ISSN 0802-3271.
- “Stress-resultant material models for reinforced concrete plates and shells”,
Jan Arve Øverli, 1998:95, ISBN 82-471-0297-8, ISSN 0802-3271.
- “Chloride binding in concrete. Effect of surrounding environment and concrete composition”,
Claus Kenneth Larsen, 1998:101, ISBN 82-471-0337-0, ISSN 0802-3271.
- “Rotational capacity of aluminium alloy beams”,
Lars A. Moen, 1999:1, ISBN 82-471-0365-6, ISSN 0802-3271.
- “Stretch Bending of Aluminium Extrusions”,
Arild H. Clausen, 1999:29, ISBN 82-471-0396-6, ISSN 0802-3271.
- “Aluminium and Steel Beams under Concentrated Loading”,
Tore Tryland, 1999:30, ISBN 82-471-0397-4, ISSN 0802-3271.
- "Engineering Models of Elastoplasticity and Fracture for Aluminium Alloys",
Odd-Geir Lademo, 1999:39, ISBN 82-471-0406-7, ISSN 0802-3271.
- "Kapasitet og duktilitet av dybelforbindelser i trekonstruksjoner",
Jan Siem, 1999:46, ISBN 82-471-0414-8, ISSN 0802-3271.
- “Etablering av distribuert ingeniørarbeid; Teknologiske og organisatoriske erfaringer fra en norsk ingeniørbedrift”,
Lars Line, 1999:52, ISBN 82-471-0420-2, ISSN 0802-3271.
- “Estimation of Earthquake-Induced Response”,
Símon Ólafsson, 1999:73, ISBN 82-471-0443-1, ISSN 0802-3271.
- “Coastal Concrete Bridges: Moisture State, Chloride Permeability and Aging Effects”

-
- Ragnhild Holen Relling, 1999:74, ISBN 82-471-0445-8, ISSN 0802-3271.
- ”Capacity Assessment of Titanium Pipes Subjected to Bending and External Pressure”,
Arve Bjørset, 1999:100, ISBN 82-471-0473-3, ISSN 0802-3271.
- “Validation of Numerical Collapse Behaviour of Thin-Walled Corrugated Panels”,
Håvar Ilstad, 1999:101, ISBN 82-471-0474-1, ISSN 0802-3271.
- “Strength and Ductility of Welded Structures in Aluminium Alloys”,
Mirosław Matusiak, 1999:113, ISBN 82-471-0487-3, ISSN 0802-3271.
- “Thermal Dilation and Autogenous Deformation as Driving Forces to Self-Induced
Stresses in High Performance Concrete”,
Øyvind Bjøntegaard, 1999:121, ISBN 82-7984-002-8, ISSN 0802-3271.
- “Some Aspects of Ski Base Sliding Friction and Ski Base Structure”,
Dag Anders Moldestad, 1999:137, ISBN 82-7984-019-2, ISSN 0802-3271.
- "Electrode reactions and corrosion resistance for steel in mortar and concrete",
Roy Antonsen, 2000:10, ISBN 82-7984-030-3, ISSN 0802-3271.
- "Hydro-Physical Conditions in Kelp Forests and the Effect on Wave Damping and
Dune Erosion. A case study on Laminaria Hyperborea",
Stig Magnar Løvås, 2000:28, ISBN 82-7984-050-8, ISSN 0802-3271.
- "Random Vibration and the Path Integral Method",
Christian Skaug, 2000:39, ISBN 82-7984-061-3, ISSN 0802-3271.
- "Buckling and geometrical nonlinear beam-type analyses of timber structures",
Trond Even Eggen, 2000:56, ISBN 82-7984-081-8, ISSN 0802-3271.
- ”Structural Crashworthiness of Aluminium Foam-Based Components”,
Arve Grønsund Hanssen, 2000:76, ISBN 82-7984-102-4, ISSN 0809-103X.
- “Measurements and simulations of the consolidation in first-year sea ice ridges, and
some aspects of mechanical behaviour”,
Knut V. Høyland, 2000:94, ISBN 82-7984-121-0, ISSN 0809-103X.
- ”Kinematics in Regular and Irregular Waves based on a Lagrangian Formulation”,
Svein Helge Gjørund, 2000-86, ISBN 82-7984-112-1, ISSN 0809-103X.
- ”Self-Induced Cracking Problems in Hardening Concrete Structures”,
Daniela Bosnjak, 2000-121, ISBN 82-7984-151-2, ISSN 0809-103X.
- "Ballistic Penetration and Perforation of Steel Plates",
Tore Børvik, 2000:124, ISBN 82-7984-154-7, ISSN 0809-103X.

"Freeze-Thaw resistance of Concrete. Effect of: Curing Conditions, Moisture Exchange and Materials",
Terje Finnerup Rønning, 2001:14, ISBN 82-7984-165-2, ISSN 0809-103X

"Structural behaviour of post tensioned concrete structures. Flat slab. Slabs on ground",
Steinar Trygstad, 2001:52, ISBN 82-471-5314-9, ISSN 0809-103X.

"Slipforming of Vertical Concrete Structures. Friction between concrete and slipform panel",
Kjell Tore Fosså, 2001:61, ISBN 82-471-5325-4, ISSN 0809-103X.

"Some numerical methods for the simulation of laminar and turbulent incompressible flows",
Jens Holmen, 2002:6, ISBN 82-471-5396-3, ISSN 0809-103X.

"Improved Fatigue Performance of Threaded Drillstring Connections by Cold Rolling",
Steinar Kristoffersen, 2002:11, ISBN: 82-421-5402-1, ISSN 0809-103X.

"Deformations in Concrete Cantilever Bridges: Observations and Theoretical Modelling",
Peter F. Takács, 2002:23, ISBN 82-471-5415-3, ISSN 0809-103X.

"Stiffened aluminium plates subjected to impact loading",
Hilde Giæver Hildrum, 2002:69, ISBN 82-471-5467-6, ISSN 0809-103X.

"Full- and model scale study of wind effects on a medium-rise building in a built up area",
Jónas Thór Snæbjörnsson, 2002:95, ISBN82-471-5495-1, ISSN 0809-103X.

"Evaluation of Concepts for Loading of Hydrocarbons in Ice-infested water",
Arnor Jensen, 2002:114, ISBN 82-417-5506-0, ISSN 0809-103X.

"Numerical and Physical Modelling of Oil Spreading in Broken Ice",
Janne K. Økland Gjøsteen, 2002:130, ISBN 82-471-5523-0, ISSN 0809-103X.

"Diagnosis and protection of corroding steel in concrete",
Franz Pruckner, 20002:140, ISBN 82-471-5555-4, ISSN 0809-103X.

"Tensile and Compressive Creep of Young Concrete: Testing and Modelling",
Dawood Atrushi, 2003:17, ISBN 82-471-5565-6, ISSN 0809-103X.

"Rheology of Particle Suspensions. Fresh Concrete, Mortar and Cement Paste with Various Types of Lignosulfonates",
Jon Elvar Wallevik, 2003:18, ISBN 82-471-5566-4, ISSN 0809-103X.

"Oblique Loading of Aluminium Crash Components",

Aase Reyes, 2003:15, ISBN 82-471-5562-1, ISSN 0809-103X.

“Utilization of Ethiopian Natural Pozzolans”,
Surafel Ketema Desta, 2003:26, ISSN 82-471-5574-5, ISSN:0809-103X.

“Behaviour and strength prediction of reinforced concrete structures with discontinuity regions”, Helge Brå, 2004:11, ISBN 82-471-6222-9, ISSN 1503-8181.

“High-strength steel plates subjected to projectile impact. An experimental and numerical study”, Sumita Dey, 2004:38, ISBN 82-471-6282-2 (printed version), ISBN 82-471-6281-4 (electronic version), ISSN 1503-8181.

“Alkali-reactive and inert fillers in concrete. Rheology of fresh mixtures and expansive reactions.”
Bård M. Pedersen, 2004:92, ISBN 82-471-6401-9 (printed version), ISBN 82-471-6400-0 (electronic version), ISSN 1503-8181.

“On the Shear Capacity of Steel Girders with Large Web Openings”.
Nils Christian Hagen, 2005:9 ISBN 82-471-6878-2 (printed version), ISBN 82-471-6877-4 (electronic version), ISSN 1503-8181.

”Behaviour of aluminium extrusions subjected to axial loading”.
Østen Jensen, 2005:7, ISBN 82-471-6873-1 (printed version), ISBN 82-471-6872-3 (electronic version), ISSN 1503-8181.

”Thermal Aspects of corrosion of Steel in Concrete”.
Jan-Magnus Østvik, 2005:5, ISBN 82-471-6869-3 (printed version), ISBN 82-471-6868 (electronic version), ISSN 1503-8181.

”Mechanical and adaptive behaviour of bone in relation to hip replacement.” A study of bone remodelling and bone grafting.
Sébastien Muller, 2005:34, ISBN 82-471-6933-9 (printed version), ISBN 82-471-6932-0 (electronic version), ISSN 1503-8181.

“Analysis of geometrical nonlinearities with applications to timber structures”.
Lars Wollebæk, 2005:74, ISBN 82-471-7050-5 (printed version), ISBN 82-471-7019-1 (electronic version), ISSN 1503-8181.

“Pedestrian induced lateral vibrations of slender footbridges”,
Anders Rönquist, 2005:102, ISBN 82-471-7082-5 (printed version), ISBN 82-471-7081-7 (electronic version), ISSN 1503-8181.

“Initial Strength Development of Fly Ash and Limestone Blended Cements at Various Temperatures Predicted by Ultrasonic Pulse Velocity”,
Tom Ivar Fredvik, 2005:112, ISBN 82-471-7105-8 (printed version), ISBN 82-471-7103-1 (electronic version), ISSN 1503-8181.

“Behaviour and modelling of thin-walled cast components”,
Cato Dørum, 2005:128, ISBN 82-471-7140-6 (printed version), ISBN 82-471-7139-2
(electronic version), ISSN 1503-8181.

“Behaviour and modelling of selfpiercing riveted connections”,
Raffaele Porcaro, 2005:165, ISBN 82-471-7219-4 (printed version), ISBN 82-471-
7218-6 (electronic version), ISSN 1503-8181.

”Behaviour and Modelling of Aluminium Plates subjected to Compressive Load”,
Lars Rønning, 2005:154, ISBN 82-471-7169-1 (printed version), ISBN 82-471-7195-3
(electronic version), ISSN 1503-8181.

”Bumper beam-longitudinal system subjected to offset impact loading”,
Satyanarayana Kokkula, 2005:193, ISBN 82-471-7280-1 (printed version), ISBN 82-
471-7279-8 (electronic version), ISSN 1503-8181.

“Control of Chloride Penetration into Concrete Structures at Early Age”,
Guofei Liu, 2006:46, ISBN 82-471-7838-9 (printed version), ISBN 82-471-7837-0
(electronic version), ISSN 1503-8181.

“Modelling of Welded Thin-Walled Aluminium Structures”,
Ting Wang, 2006:78, ISBN 82-471-7907-5 (printed version), ISBN 82-471-7906-7
(electronic version), ISSN 1503-8181.

”Time-variant reliability of dynamic systems by importance sampling and probabilistic
analysis of ice loads”,
Anna Ivanova Olsen, 2006:139, ISBN 82-471-8041-3 (printed version), ISBN 82-471-
8040-5 (electronic version), ISSN 1503-8181.

“Fatigue life prediction of an aluminium alloy automotive component using finite
element analysis of surface topography”,
Sigmund Kyrre Ås, 2006:25, ISBN 82-471-7791-9 (printed version), ISBN 82-471-
7791-9 (electronic version), ISSN 1503-8181.

”Constitutive models of elastoplasticity and fracture for aluminium alloys under strain
path change”,
Dasharatha Achani, 2006:76, ISBN 82-471-7903-2 (printed version), ISBN 82-471-
7902-4 (electronic version), ISSN 1503-8181.

“Simulations of 2D dynamic brittle fracture by the Element-free Galerkin method and
linear fracture mechanics”,
Tommy Karlsson, 2006:125, ISBN 82-471-8011-1 (printed version), ISBN 82-471-
8010-3 (electronic version), ISSN 1503-8181.

“Penetration and Perforation of Granite Targets by Hard Projectiles”,

Chong Chiang Seah, 2006:188, ISBN 82-471-8150-9 (printed version), ISBN 82-471-8149-5 (electronic version), ISSN 1503-8181.

“Deformations, strain capacity and cracking of concrete in plastic and early hardening phases”,

Tor Arne Hammer, 2007:234, ISBN 978-82-471-5191-4 (printed version), ISBN 978-82-471-5207-2 (electronic version), ISSN 1503-8181.

“Crashworthiness of dual-phase high-strength steel: Material and Component behaviour”, Venkatapathi Tarigopula, 2007:230, ISBN 82-471-5076-4 (printed version), ISBN 82-471-5093-1 (electronic version), ISSN 1503-8181.

“Fibre reinforcement in load carrying concrete structures”,

Åse Lyslo Døssland, 2008:50, ISBN 978-82-471-6910-0 (printed version), ISBN 978-82-471-6924-7 (electronic version), ISSN 1503-8181.

“Low-velocity penetration of aluminium plates”,

Frode Grytten, 2008:46, ISBN 978-82-471-6826-4 (printed version), ISBN 978-82-471-6843-1 (electronic version), ISSN 1503-8181.

“Robustness studies of structures subjected to large deformations”,

Ørjan Fyllingen, 2008:24, ISBN 978-82-471-6339-9 (printed version), ISBN 978-82-471-6342-9 (electronic version), ISSN 1503-8181.

“Constitutive modelling of morsellised bone”,

Knut Birger Lunde, 2008:92, ISBN 978-82-471-7829-4 (printed version), ISBN 978-82-471-7832-4 (electronic version), ISSN 1503-8181.

“Experimental Investigations of Wind Loading on a Suspension Bridge Girder”,

Bjørn Isaksen, 2008:131, ISBN 978-82-471-8656-5 (printed version), ISBN 978-82-471-8673-2 (electronic version), ISSN 1503-8181.

“Cracking Risk of Concrete Structures in The Hardening Phase”,

Guomin Ji, 2008:198, ISBN 978-82-471-1079-9 (printed version), ISBN 978-82-471-1080-5 (electronic version), ISSN 1503-8181.

“Modelling and numerical analysis of the porcine and human mitral apparatus”,

Victorien Emile Prot, 2008:249, ISBN 978-82-471-1192-5 (printed version), ISBN 978-82-471-1193-2 (electronic version), ISSN 1503-8181.

“Strength analysis of net structures”,

Heidi Moe, 2009:48, ISBN 978-82-471-1468-1 (printed version), ISBN 978-82-471-1469-8 (electronic version), ISSN 1503-8181.

“Numerical analysis of ductile fracture in surface cracked shells”,

Espen Berg, 2009:80, ISBN 978-82-471-1537-4 (printed version), ISBN 978-82-471-1538-1 (electronic version), ISSN 1503-8181.

“Subject specific finite element analysis of bone – for evaluation of the healing of a leg lengthening and evaluation of femoral stem design”,

Sune Hansborg Pettersen, 2009:99, ISBN 978-82-471-1579-4 (printed version), ISBN 978-82-471-1580-0 (electronic version), ISSN 1503-8181.

“Evaluation of fracture parameters for notched multi-layered structures”,

Lingyun Shang, 2009:137, ISBN 978-82-471-1662-3 (printed version), ISBN 978-82-471-1663-0 (electronic version), ISSN 1503-8181.

“Modelling of Dynamic Material Behaviour and Fracture of Aluminium Alloys for Structural Applications”

Yan Chen, 2009:69, ISBN 978-82-471-1515-2 (printed version), ISBN 978-82-471-1516-9 (electronic version), ISSN 1503-8181.

“Nanomechanics of polymer and composite particles”

Jiaying He 2009:213, ISBN 978-82-471-1828-3 (printed version), ISBN 978-82-471-1829-0 (electronic version), ISSN 1503-8181.

“Mechanical properties of clear wood from Norway spruce”

Kristian Berbom Dahl 2009:250, ISBN 978-82-471-1911-2 (printed version) ISBN 978-82-471-1912-9 (electronic version), ISSN 1503-8181.

“Modeling of the degradation of TiB₂ mechanical properties by residual stresses and liquid Al penetration along grain boundaries”

Micol Pezzotta 2009:254, ISBN 978-82-471-1923-5 (printed version) ISBN 978-82-471-1924-2 (electronic version) ISSN 1503-8181.

“Effect of welding residual stress on fracture”

Xiabo Ren 2010:77, ISBN 978-82-471-2115-3 (printed version) ISBN 978-82-471-2116-0 (electronic version), ISSN 1503-8181.

“Pan-based carbon fiber as anode material in cathodic protection system for concrete structures”

Mahdi Chini 2010:122, ISBN 978-82-471-2210-5 (printed version) ISBN 978-82-471-2213-6 (electronic version), ISSN 1503-8181.

“Structural Behaviour of deteriorated and retrofitted concrete structures”

Irina Vasililjeva Sæther 2010:171, ISBN 978-82-471-2315-7 (printed version) ISBN 978-82-471-2316-4 (electronic version) ISSN 1503-8181.

“Prediction of local snow loads on roofs”

Vivian Meløysund 2010:247, ISBN 978-82-471-2490-1 (printed version) ISBN 978-82-471-2491-8 (electronic version) ISSN 1503-8181.

“Behaviour and modelling of polymers for crash applications”

Virgile Delhaye 2010:251, ISBN 978-82-471-2501-4 (printed version) ISBN 978-82-471-2502-1 (electronic version) ISSN 1503-8181.

“Blended cement with reduced CO₂ emission – Utilizing the Fly Ash-Limestone Synergy”,

Klaartje De Weerd 2011:32, ISBN 978-82-471-2584-7 (printed version) ISBN 978-82-471-2584-4 (electronic version) ISSN 1503-8181.

“Chloride induced reinforcement corrosion in concrete” Concept of critical chloride content – methods and mechanisms.

Ueli Angst 2011:113, ISBN 978-82-471-2769-9 (printed version) ISBN 978-82-471-2763-6 (electronic version) ISSN 1503-8181.

“A thermo-electric-Mechanical study of the carbon anode and contact interface for Energy savings in the production of aluminium”.

Dag Herman Andersen 2011:157, ISBN 978-82-471-2859-6 (printed version) ISBN 978-82-471-2860-2 (electronic version) ISSN 1503-8181.

“Structural Capacity of Anchorage Ties in Masonry Veneer Walls Subjected to Earthquake”. The implications of Eurocode 8 and Eurocode 6 on a typical Norwegian veneer wall.

Ahmed Mohamed Yousry Hamed 2011:181, ISBN 978-82-471-2911-1 (printed version) ISBN 978-82-471-2912-8 (electronic ver.) ISSN 1503-8181.

“Work-hardening behaviour in age-hardenable Al-Zn-Mg(-Cu) alloys”.

Ida Westermann , 2011:247, ISBN 978-82-471-3056-8 (printed ver.) ISBN 978-82-471-3057-5 (electronic ver.) ISSN 1503-8181.

“Behaviour and modelling of selfpiercing riveted connections using aluminium rivets”.

Nguyen-Hieu Hoang, 2011:266, ISBN 978-82-471-3097-1 (printed ver.) ISBN 978-82-471-3099-5 (electronic ver.) ISSN 1503-8181.

“Fibre reinforced concrete”.

Sindre Sandbakk, 2011:297, ISBN 978-82-471-3167-1 (printed ver.) ISBN 978-82-471-3168-8 (electronic ver.) ISSN 1503-8181.

“Dynamic behaviour of cablesupported bridges subjected to strong natural wind”.

Ole Andre Øiseth, 2011:315, ISBN 978-82-471-3209-8 (printed ver.) ISBN 978-82-471-3210-4 (electronic ver.) ISSN 1503-8181.

“Constitutive modeling of solargrade silicon materials”

Julien Cochard, 2011:307, ISBN 978-82-471-3189-3 (printed ver.) ISBN 978-82-471-3190-9 (electronic ver.) ISSN 1503-8181.

“Constitutive behavior and fracture of shape memory alloys”

Jim Stian Olsen, 2012:57, ISBN 978-82-471-3382-8 (printed ver.) ISBN 978-82-471-3383-5 (electronic ver.) ISSN 1503-8181.

“Field measurements in mechanical testing using close-range photogrammetry and digital image analysis”

Egil Fagerholt, 2012:95, ISBN 978-82-471-3466-5 (printed ver.) ISBN 978-82-471-3467-2 (electronic ver.) ISSN 1503-8181.

“Towards a better understanding of the ultimate behaviour of lightweight aggregate concrete in compression and bending”,

Håvard Nedrelid, 2012:123, ISBN 978-82-471-3527-3 (printed ver.) ISBN 978-82-471-3528-0 (electronic ver.) ISSN 1503-8181.

“Numerical simulations of blood flow in the left side of the heart”

Sigrid Kaarstad Dahl, 2012:135, ISBN 978-82-471-3553-2 (printed ver.) ISBN 978-82-471-3555-6 (electronic ver.) ISSN 1503-8181.

“Moisture induced stresses in glulam”

Vanessa Angst-Nicollier, 2012:139, ISBN 978-82-471-3562-4 (printed ver.) ISBN 978-82-471-3563-1 (electronic ver.) ISSN 1503-8181.

“Biomechanical aspects of distraction osteogenesis”

Valentina La Russa, 2012:250, ISBN 978-82-471-3807-6 (printed ver.) ISBN 978-82-471-3808-3 (electronic ver.) ISSN 1503-8181.

“Ductile fracture in dual-phase steel. Theoretical, experimental and numerical study”

Gaute Gruben, 2012:257, ISBN 978-82-471-3822-9 (printed ver.) ISBN 978-82-471-3823-6 (electronic ver.) ISSN 1503-8181.

“Damping in Timber Structures”

Nathalie Labonnote, 2012:263, ISBN 978-82-471-3836-6 (printed ver.) ISBN 978-82-471-3837-3 (electronic ver.) ISSN 1503-8181.

“Biomechanical modeling of fetal veins: The umbilical vein and ductus venosus bifurcation”

Paul Roger Leinan, 2012:299, ISBN 978-82-471-3915-8 (printed ver.) ISBN 978-82-471-3916-5 (electronic ver.) ISSN 1503-8181.

“Large-Deformation behaviour of thermoplastics at various stress states”

Anne Serine Ognedal, 2012:298, ISBN 978-82-471-3913-4 (printed ver.) ISBN 978-82-471-3914-1 (electronic ver.) ISSN 1503-8181.

“Hardening accelerator for fly ash blended cement”

Kien Dinh Hoang, 2012:366, ISBN 978-82-471-4063-5 (printed ver.) ISBN 978-82-471-4064-2 (electronic ver.) ISSN 1503-8181.

“From molecular structure to mechanical properties”

Jiayang Wu, 2013:186, ISBN 978-82-471-4485-5 (printed ver.) ISBN 978-82-471-4486-2 (electronic ver.) ISSN 1503-8181.

“Experimental and numerical study of hybrid concrete structures”

Linn Grepstad Nes, 2013:259, ISBN 978-82-471-4644-6 (printed ver.) ISBN 978-82-471-4645-3 (electronic ver.) ISSN 1503-8181.

“Mechanics of ultra-thin multi crystalline silicon wafers”

Saber Saffar, 2013:199, ISBN 978-82-471-4511-1 (printed ver.) ISBN 978-82-471-4513-5 (electronic ver.) ISSN 1503-8181.

“Through process modelling of welded aluminium structures”

Anizahyati Alisibramulisi, 2013:325, ISBN 978-82-471-4788-7 (printed ver.) ISBN 978-82-471-4789-4 (electronic ver.) ISSN 1503-8181.

“Combined blast and fragment loading on steel plates”

Knut Gaarder Rakvåg, 2013:361, ISBN 978-82-471-4872-3 (printed ver.) ISBN 978-82-4873-0 (electronic ver.) ISSN 1503-8181.

“Characterization and modelling of the anisotropic behaviour of high-strength aluminium alloy”

Marion Fourmeau, 2014:37, ISBN 978-82-326-0008-3 (printed ver.) ISBN 978-82-326-0009-0 (electronic ver.) ISSN 1503-8181.

“Behaviour of threaded steel fasteners at elevated deformation rates”

Henning Fransplass, 2014:65, ISBN 978-82-326-0054-0 (printed ver.) ISBN 978-82-326-0055-7 (electronic ver.) ISSN 1503-8181.

“Sedimentation and Bleeding”

Ya Peng, 2014:89, ISBN 978-82-326-0102-8 (printed ver.) ISBN 978-82-326-0103-5 (electronic ver.) ISSN 1503-8181.

“Impact against X65 offshore pipelines”

Martin Kristoffersen, 2014:362, ISBN 978-82-326-0636-8 (printed ver.) ISBN 978-82-326-0637-5 (electronic ver.) ISSN 1503-8181.

“Formability of aluminium alloy subjected to prestrain by rolling”

Dmitry Vysochinskiy, 2014:363, ISBN 978-82-326-0638-2 (printed ver.) ISBN 978-82-326-0639-9 (electronic ver.) ISSN 1503-8181.

“Experimental and numerical study of Yielding, Work-Hardening and anisotropy in textured AA6xxx alloys using crystal plasticity models”

Mikhail Khadyko, 2015:28, ISBN 978-82-326-0724-2 (printed ver.) ISBN 978-82-326-0725-9 (electronic ver.) ISSN 1503-8181.

“Behaviour and Modelling of AA6xxx Aluminium Alloys Under a Wide Range of Temperatures and Strain Rates”

Vincent Vilamosa, 2015:63, ISBN 978-82-326-0786-0 (printed ver.) ISBN 978-82-326-0787-7 (electronic ver.) ISSN 1503-8181.

“A Probabilistic Approach in Failure Modelling of Aluminium High Pressure Die-Castings”

Octavian Knoll, 2015:137, ISBN 978-82-326-0930-7 (printed ver.) ISBN 978-82-326-0931-4 (electronic ver.) ISSN 1503-8181.

“Ice Abrasion on Marine Concrete Structures”

Egil Møen, 2015:189, ISBN 978-82-326-1034-1 (printed ver.) ISBN 978-82-326-1035-8 (electronic ver.) ISSN 1503-8181.

“Fibre Orientation in Steel-Fibre-Reinforced Concrete”

Giedrius Zirgulis, 2015:229, ISBN 978-82-326-1114-0 (printed ver.) ISBN 978-82-326-1115-7 (electronic ver.) ISSN 1503-8181.

“Effect of spatial variation and possible interference of localised corrosion on the residual capacity of a reinforced concrete beam”

Mohammad Mahdi Kioumarsi, 2015:282, ISBN 978-82-326-1220-8 (printed ver.) ISBN 978-82-1221-5 (electronic ver.) ISSN 1503-8181.

“The role of concrete resistivity in chloride-induced macro-cell corrosion”

Karla Horbostel, 2015:324, ISBN 978-82-326-1304-5 (printed ver.) ISBN 978-82-326-1305-2 (electronic ver.) ISSN 1503-8181.

“Flowable fibre-reinforced concrete for structural applications”

Elena Vidal Sarmiento, 2015:335, ISBN 978-82-326-1324-3 (printed ver.) ISBN 978-82-326-1325-0 (electronic ver.) ISSN 1503-8181.

“Development of chushed sand for concrete production with microproportioning”

Rolands Cepuritis, 2016:19, ISBN 978-82-326-1382-3 (printed ver.) ISBN 978-82-326-1383-0 (electronic ver.) ISSN 1503-8181.

“Withdrawal properties of threaded rods embedded in glued-laminated timber elements”

Haris Stamatopoulos, 2016:48, ISBN 978-82-326-1436-3 (printed ver.) ISBN 978-82-326-1437-0 (electronic ver.) ISSN 1503-8181.

“An Experimental and numerical study of thermoplastics at large deformation”

Marius Andersen, 2016:191, ISBN 978-82-326-1720-3 (printed ver.) ISBN 978-82-326-1721-0 (electronic ver.) ISSN 1503-8181.

“Modeling and Simulation of Ballistic Impact”

Jens Kristian Holmen, 2016:240, ISBN 978-82-326-1818-7 (printed ver.) ISBN 978-82-326-1819-4 (electronic ver.) ISSN 1503-8181.

“Early age crack assessment of concrete structures”

Anja B. Estensen Klausen, 2016:256, ISBN 978-82-326-1850-7 (printed ver.) ISBN 978-82-326-1851-4 (electronic ver.) ISSN 1503-8181.

“Uncertainty quantification and sensitivity analysis for cardiovascular models”

Vinzenz Gregor Eck, 2016:234, ISBN 978-82-326-1806-4 (printed ver.) ISBN 978-82-326-1807-1 (electronic ver.) ISSN 1503-8181.

“Dynamic behaviour of existing and new railway catenary systems under Norwegian conditions”

Petter Røe Nåvik, 2016:298, ISBN 978-82-326-1935-1 (printed ver.) ISBN 978-82-326-1934-4 (electronic ver.) ISSN 1503-8181.

“Mechanical behaviour of particle-filled elastomers at various temperatures”

Arne Ilseeng, 2016:295, ISBN 978-82-326-1928-3 (printed ver.) ISBN 978-82-326-1929-0 (electronic ver.) ISSN 1503-8181.

“Nanotechnology for Anti-Icing Application”

Zhiwei He, 2016:348, ISBN 978-82-326-2038-8 (printed ver.) ISBN 978-82-326-2019-5 (electronic ver.) ISSN 1503-8181.

“Conduction Mechanisms in Conductive Adhesives with Metal-Coated Polymer Spheres”

Sigurd Rolland Pettersen, 2016:349, ISBN 978-82-326-2040-1 (printed ver.) ISBN 978-82-326-2041-8 (electronic ver.) ISSN 1503-8181.

“The interaction between calcium lignosulfonate and cement”

Alessia Colombo, 2017:20, ISBN 978-82-326-2122-4 (printed ver.) ISBN 978-82-326-2123-1 (electronic ver.) ISSN 1503-8181.

“Behaviour and Modelling of Flexible Structures Subjected to Blast Loading”

Vegard Aune, 2017:101, ISBN 978-82-326-2274-0 (printed ver.) ISBN 978-82-326-2275-7 (electronic ver.) ISSN 1503-8181.

“Behaviour of steel connections under quasi-static and impact loading”

Erik Løhre Grimsmo, 2017:159, ISBN 978-82-326-2390-7 (printed ver.) ISBN 978-82-326-2391-4 (electronic ver.) ISSN 1503-8181.

“An experimental and numerical study of cortical bone at the macro and Nano-scale”

Masoud Ramenzanzadehkoldeh, 2017:208, ISBN 978-82-326-2488-1 (printed ver.) ISBN 978-82-326-2489-8 (electronic ver.) ISSN 1503-8181.

“Optoelectrical Properties of a Novel Organic Semiconductor: 6,13-Dichloropentacene”

Mao Wang, 2017:130, ISBN 978-82-326-2332-7 (printed ver.) ISBN 978-82-326-2333-4 (electronic ver.) ISSN 1503-8181.

“Core-shell structured microgels and their behavior at oil and water interface”

Yi Gong, 2017:182, ISBN 978-82-326-2436-2 (printed. ver.) ISBN 978-82-326-2437-9 (electronic ver.) ISSN 1503-8181.

“Aspects of design of reinforced concrete structures using nonlinear finite element analyses”

Morten Engen, 2017:149, ISBN 978-82-326-2370-9 (printed ver.) ISBN 978-82-326-2371-6 (electronic ver.) ISSN 1503-8181.

“Numerical studies on ductile failure of aluminium alloys”

Lars Edvard Dæhli, 2017:284, ISBN 978-82-326-2636-6 (printed ver.) ISBN 978-82-326-2637-3 (electronic ver.) ISSN 1503-8181.

“Modelling and Assessment of Hydrogen Embrittlement in Steels and Nickel Alloys”

Haiyang Yu, 2017:278, ISBN 978-82-326-2624-3 (printed. ver.) ISBN 978-82-326-2625-0 (electronic ver.) ISSN 1503-8181.

“Network arch timber bridges with light timber deck on transverse crossbeams”

Anna Weronika Ostrycharczyk, 2017:318, ISBN 978-82-326-2704-2 (printed ver.) ISBN 978-82-326-2705-9 (electronic ver.) ISSN 1503-8181.

“Splicing of Large Glued Laminated Timber Elements by Use of Long Threaded Rods”

Martin Cepelka, 2017:320, ISBN 978-82-326-2708-0 (printed ver.) ISBN 978-82-326-2709-7 (electronic ver.) ISSN 1503-8181.

“Thermomechanical behaviour of semi-crystalline polymers: experiments, modelling and simulation”

Joakim Johnsen, 2017:317, ISBN 978-82-326-2702-8 (printed ver.) ISBN 978-82-326-2703-5 (electronic ver.) ISSN 1503-8181.

“Small-Scale Plasticity under Hydrogen Environment”

Kai Zhao, 2017:356, ISBN 978-82-326-2782-0 (printed ver.) ISBN 978-82-326-2783-7 (electronic er.) ISSN 1503-8181.

“Risk and Reliability Based Calibration of Structural Design Codes”

Michele Baravalle, 2017:342, ISBN 978-82-326-2752-3 (printed ver.) ISBN 978-82-326-2753-0 (electronic ver.) ISSN 1503-8181.

“Dynamic behaviour of floating bridges exposed to wave excitation”

Knut Andreas Kvåle, 2017:365, ISBN 978-82-326-2800-1 (printed ver.) ISBN 978-82-326-2801-8 (electronic ver.) ISSN 1503-8181.

“Dolomite calcined clay composite cement – hydration and durability”

Alisa Lydia Machner, 2018:39, ISBN 978-82-326-2872-8 (printed ver.) ISBN 978-82-326-2873-5 (electronic ver.) ISSN 1503-8181.

“Modelling of the self-excited forces for bridge decks subjected to random motions: an experimental study”

Bartosz Siedziako, 2018:52, ISBN 978-82-326-2896-4 (printed ver.) ISBN 978-82-326-2897-1 (electronic ver.) ISSN 1503-8181.

“A probabilistic-based methodology for evaluation of timber facade constructions”

Klodian Gradeci, 2018:69, ISBN 978-82-326-2928-2 (printed ver.) ISBN 978-82-326-2929-9 (electronic ver.) ISSN 1503-8181.

“Behaviour and modelling of flow-drill screw connections”

Johan Kolstø Sønstabø, 2018:73, ISBN 978-82-326-2936-7 (printed ver.) ISBN 978-82-326-2937-4 (electronic ver.) ISSN 1503-8181.

“Full-scale investigation of the effects of wind turbulence characteristics on dynamic behavior of long-span cable-supported bridges in complex terrain”

Aksel Fenerci, 2018 100, ISBN 978-82-326-2990-9 (printed ver.) ISBN 978-82-326-2991-6 (electronic ver.) ISSN 1503-8181.

“Modeling and simulation of the soft palate for improved understanding of the obstructive sleep apnea syndrome”

Hongliang Liu, 2018:101, ISBN 978-82-326-2992-3 (printed ver.) ISBN 978-82-326-2993-0 (electronic ver.) ISSN 1503-8181.

“Long-term extreme response analysis of cable-supported bridges with floating pylons subjected to wind and wave loads”.

Yuwang Xu, 2018:229, ISBN 978-82-326-3248-0 (printed ver.) ISBN 978-82-326-3249-7 (electronic ver.) ISSN 1503-8181.

“Reinforcement corrosion in carbonated fly ash concrete”

Andres Belda Revert, 2018:230, ISBN 978-82-326-3250-3 (printed ver.) ISBN 978-82-326-3251-0 (electronic ver.) ISSN 1503-8181.

“Direct finite element method for nonlinear earthquake analysis of concrete dams including dam-water-foundation rock interaction”

Arnkjell Løkke, 2018:252, ISBN 978-82-326-3294-7 (printed ver.) ISBN 978-82-326-3295-4 (electronic ver.) ISSN 1503-8181.

“Electromechanical characterization of metal-coated polymer spheres for conductive adhesives”

Molly Strimbeck Bazilchuk, 2018:295, ISBN 978-82-326-3380-7 (printed. ver.) ISBN 978-82-326-3381-4 (electrical ver.) ISSN 1503-8181.

“Determining the tensile properties of Artic materials and modelling their effects on fracture”

Shengwen Tu, 2018:269, ISBN 978-82-326-3328-9 (printed ver.) ISBN 978-82-326-3329-6 (electronic ver.) ISSN 1503-8181.

“Atomistic Insight into Transportation of Nanofluid in Ultra-confined Channel”
Xiao Wang, 2018:334, ISBN978-82-326-3456-9 (printed ver.) ISBN 978-82-326-3457-6 (electronic ver.) ISSN 1503-8181.

“An experimental and numerical study of the mechanical behaviour of short glass-fibre reinforced thermoplastics”.

Jens Petter Henrik Holmstrøm, 2019:79, ISBN 978-82-326-3760-7 (printed ver.) ISBN 978-82-326-3761-4 (electronic ver.) ISSN 1503-8181.

“Uncertainty quantification and sensitivity analysis informed modeling of physical systems”

Jacob Sturdy, 2019:115, ISBN 978-82-326-3828-4 (printed ver.) ISBN 978-82-326-3829-1 (electric ver.) ISSN 1503-8181.

“Load model of historic traffic for fatigue life estimation of Norwegian railway bridges”
Gunnstein T. Frøseth, 2019:73, ISBN 978-82-326-3748-5 (printed ver.) ISBN 978-82-326-3749-2 (electronic ver.) ISSN 1503-8181.

“Force identification and response estimation in floating and suspension bridges using measured dynamic response”

Øyvind Wiig Petersen, 2019:88, ISBN 978-82-326-3778-2 (printed ver.) ISBN 978-82-326-3779-9 (electronic ver.) ISSN 1503-8181.

“Consistent crack width calculation methods for reinforced concrete elements subjected to 1D and 2D stress states”

Reignard Tan, 2019:147, ISBN 978-82-326-3892-5 (printed ver.) ISBN 978-82-326-3893-2 (electronic ver.) ISSN 1503-8181.

“Nonlinear static and dynamic isogeometric analysis of slender spatial and beam type structures”

Siv Bente Raknes, 2019:181, ISBN 978-82-326-3958-8 (printed ver.) ISBN 978-82-326-3959-5 (electronic ver.) ISSN 1503-8181.

“Experimental study of concrete-ice abrasion and concrete surface topography modification”

Guzel Shamsutdinova, 2019:182, ISBN978-82-326-3960-1 (printed ver.) ISBN 978-82-326-3961-8 (electronic ver.) ISSN 1503-8181.

“Wind forces on bridge decks using state-of-the art FSI methods”

Tore Andreas Helgedagsrud, 2019:180, ISBN 978-82-326-3956-4 (printed ver.) ISBN 978-82-326-3957-1 (electronic ver.) ISSN 1503-8181.

“Numerical Study on Ductile-to-Brittle Transition of Steel and its Behavior under Residual Stresses”

Yang Li, 2019:227, ISBN 978-82-326-4050-8 (printed ver.) ISBN 978-82-326-4015-5 (electronic ver.) ISSN 1503-8181.

“Micromechanical modelling of ductile fracture in aluminium alloys”

Bjørn Håkon Frodal, 2019:253, ISBN 978-82-326-4102-4 (printed ver.) ISBN 978-82-326-4103-1 (electronic ver.) ISSN 1503-8181.

“Monolithic and laminated glass under extreme loading: Experiments, modelling and simulations”

Karoline Osnes, 2019:304, ISBN 978-82-326-4204-5 (printed ver.) ISBN 978-82-326-4205-2 (electronic ver.) ISSN 1503-8181.

ISBN 978-82-326-5530-4 (printed ver.)
ISBN 978-82-326-6894-6 (electronic ver.)
ISSN 1503-8181 (printed ver.)
ISSN 2703-8084 (online ver.)



NTNU

Norwegian University of
Science and Technology